

*Environment Agency*  
*Operational Investigation*  
x Anglian Region OI Project OI/569

WAVE ATTENUATION  
OVER SALT MARSH SURFACES

x ~~Department of Geography~~

University of Cambridge

x August 1996

Anglian Region Final Report OI/569/3/A

ENVIRONMENT AGENCY



124646

## WAVE ATTENUATION OVER SALT MARSH SURFACES

- ✖ Final Report for ~~Anglian Region~~ OI Project OI/569
- ✖ T Spencer ✕  
I. Moeller ↗
- ✖ Research Contractor: DEPT OF GEOGRAPHY  
Cambridge University
- ✖ Environment Agency (~~Anglian Region~~)  
Kingfisher House  
Goldhay Way  
Orton Goldhay  
Peterborough  
PE2 5ZR
- ✖ ~~Anglian Region~~ OI Final Report OI/569/3/A

**Publisher**

Environment Agency, ~~Anglian Region~~  
Kingfisher House  
Goldhay Way  
Orton Goldhay  
Peterborough PE2 5ZR

Tel: 01733 371811

Fax: 01733 231840

© Environment Agency 1996

All rights reserved. No part of this document may be produced, stored in a retrieval system, or transmitted, in any form or by any means, electronic, mechanical, photocopying, recording or otherwise without the prior permission of the Environment Agency.

The views expressed in this document are not necessarily those of the Environment Agency. Its officers, servants or agents accept no liability whatsoever for any loss or damage arising from the interpretation, or reliance upon the views contained herein.

**Dissemination Status**

Internal: Limited Release  
External: Restricted

Why?

**Statement of Use:**

The report is for use by coastal managers and researchers concerned with flood defence, with particular reference to the use of salt marshes in flood defence.

**Research Contractor:**

The Research Contractor for this work was:

Dr T Spencer  
Department of Geography  
University of Cambridge  
Downing Place  
Cambridge  
CB2 3EN

Tel: 01223 333399

Fax: 01223 333392

**Environment Agency Project Leader:**

The Environment Agency Project Manager, ~~Anglian Region~~ was:

Mr DJ Leggett - Environment Agency, Anglian Region

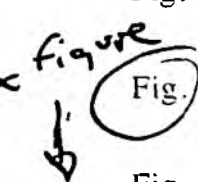
**Further Information:**

Further information relating to this document may be obtained from the ~~Anglian Region~~ R&D Management Support Officer in our Peterborough Office.

# CONTENTS

	Page
LIST OF FIGURES	ii
LIST OF TABLES	iv
LIST OF SYMBOLS <span style="margin-left: 20px;">← GLOSSARY OF TERMS</span>	v
LIST OF APPENDICES	vi
EXECUTIVE SUMMARY	vii
<del>SUMMARY</del>	viii
KEY WORDS	viii
 1. INTRODUCTION	 1
2. WAVE CLIMATE OF THE NORTH NORFOLK COAST	7
2.1. Wind and wave measurements	7
2.2. Environmental synthesis	17
2.3. Conclusions	20
3. DATA COLLECTION AND PROCESSING	21
3.1. Field experimental design	21
3.2. Field calibration	23
3.3. Timing and duration of wave measurements	25
4. RESULTS: WAVE ATTENUATION OVER THE STIFFKEY SANDFLAT / SALT MARSH	27
4.1. Introduction	27
4.2. General wave conditions at Stiffkey during the field monitoring period	27
4.3. Wave attenuation over sandflat and salt marsh	35
5. MODELLING WAVE ATTENUATION	47
5.1. Introduction	47
5.2. Wave attenuation: formulating the problem	50
5.3. Theoretical and semi-empirical equations	51
5.4. Model formulation and sensitivity analysis	62
5.5. Model application to the Stiffkey sandflat / salt marsh transect	78
6. CONCLUSIONS	99
7. RECOMMENDATIONS	101
8. REFERENCES	103
9. APPENDICES	107

## LIST OF FIGURES

- Summary Figure: Comparison of total wave energy reduction (%) and wave height change (%) over 200 m width of sandflat and 200 m of salt marsh from experimental field studies at Stiffkey, north Norfolk. p.ix
- x figure*  

 Fig. 1.1: Location of the Stiffkey marshes, north Norfolk, with location of wave recording stations (D) (source: 1:25 000 Ordnance Survey map, 1984) p.4
- Fig. 1.2: Generalised cross-section through the Stiffkey marshes (based on NRA/Environment Agency beach profile N2D4, Summer 1994). For location see Figure 1.1. p.5
- Fig. 2.1: Cumulative (%) frequency of 3-hourly offshore wind velocities during field season, 20.9.94 to 29.5.95. p.9
- Fig. 2.2: Monthly mean offshore wind speeds (1991-1995). p.10
- Fig. 2.3: Monthly means of offshore wave H, wind sea H, and swell H, 1991-95. p.12
- Fig. 2.4: Three-hourly significant wave heights at Blakeney, 19.11.94 to 3.3.95. p.13
- Fig. 2.5: Frequency distribution of coastal  $H_s$  at three coastal stations, Norfolk, for water depths exceeding 1m at Thornham (data from 19.11.94 to 4.3.95). p.14
- Fig. 2.6: Three-hourly wave heights offshore (spectral peak height) and at coastal stations ( $H_s$ ), January 1995 (note: different y-axis scales) (coastal records incomplete). p.16
- Fig. 2.7: Normalised non-tidal water elevation residuals for 5 Norfolk stations (November 1994 - March 1995) a) Thornham, b) Brancaster, c) Wells, d) Blakeney, e) Stiffkey. p.18
- Fig. 3.1: Photograph of dataloggers in casing. p.22
- Fig. 3.2: Observed and videoed time series of water surface at the middle station, 22 Sept 1994. p.24
- Fig. 4.1: Frequency distributions of  $H_{rms}$ ,  $E_{tot}$ ,  $T_p$ , and  $T_z$  at the outer station, Stiffkey (54 records, 21.9.94 to 17.5.95). p.28
- Fig. 4.2: Significant wave heights at (a) Stiffkey and Blakeney, and (b) Stiffkey and Brancaster. p.30
- Fig. 4.3: Offshore wind speed and direction during 54 wave records. p.33
- Fig. 4.4: (a) Relationship between wind direction measured offshore and incident wave height at Stiffkey, (b) Relationship between velocity of onshore winds and incident wave height at Stiffkey. p.34
- Fig. 4.5: Frequency distribution of change in  $E_{tot}$  and  $H_{rms}$  between stations at Stiffkey. p.38
- Fig. 4.6: Frequency distribution of  $T_p$  and  $T_z$  at the three stations at Stiffkey. p.40

- Fig. 4.7: Relationship between water depth at seaward station of section and  $H_{rms}$  change over respective section. p.41
- Fig. 4.8: Relationship between onshore wind velocity and  $H_{rms}$  change across sandflat and salt marsh. p.44
- Fig. 4.9: Diagram showing partial regression coefficients for the links between wave attenuation, tidal, offshore wave, and meteorological conditions. p.45
- Fig. 5.1: Meerschaert's (1993) 5-step approach towards mathematical modelling. p.49
- Fig. 5.2: Viscous friction factors, theory and experiment (Sleath, 1984). p.53
- Fig. 5.3: The variation of friction factors for a range of surfaces with water depth (CERC, 1984). p.56
- Fig. 5.4: The variation of wave length,  $L$ , with wave period,  $T$ , for varying water depths,  $h$ , as predicted from the model computations. p.64
- Fig. 5.5: The variation of relative water depth,  $h/L$ , with wave period,  $T$ , for varying water depths,  $h$ , as predicted from the model computations. p.65
- Fig. 5.6: The variation of modelled  $K_s$  with  $h/L$  for (a) varying slopes ( $dh$ ) and (b) varying water depths ( $h$ ). p.66
- Fig. 5.7: The variation of modelled  $K_v$  with  $h/L$  for varying  $T$  and  $h$ . p.68
- Fig. 5.8: The variation of modelled  $K_p$  with  $h/L$  for varying  $T$  and  $h$ . (a)  $d = 0.2$ , (b)  $d = 1.0$ , (c)  $d = \infty$ . p.69 - 71
- Fig. 5.9: The variation of modelled  $K_f$  with  $h/L$  for (a) varying  $f$  ( $h = 1.5\text{m}$ ,  $H = 0.2\text{m}$ ,  $dh = 0.25\text{m}$ ), varying  $T$  and  $h$  for (b)  $f = 0.1$ ,  $H = 0.6\text{m}$ , (c)  $f = 0.1$ ,  $H = 0.2\text{m}$ , (d)  $f = 0.1$ ,  $H = 0.05\text{m}$ . p.72 - 75
- Fig. 5.10: The variation of  $K$  with  $h/L$ . p.77
- Fig. 5.11: Variation of  $K_s$ ,  $K_p$ ,  $K_v$  for the 54 records for (a) the sandflat, (b) the salt marsh. p.81
- Fig. 5.12: Variation of  $K_s$ ,  $K_p$ ,  $K_v$  with  $h/L$  for (a) the sandflat, (b) the salt marsh. p.82
- Fig. 5.13: Variation of  $K_s$ ,  $K_p$ ,  $K_v$  with  $h/L$  for sandflat (note: y-axis scaled different to Figure 5.12). p.83
- Fig. 5.14: Variation of  $K_{obs}/K_{mod}$  for sandflat and salt marsh. p.85
- Fig. 5.15: Variation of  $f_{mod}$  with (a)  $h$ , (b)  $T$ , and (c). p.89 - 90
- Fig. 5.16: Variation of  $f_{mod}$  with  $h/L$ . p.91
- Fig. 5.17: Variation of  $f_{mod}$  with  $h/L$  for sandflat only. p.93

## LIST OF TABLES

Table 1.1:	Date, time, tidal conditions, and length of 54 wave record time-series collected at Stiffkey. p.3
Table 2.1:	$H_s$ at four coastal stations (Nov 94 - Feb 95) (for water depths > 1m at Thornham). p.15
Table 2.2:	Correlation coefficients ( $r$ values) relating coastal wave heights to offshore meteorological conditions. p.15
Table 4.1:	Summary statistics of main wave parameters calculated from all 54 'burst' records, September 1994 - March 1995. p.29
Table 4.2:	Water depth ( $h$ ), offshore ( $U_o$ ) and local ( $U_s$ ) wind speeds, and offshore wave (total, wind, and swell wave) conditions during wave recording at Stiffkey. p.31
Table 4.3:	Water depth ( $h$ ), offshore ( $U_o$ ) and local ( $U_s$ ) wind speeds, and offshore wave (total, wind, and swell wave) conditions for wave records obtained in onshore wind conditions. p.32
Table 4.4:	Wave parameter changes between the three stations at Stiffkey - summary statistics. p.36 - 37
Table 5.1:	Model input variables. p.62
Table 5.2:	Values of $K_{obs}/K_{mod}$ for the sandflat and salt marsh transects, Stiffkey ( $N = 54$ ). p.86
Table 5.3:	Observed and modelled wave height attenuation (excluding effect of surface friction in model). p.86
Table 5.4:	Percentage difference between expected wave heights (on basis of shoaling, viscous friction, and percolation) and observed wave heights ( $N = 54$ ). p.87
Table 5.5:	Values for the friction factor, $f$ , derived from the attenuation model. p.88
Table 5.6:	Friction factors as estimated from various equations and from the wave attenuation model. p.95
Table 5.7:	Observed values of wave height decrease over the salt marsh compared to computed values for salt marsh-to-sandflat conversion assuming three different values of $f$ . p.96

# + GLOSSARY OF TERMS

## LIST OF SYMBOLS

$h$	Viscosity of water
$\rho$	Water density
$\tau_0$	Amplitude of shear stress
$Dx$	Distance between two stations on transect parallel to wave path
$a$	Amplitude of horizontal displacement of water particles at the bottom
$A$	Surface area ( $m^2$ ) or (eq. (16)) packing factor of sediment
$a_0$	Damping coefficient
$a_1$	Coefficient for damping due to viscous boundary layer friction
$a_2$	Coefficient for damping due to percolation
$B$	Sand shape factor
$CD$	Drag coefficient
$C_{lim}$	Upper limit of volume concentration of particles ('packing density')
$c_x$	Wave celerity at station $x$ , calculated from wave number, $k$
$De$	Change in average wave energy transported through a vertical section with unit crest width
$d$	Depth of permeable layer
$D_s$	Sediment particle diameter
$D_{90}$	Grain size exceeded by 10% by weight of a sediment sample
$D_{gm}$	Geometric mean of two mesh sizes
$D_p$	rate of energy dissipation per unit surface area due to percolation
$E$	Wave energy ( $Joules\ m^{-2}$ )
$f$	Surface friction factor
$f_d$	Friction factor associated with surface drag
$f_{mod}$	Friction factor derived from modelled wave attenuation
$g$	gravitational acceleration
$h$	Water depth (m)
$H$	Wave height
$H_1$	wave height at seaward station on transect parallel to wave path
$H_2$	wave height at landward station on transect parallel to wave path
$H_{max}$	Maximum possible $H$ for given $h$ and $L$
$h_r$	Ripple height
$K$	Specific permeability or wave height decay factor

$k$	Permeability coefficient
$K_f$	Friction coefficient
$K_{mod}$	Modelled combined decay factor
$K_{obs}$	Decay factor derived from observed wave height ratio
$K_p$	Percolation coefficient
$k_s$	Nikuradse grain roughness (approx. by $2D_{90}$ or $25h_r^2/L_r$ )
$K_s$	Shoaling coefficient
$L$	Wave length (m)
$L_r$	Spacing of ripples associated with surface drag on sand
$m$	Slope ( $-dh/dx$ )
$n_p$	Porosity of sediment
$p$	Pressure
$P$	% of sand held between two adjacent sieves
$Q$	Rate of water movement through soil (discharge)
$R$	Half-amplitude of horizontal displacement of water particles at the bottom
$Re$	Reynold's number
$S_p$	Area of object projected into the direction of flow
$T$	Wave period (s)
$u$	Horizontal fluid velocity
$U$	Amplitude of horizontal component of velocity just outside oscillatory boundary layer
$U, u$	horizontal velocity just outside the boundary layer
$\nu$	Kinematic viscosity
$x$	Distance in direction of wave travel (m)



## LIST OF APPENDICES

- Appendix 1: Time periods for which water level and wave records were available from the NRA / Environment Agency at individual locations along the north Norfolk coast. p.107
- Appendix 2: Davis' method for calculating directional means. p.107
- Appendix 3: Regression analysis ( $r$  values) of offshore wave heights versus wave heights ( $H_s$ ) at coastal stations. p.107
- Appendix 4: Calculated wave parameters and summary statistics for the 54 wave record time-series. p.108

## EXECUTIVE SUMMARY

Over large areas of lowland Britain, agricultural land and settlements are protected from flooding by walls, embankments and fronting salt marshes. Salt marshes are an important asset for flood defence because they act as a buffer which helps dissipate wave and tidal energy. This has implications for the cost of defence structures.

This project provides the first comprehensive datasets on wave energy dissipation over 'open coast' intertidal salt marsh surfaces on the UK coastline. This report describes the measurement of water level variations using a pressure gauge methodology, and the processing of these records for the extraction of wind wave statistics.

Field measurements were made at Stiffkey, North Norfolk for a range of tidal and meteorological conditions across a 300m sandflat - salt marsh transect. Over the sandflat, wave height decreased on average by ca. 15%; across the salt marsh by 58% (range: 27 - 99%). Total spectral energy loss was 26% and 80% respectively.

*In what cycle? high tide/  
low tide?*

Preliminary mathematical modelling of wave attenuation showed that shoaling, viscous friction and percolation are negligible controls on attenuation and that friction from surface roughness accounts for at least 70% of wave energy dissipation over the sandflat and at least 90% over the salt marsh.

Wave attenuation can be accurately reproduced by a model on the basis of known surface slope, grain size of surface sediments, incident wave and water depth conditions and estimated friction factors. The replacement of 200 m of salt marsh by sandflat would, for example, result on waves heights ca. 78% higher at the landward margin.

*At what time?*

A future wave attenuation research programme should seek to provide a series of guidelines for field managers to rapidly assess salt marsh characteristics in relation to wave attenuation potential at individual sites and to evaluate the likely flood defence impacts of natural and anthropogenic modification to the salt marsh environment.

## SUMMARY

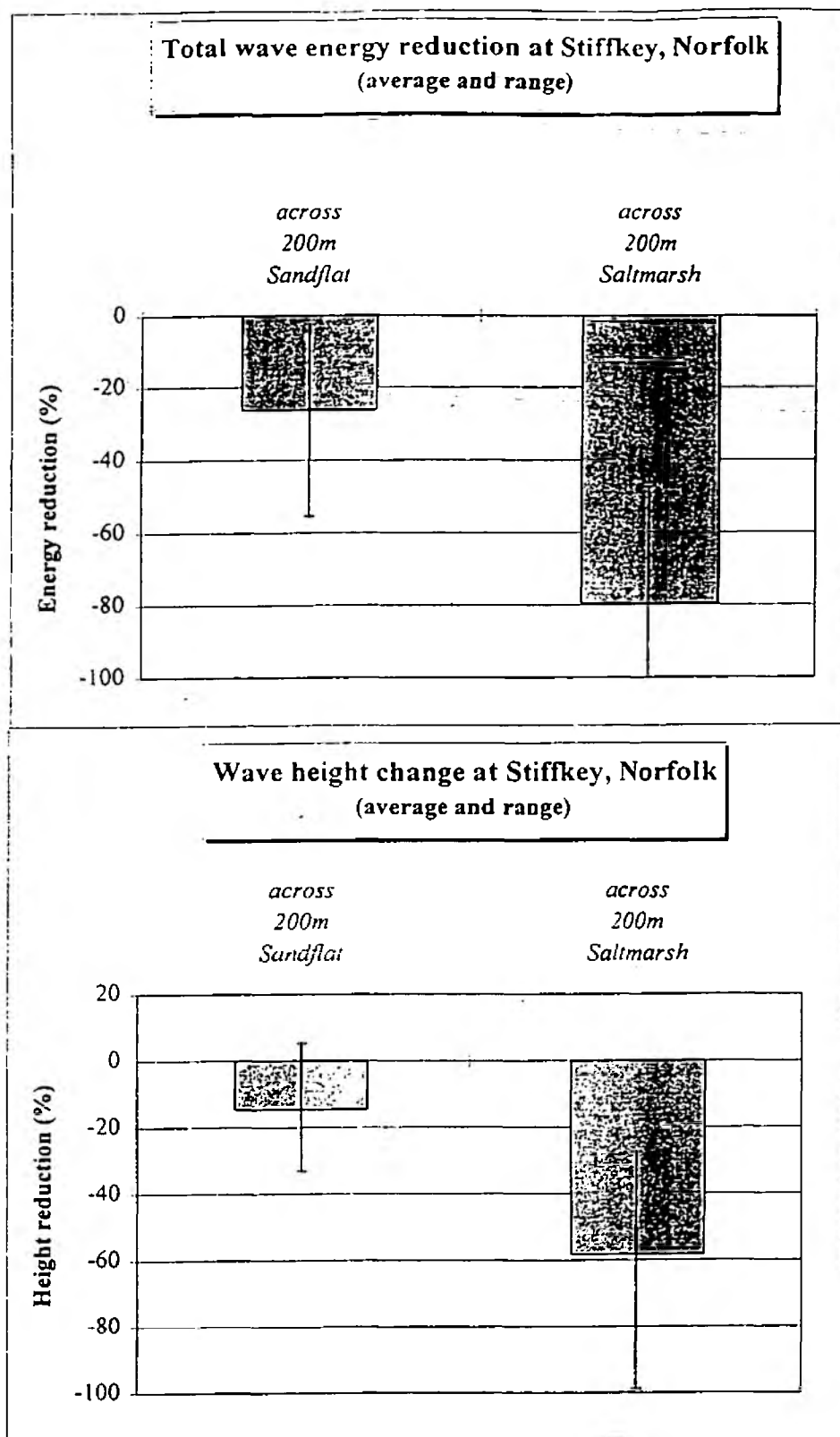
*why do we have a  
SUMMARY + EXECUTIVE SUMMARY?*

This report describes the measurement of water level variations over salt marsh surfaces, using a pressure gauge methodology, and the processing of these records for the extraction of wind wave statistics. Record calibration using videographic techniques is reported. Instrumentation was deployed at Stiffkey, North Norfolk. The general wave climate of the site is discussed through preliminary evaluation of three-hourly datasets from EA-maintained wave/tide stations at Thornham, Brancaster and Blakeney. Measurements at Stiffkey were undertaken with three stations equally spaced along a 300m sandflat to salt marsh transect, under a range of tidal and meteorological conditions. This allowed the calculation of wave attenuation with the passage of waves onshore. Mean, median and range of wave heights; spectral energy and wave periods for the field monitoring period are reported. Over the sandflat, wave height decreased on average by approximately 15%; across the salt marsh by 58% (range: 27 - 99%). Total spectral energy loss was 26% and 80% respectively. Preliminary mathematical modelling of wave attenuation - covering problem formulation, theoretical and semi-empirical equations, model construction and sensitivity analyses, and application to the Stiffkey transect - is described. Modelling showed that shoaling, viscous friction and percolation are negligible controls on attenuation and that friction from surface roughness accounts for at least 70% of wave energy dissipation over the sandflat and at least 90% over the salt marsh. Wave attenuation can be accurately reproduced by a model on the basis of known surface slope, grain size of surface sediments, incident wave and water depth conditions and estimated friction factors. The replacement of 200 m of salt marsh by sandflat would, for example, result on waves heights ca. 78% higher at the landward margin. Further research is required on the relative importance of the frictional role of marsh vegetation on the one hand and the more neglected control of marsh surface topography on the other. Wave diffraction, reflection, and refraction around and over mud-mounds and creeks may be responsible for a substantial proportion of the wave attenuation which has been attributed to surface friction. Further detailed field experiments investigating wave attenuation over marsh surfaces of varying topography, with and without creek channels, are needed to extend the model and determine the relative importance of these processes. A future wave attenuation research programme should, by looking at wave attenuation processes in a much wider set of salt marsh types and settings, seek to provide a series of guidelines for field managers to rapidly assess salt marsh characteristics in relation to wave attenuation potential at individual sites and to evaluate the likely flood defence impacts of natural and anthropogenic modification to the salt marsh environment.

## KEYWORDS

Salt marsh    Wave attenuation    Nearshore mathematical modelling    Flood defence

OI/569/3/A



Summary Figure: Comparison of total wave energy reduction (%) and wave height change (%) over 200 m width of sandflat and 200 m of salt marsh from experimental field studies at Stiffkey, north Norfolk.

## I. INTRODUCTION

Open-coast, open embayment and many estuarine salt marshes in England and Wales are exposed to significant incident energy from wind-generated waves. Salt marshes buffer this energy, as seen in the reduction of wave heights across marsh surfaces. This energy dissipation function has engineering significance since it permits the relaxation of design criteria for flood defence embankments where these are fronted by saltmarsh (Brampton 1992). Conversely, where salt marsh has been eroding (as on the Essex coast) defences have become subject to great forces than their design capability (Leggett and Dixon 1994).

Concern over near-future accelerated sea level rise and the potential costs of raising and strengthening existing lines of coastal defence has stimulated i) general interest in how natural coastal systems function and the ways in which flood defence works alter these dynamics, and ii) specific interest in the mechanisms by which mudflat and saltmarsh surfaces dissipate wave energy and the efficiency with which they do so. Better understanding of the physical effect of saltmarshes upon wave hydrodynamics is necessary in order to i) inform policies of 'coastal realignment' (or 'managed retreat'), where an expanded intertidal zone is created between existing and newly constructed landward defences (Burd 1995); and ii) provide design criteria for the restoration of degraded marsh systems or the creation of new protective marshes in front of threatened defences. Such concerns form part of a general philosophy of coastal management which seeks to work with natural processes rather than against them.

Scale physical model experiments undertaken in the UK during the 1980s suggest a wave height reduction of approximately 40% over an 80m wide saltmarsh from shoaling and breaking processes and from frictional losses (Brampton 1992). These results were not, however, validated by complementary field observations; <sup>although</sup> there have been remarkably few such studies. Wayne's (1976) work indicates substantial reduction of wave height and total energy (71% and 92% respectively) over a 20m transect, although it is difficult to reconstruct the methods and tidal sampling strategy employed. Knutson *et al.* (1982) reported similarly large reductions within the marshes of Chesapeake Bay <sup>where</sup> virtually all the incident wind-wave energy was removed at the end of a 30m transect. Both these studies were conducted in densely vegetated stands of tall *Spartina alterniflora* (cordgrass), under very low incident wave energies. Laboratory studies (e.g. Fonseca and Cahalan 1992) suggest a significant influence of vegetation density, and leaf area on wave height reduction over seagrasses and scale physical model experiments undertaken in the UK during the 1980s suggest a wave height reduction of approximately 40% over an 80m wide salt marsh from shoaling and breaking processes and from frictional losses (Brampton 1992). These results, however, were not validated by complementary field observations. There has been no published work on wave energy transformations within European locations subject to a storm wave climate.

hits as  
gullets

lists as  
bullets

x

x

repeat of  
above.

The simplest (and cheapest) way to measure wave heights in shallow water is by means of visual estimation. Although these techniques have been widely used, it has been shown that visual wave height observations made from the shore or from a ship tend to overestimate wave heights. Even with the aid of a calibrated staff, the visual observation of a full record of relatively high frequency waves is not feasible. Mechanical devices such as floats, wave rider buoys, accelerometer gauges, or remote sensing techniques are unsuitable for shallow water wave studies because of their inability to resolve small, high frequency waves. As a result, bottom-mounted resistance wire or capacitance gauges have been developed. These devices translate the fluctuating sea surface into a fluctuating voltage output and are able to resolve high frequency waves. Water elevations are calculated based on the relationship between the height of the water column,  $h$ , and hydrostatic pressure,  $P$ :

$$P = \rho gh + P_a \quad (1)$$

where  $P_a$  is the atmospheric pressure. (Many pressure sensors are fitted with an air vent, so that this term can be excluded.)

The project provided the first comprehensive datasets (Table 1.1) on wave attenuation over 'open coast' intertidal marsh surfaces in the UK using such pressure gauges. Investigations were based at Stiffkey on the North Norfolk coast of Eastern England (Figures 1.1, 1.2). This Final Report summarises previous reports, provides final datasets, and considers implications of these field-based investigations, and associated numerical modelling, for flood defence purposes.

The Anglian Region OI Interim Report (OI/569) (January 1994) outlined the main project objectives, site selection criteria, initial project activities and direction of research. The Annual Interim Report (OI/569) (August 1994) included a literature review on the role of salt marshes in coastal defence management, and an introduction to the physics of wind-generated surface gravity waves. It also described the project objectives, field methods and techniques, and the preliminary data collected in February 1994 in more detail. The Annual Interim Report (OI/569) (August 1995) reported comprehensive datasets from the 1994 / 95 winter wave monitoring campaign and further details of signal processing of pressure time-series, derivation of wave parameters and validation of computed water level time-series.

should be reproduced in this report if important in project result  
6-text

Table 1.1: Date, time, tidal conditions, and length of 54 wave record time-series collected at Stiffkey.

Burst Nr.	Date	Predicted HW height at Wells (m OD)	Predicted time HW at Stiffkey (GMT)	Measured time of HW, Stiffkey (if avail.)	Start of 'burst' recording	Duration of 'burst' (minutes)
1	21.09.94	2.78	08:08	n.a.	07:50	5
2					08:00	5
3					08:10	5
4	22.09.94	2.68	08:40	n.a.	08:30	5
5					08:45	5
6	05.10.94	3.05	06:55	n.a.	06:59	15
7	06.10.94	3.25	07:40	n.a.	07:20	5
8					07:40	5
9	07.10.94	3.25	08:25	n.a.	08:15	7
10					08:30	7
11	08.10.94	3.15	09:10	n.a.	09:00	7
12					09:15	7
13	04.11.94	2.98	18:50	n.a.	18:50	7
14	05.11.94	3.25	07:09	n.a.	06:30	5
15					06:50	5
16					07:10	5
17					07:30	5
18	04.12.94	3.05	06:55	06:51	06:55	7
19		3.05	19:15	19:05	19:20	7
20					19:40	5
21	05.12.94	2.95	07:45	07:59	07:45	5
22	06.01.95	2.48	21:54	21:35	21:45	7
23					22:00	7
24	03.02.95	2.83	20:53	20:40	20:50	7
25	17.02.95	2.91	19:53	19:48	19:40	7
26					19:50	7
27	18.02.95	2.62	08:20	08:00	08:20	7
28	19.02.95	2.85	21:05	20:40	20:50	7
29					21:00	7
30	20.02.95	2.40	09:32	09:25	09:30	7
31	02.03.95	2.93	19:17	19:00	19:00	7
32					19:20	7
33	03.03.95	2.60	07:52	07:30	07:50	5
34		2.93	19:53	19:10	19:40	7
35					20:00	7
36	04.03.95	2.53	08:24	08:20	08:20	5
37	17.03.95	2.88	18:54	18:15	18:50	7
38					19:05	7
39	18.03.95	2.71	07:21	06:55	07:20	5
40		3.03	19:31	19:05	19:25	7
41					19:40	7
42	19.03.95	2.78	07:57	07:40	07:55	5
43		3.06	20:10	19:50	20:10	7
44					20:25	7
45	20.03.95	2.73	08:35	08:15	08:30	5
46		2.93	20:48	20:50	20:45	7
47					21:00	7
48	21.03.95	2.56	09:14	09:25	09:10	5
49	15.04.95	2.88	18:11	18:10	18:03	7
50	16.04.95	3.02	18:54	18:50	18:47	7
51	15.05.95	2.76	06:19	06:20	06:30	7
52	16.05.95	2.85	07:01	07:00	07:00	7
53		2.91	19:25	19:30	19:30	7
54	17.05.95	2.83	07:45	07:30	07:40	5

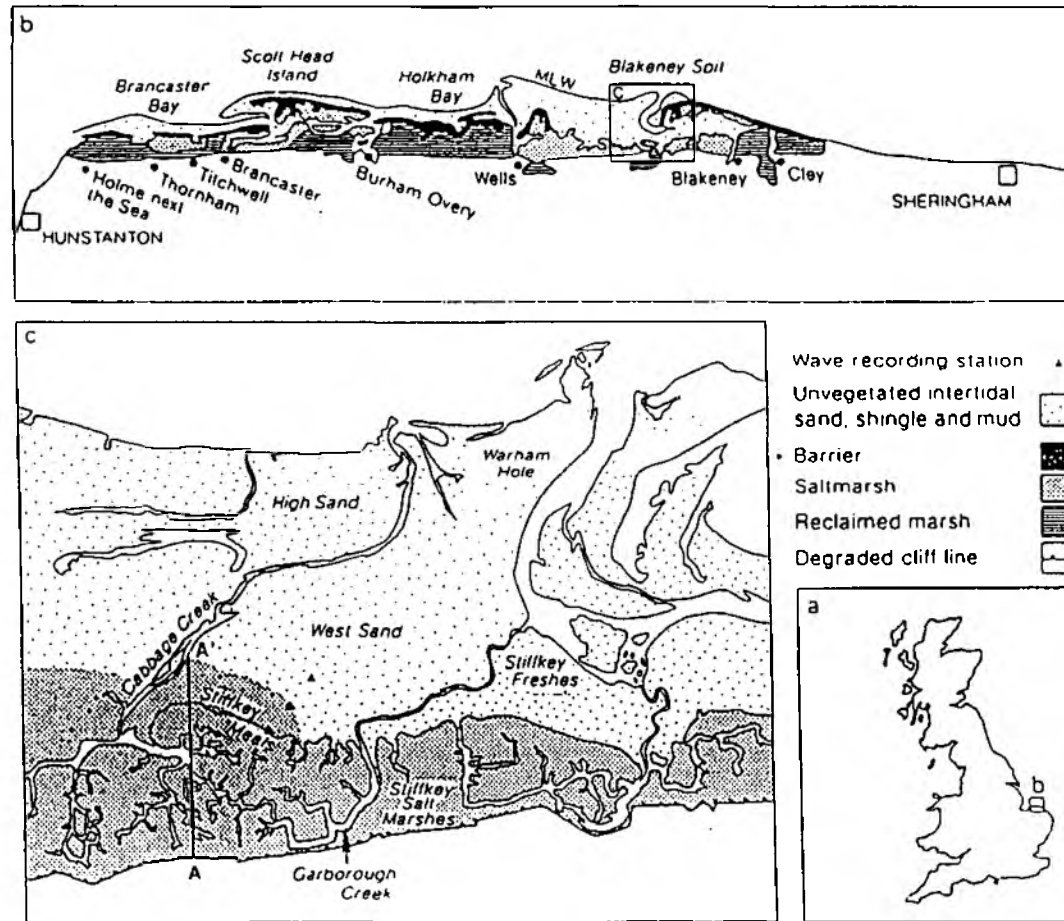


(Fig. 1.1)

1.1: Location of the Stiffkey marshes, north Norfolk, with location of wave recording stations (D) (source: 1:25 000 Ordnance Survey map, 1984)



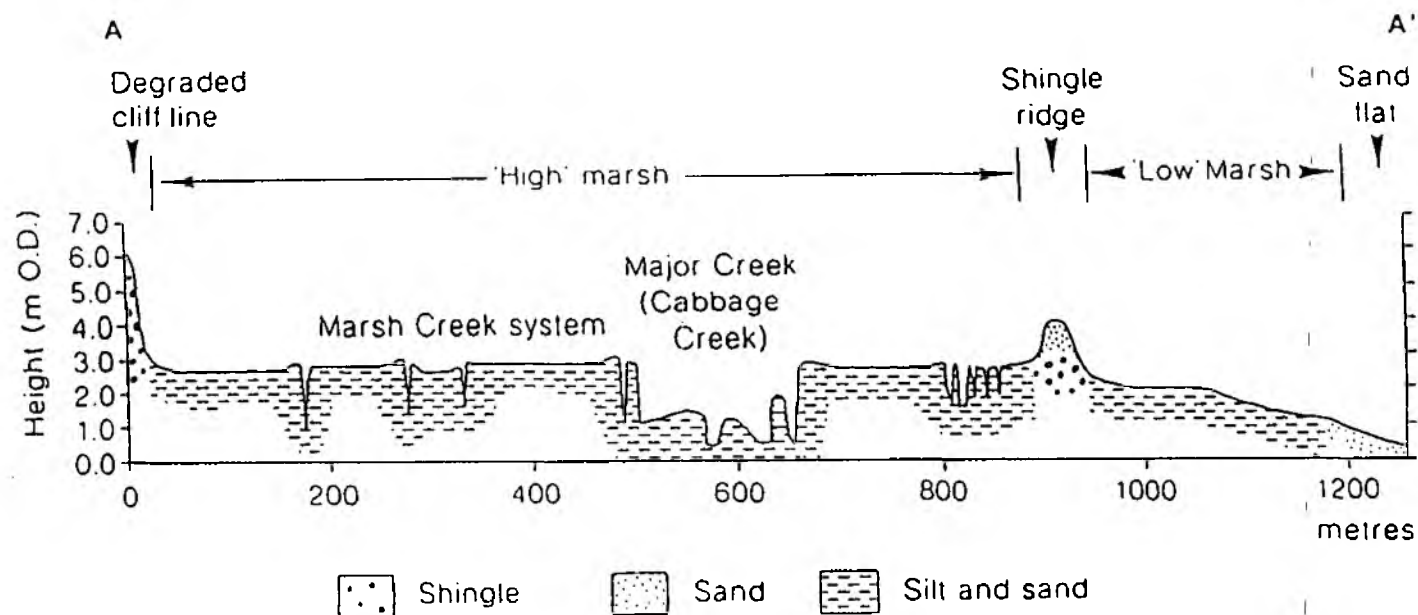


Fig. 1.2: Generalised cross-section through the Stiffkey marshes (based on NRA/Environment Agency beach profile N2D4, Summer 1994). For location see Figure 1.1.

## 2. CONTEXT: WAVE CLIMATE OF THE NORTH NORFOLK COAST

### 2.1 Wind and Wave Measurements

The height, period, and direction of incident waves on the Stiffkey sandflat is likely to be determined by offshore wave conditions as well as locally generated waves. Information on local wind conditions (see below) and offshore wave climate is therefore crucial to an interpretation of measured wave heights at Stiffkey. In addition, seasonal and inter-annual variations of wind and wave conditions are important in relation to salt marsh development as incident waves are likely to influence patterns of sediment deposition and/or erosion (see, for example, Pringle (1995)). This section focuses on offshore and coastal wave conditions in the southern North Sea and the north Norfolk coast.

#### 2.1.1 Data sources

Data on offshore wave conditions was obtained from the Environment Agency to whom it is supplied by the Meteorological Office. Three-hourly average wave heights, periods, and directions are computed on the basis of synoptic meteorological information and local wind speed and direction for several locations around the British Isles. The height, period and direction of waves associated with the energy transfer from the wind to the sea surface (wind waves) is also given, as well as the height, period and direction of waves outside their original generating area (swell). The data was available for 6-month periods (April to September, and October to March) over a total of four and a half years (from April 1991 to September 1995) with the exception of the two summer periods of 1992 and 1993. Since the 12th of June 1991, wind-sea direction has been calculated as a separate value to wind direction. Previous to that date, wind-sea direction was taken to be equal to wind direction. The model grid point closest to the north Norfolk coast is located at  $53.25^{\circ}\text{N}$  and  $1.53^{\circ}\text{E}$ . The water depth at this point is 21 km; the point is approximately 62.5 km offshore from Cromer and has been classed as 'open sea' by the Met Office. A programme written in ~~Matlab~~ <sup>Standard?</sup> was used to divide each of the datafiles covering a 6-month period into monthly data files. Monthly summary statistics were subsequently calculated and output stored in a separate file.

Three-hourly wave data was available for the Environment Agency-maintained coastal stations at Thornham, Brancaster, and Blakeney for the same time periods as the water level data (Appendix 1).

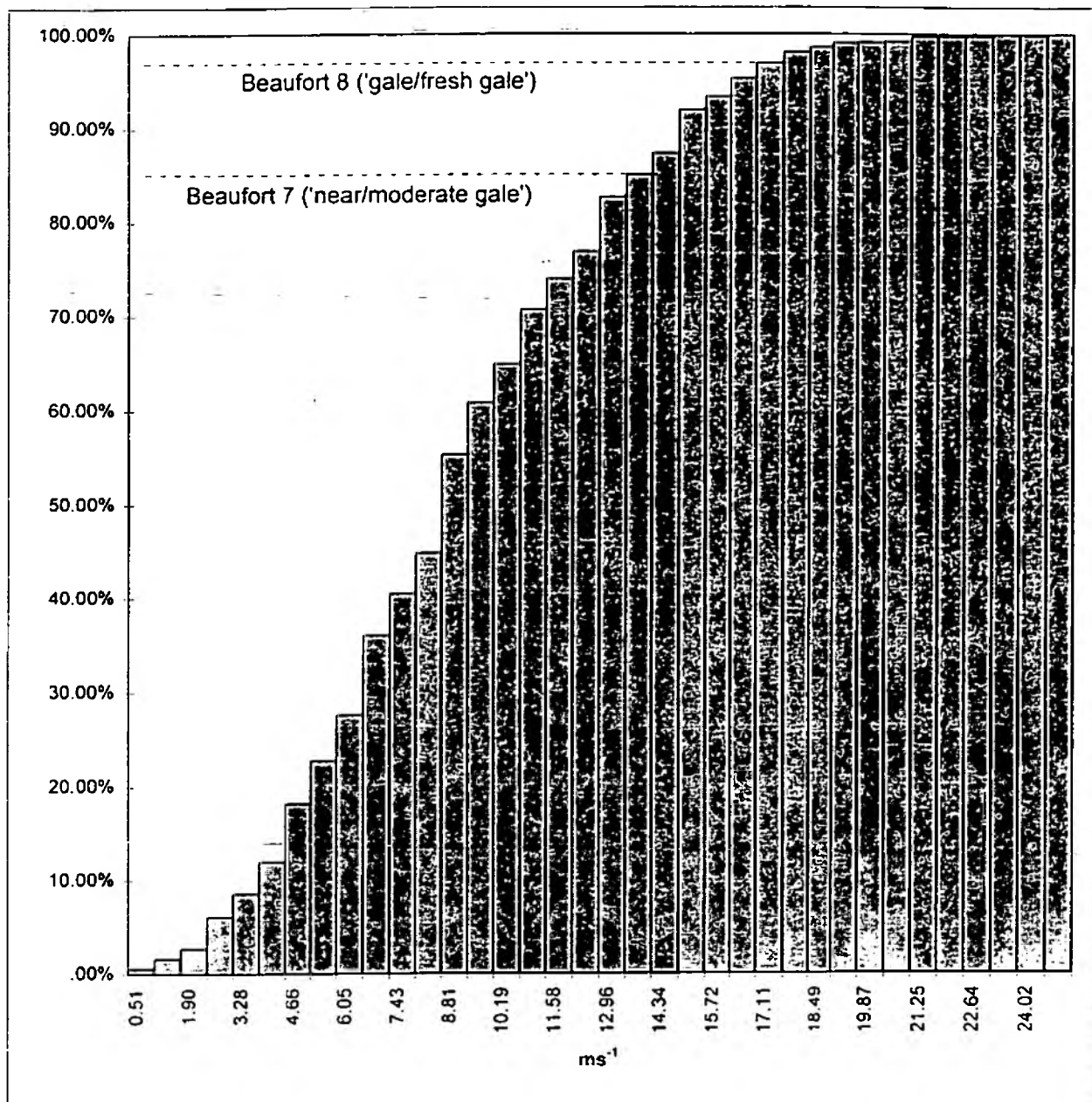
### 2.1.2 Offshore wind and wave climate

The highest individual offshore wind velocity observed over the whole period ~~(1991 to 1995 with the exception of the summer months of 1992 and 1993)~~ was  $29.3 \text{ ms}^{-1}$  (Beaufort force 11, 'violent storm' (Gardiner and Dackombe, 1983)) (direction:  $279^\circ$  from N) and occurred on the 9th of December 1993. Over the whole offshore record wind speeds averaged  $8.34 \text{ ms}^{-1}$ , with a mean direction of  $230^\circ$  (this and all following directional means were calculated using Davis' (1986) method (Appendix 2)).

Over the field work period from September 1994 to May 1995, only approximately 15% (194) values) of 3-hourly wind velocities exceeded near to moderate gale force (Beaufort force 7,  $14 \text{ ms}^{-1}$  (Gardiner and Dackombe, 1983)) (Figure 2.1). Of these 194 values, only 34 (i.e. 2.6% of all values during the season) coincided with onshore wind directions (between  $270^\circ$  and  $90^\circ$  from N) and all but one of these 34 high velocity onshore wind conditions occurred on a total of 8 days in January 1995.

During the field season, the average wind velocities of  $8.84 \text{ ms}^{-1}$  only slightly exceeded the mean over the whole record period ( $8.34 \text{ ms}^{-1}$ ). The maximum recorded offshore velocity of  $24.7 \text{ ms}^{-1}$  (Beaufort force 10, 'storm or whole gale' (Gardiner and Dackombe, 1983)) occurred on the 19th of January 1995. On the 1st of January, when exceptionally high tidal elevations were recorded by the gauges on the Norfolk coast, offshore winds ranged from  $16$  to  $17 \text{ ms}^{-1}$  from a northwesterly direction. Monthly means and standard deviations of offshore wind velocity ( $U_0$ ) are shown in Figure 2.2. These monthly means show a similar seasonal cycle as those of average offshore wave heights with relatively low values of wind speed (monthly means of around  $6 \text{ ms}^{-1}$ ) in the summer months (May to August/September) and relatively high values (monthly mean wind speeds between  $8$  and  $11 \text{ ms}^{-1}$ ) in the winter months (October to April). Highest monthly means (around  $13 \text{ ms}^{-1}$ ) were observed during December 1993 and January 1994. Both winter periods of 1992/93 and 1993/94 are characterised by an early peak of  $U_0$  in November and a later peak in March (1992) or January (1993). In the following winter, the first peak (December 1993) was followed by a second peak in March (1994). In the winter of 1994/95, however, only one maximum monthly mean occurred (January 1995).

The average predicted three-hourly wave height and period for grid point  $53.25^\circ \text{N}/1.53^\circ \text{E}$  for the period April 1991 to September 1995 was  $1.43 \text{ m}$  and  $4.68 \text{ s}$ . Swell waves, with an average height of  $0.43 \text{ m}$  over the whole period contributed relatively little to overall predicted wave heights. The maximum swell wave height of  $2.9 \text{ m}$  was calculated on the 20th December 1991 when wind generated waves were calculated to have been  $2.4 \text{ m}$  high. The largest calculated wind wave height of  $4.7 \text{ m}$  for the whole period April 1991 to September 1995 occurred on the



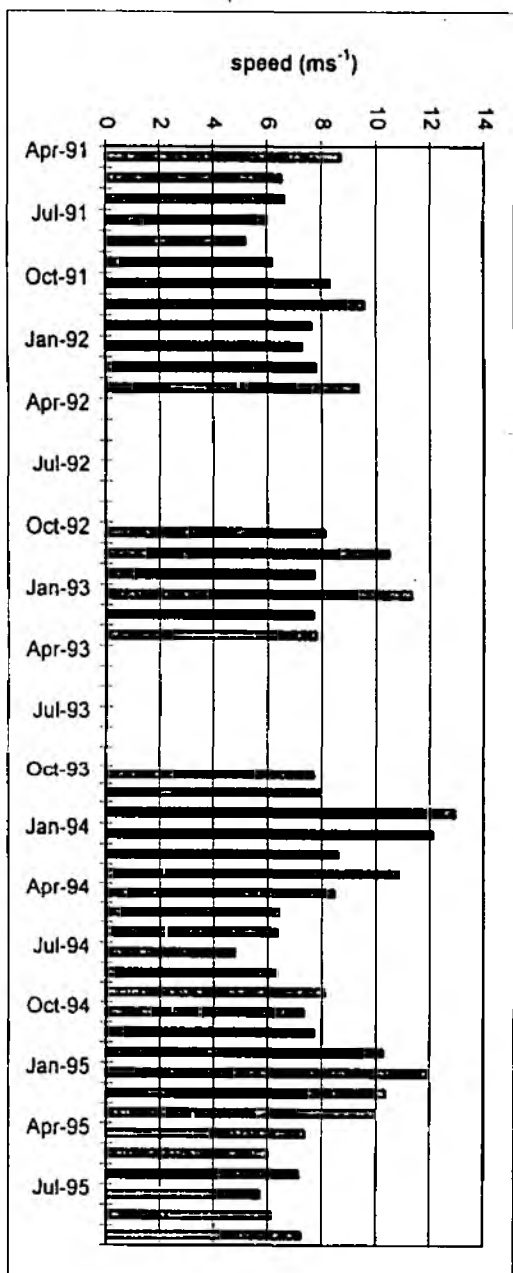
Fig

2.1: Cumulative (%) frequency of 3-hourly offshore wind velocities during field season, 20.9.94 to 29.5.95

notation ~

01/569/3/A

2.2: Monthly mean offshore wind speeds (1991-1995)



does not read well, if correct.

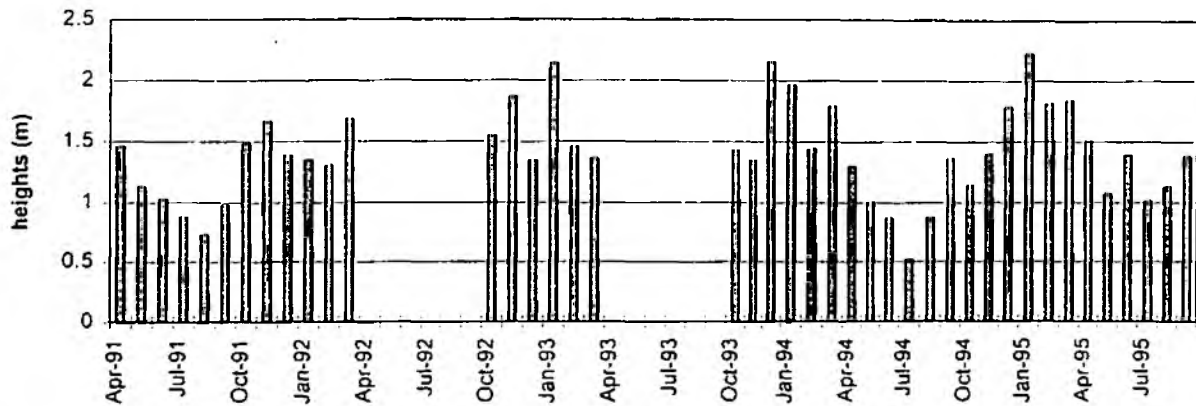
9th December 1993 when swell was negligible and total wave height (4.8m) was the largest within the record. Figure 2.3(a to c) shows the variation of monthly means of offshore wave height ( $H_0$ ), wind-sea height ( $H_{w0}$ ), and swell height ( $H_{sw0}$ ). A seasonal cycle with relatively low wave heights (monthly means of <1m) in the months of May to August/September and relatively high wave heights (monthly mean wave heights between 1 and 2m) from October to April is apparent.

### 2.1.3 Coastal wave conditions

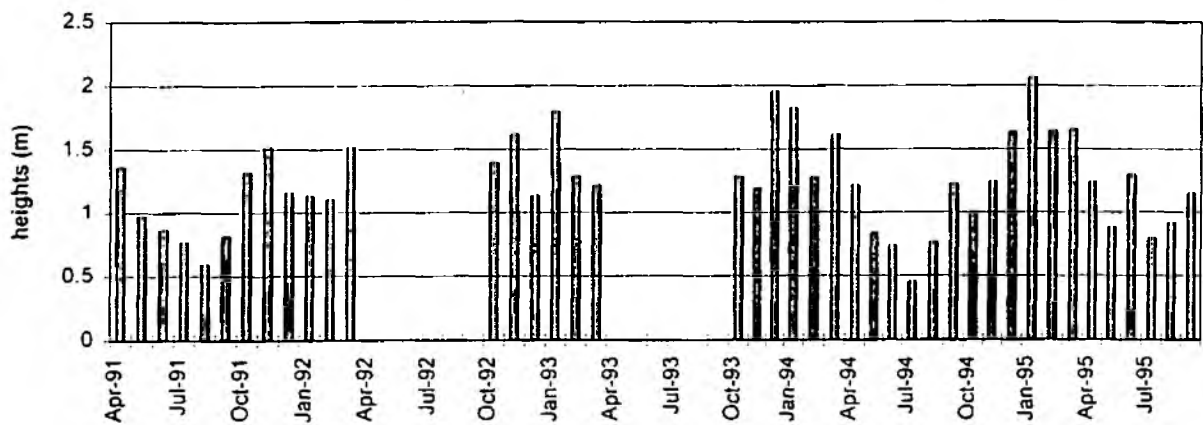
An example of a coastal record of significant wave heights ( $H_s$ ) is shown in Figure 2.4. This illustrates the strong influence of tidal fluctuations on waves as well as the low frequency of extreme wave conditions. Wave conditions measured at the three Environment Agency coastal stations largely depend on water depth above the pressure gauges. As tide gauge elevations differ between stations, the simultaneously recorded wave records at the three coastal stations are not directly comparable. At water elevations just over 0m OD, for example, no waves will be present over the Thornham gauge due to the low water depths, whereas at Brancaster and Blakeney, water depths still exceed 1.5m and waves may still be observed. To allow a better comparison between the data sets, only those wave records for which water depths exceed 1m at Thornham were considered for statistical analysis. These data sets are summarised in Table 2.1 and Figure 2.5. Significant wave heights were less than 1.4m at all three stations throughout this period. Frequency distributions of  $H_s$  are shown in Figure 2.5 which illustrates the high degree of negative skewedness of the datasets due to a very low number of observed  $H_s$  exceeding 0.3m. Average peak wave periods ( $T_p$ ) appear much larger than expected (Pearson (1986) suggests an average wave period of 6s for the Norfolk coast) and may be an artefact of the spectral analysis procedures used to derive these variables. Zero-upcrossing-periods ( $T_z$ ) seem to be a more realistic representation of actual dominant wave periods. At Thornham and Blakeney, maximum wave heights occurred on the 1st of January 1995 (see also Figure 2.4). The timing and height of these maxima, however, varied, with the largest significant wave height recorded at Blakeney at 18:00GMT and the smallest recorded at Thornham at 6:00GMT. At Blakeney, a wave height of 1.74m was recorded on the same date at 00:00GMT, although water elevations during this record were low (-1.79m OD) so that the gauge at Thornham was not inundated. Other occasions with exceptionally large  $H_s$  at Blakeney include the 7th, 10th, 26th and 30th of January.

not square on page

a) Monthly mean wave heights (m)



b) Monthly mean wind wave heights (m)



c) Monthly mean swell heights (m)

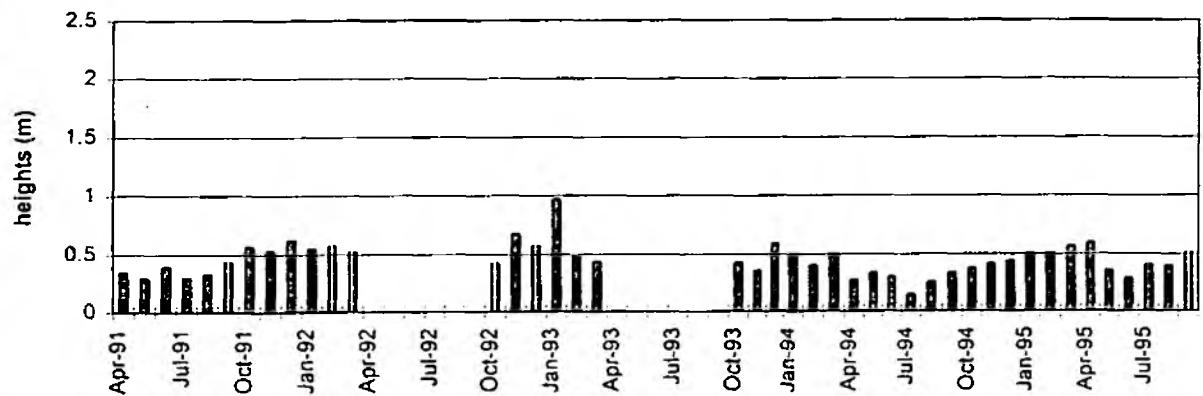


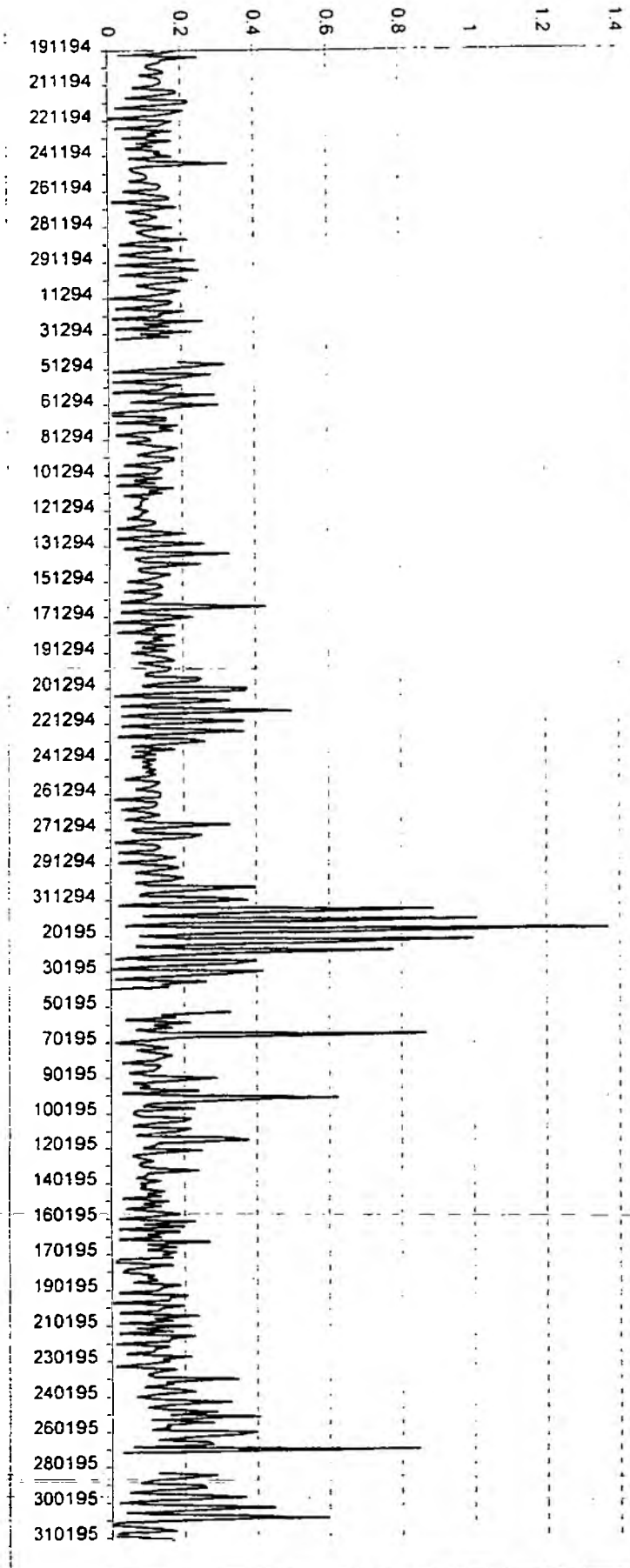
Fig. 2.3: Monthly means of offshore wave H, wind sea H, and swell H. 1991-95



X

Fig.

2.4: Three-hourly significant wave heights at Blakeney, 19.11.94 to 3.3.95.



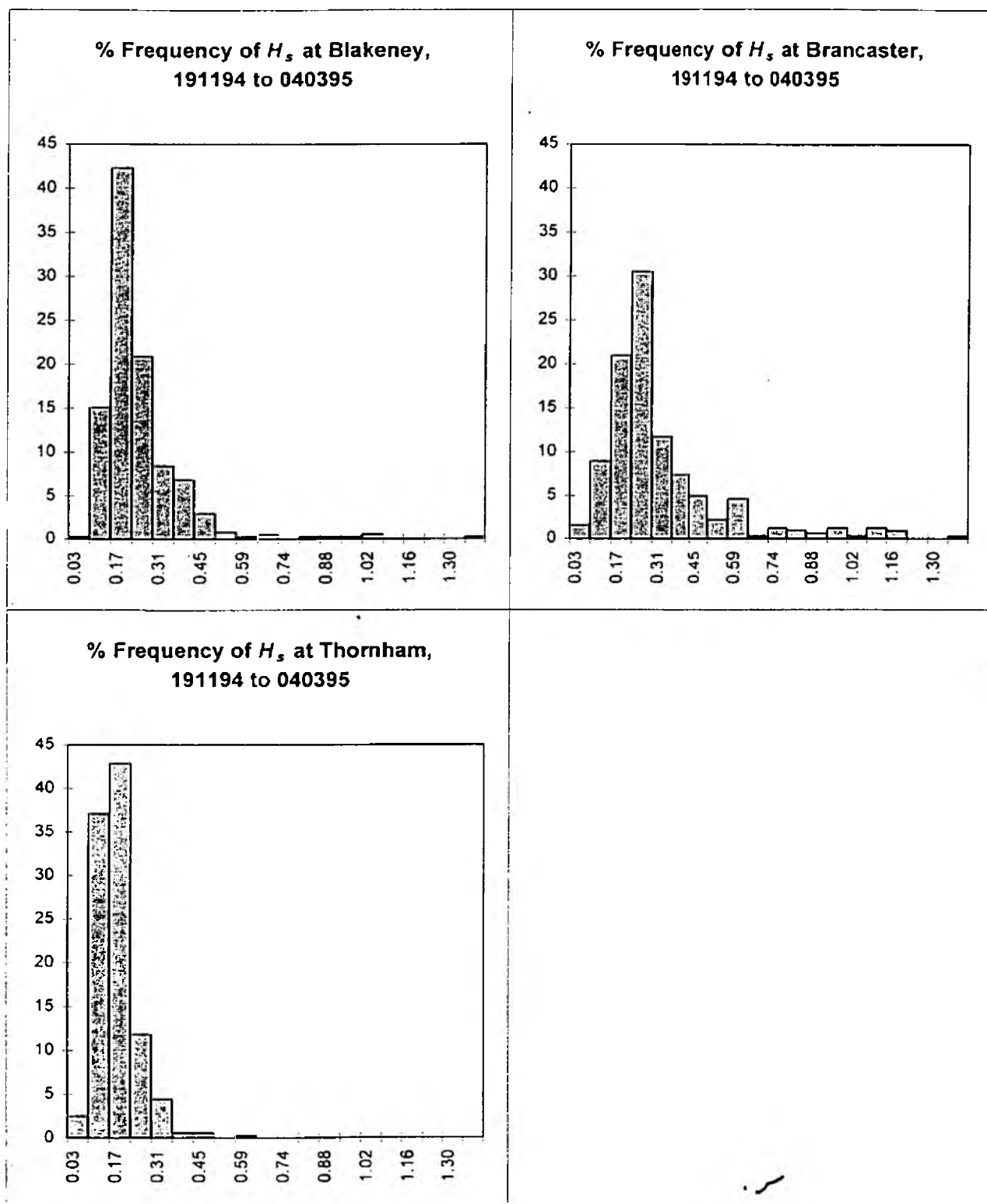


Fig.

2.5:

Frequency distribution of coastal  $H_s$  at three coastal stations, Norfolk, for water depths exceeding 1m at Thornham (data from 19.11.94 to 4.3.95).

Table 2.1: *explain table.*  $H_s$  at four coastal stations (Nov 94 - Feb 95) (for water depths > 1m at Thornham)

	Median $H_s$	Max $H_s$	Date of max $H_s$	Mean $T_p$	Mean $T_z$	Min $T_z$
Thornham	0.12	0.58	010195, 6am	28.75s	28.35s	5.4s
Brancaster	0.21	1.35*	260195, 3pm*	11.02s	7.80s	5.1s
Blakeney	0.16	1.37	010195, 6pm	23.05s	8.70s	5.0s

\* note: a higher  $H_s$  (1.74m) was recorded on the 010195 at 0am (see text)

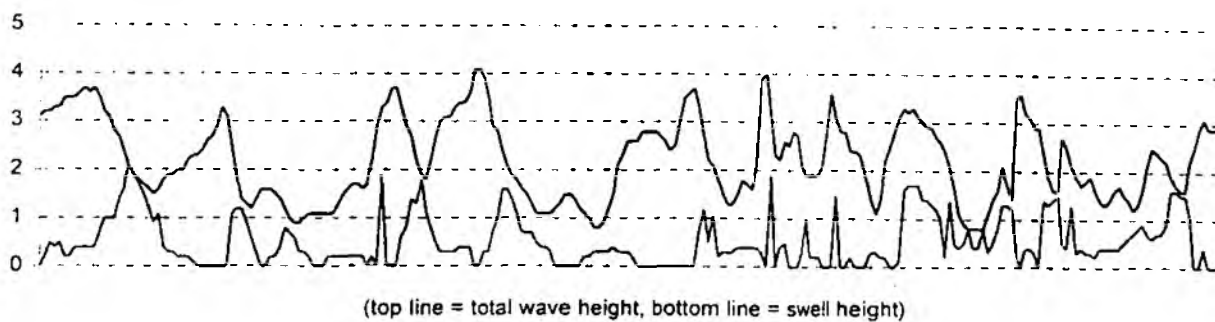
Waves at the coastal stations result from the interaction of swell waves generated offshore and transformed through refraction, diffraction, and shoaling processes, and locally generated wind waves. A positive relationship between offshore waves and coastal waves can therefore be expected. The strength of this relationship, however, depends on the distance of the location of offshore measurements from the coast, water depth above the coastal gauges, the relative influence of locally generated waves, and the prevailing meteorological conditions. Correlation coefficients ( $r$  values) for the relationships between offshore wave heights (swell, wind, and combined heights) and significant wave heights measured at the coastal stations were smaller than 0.3 in all cases (Table 2.2, Appendix 3). The large number of data values, however, meant that  $r$  values were still significant in the case of offshore total wave, wind wave, and swell height correlation with Brancaster  $H_s$ , and in the case of offshore total wave and wind wave height correlation with Blakeney  $H_s$ . Thornham waves, recorded at the station furthest away from the offshore model point, were not significantly correlated to either offshore total wave, wind wave, or swell heights.

Table 2.2: Regression analysis ( $r$  values) of offshore wave heights versus wave heights ( $H_s$ ) at coastal stations:

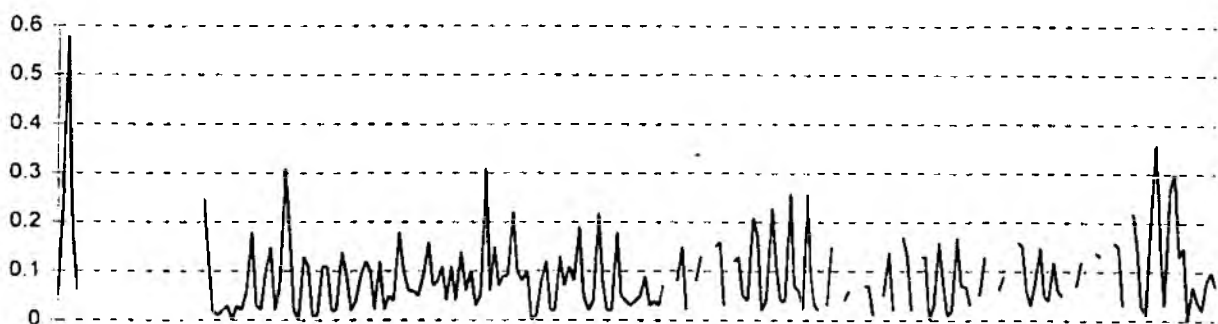
$H_s$ at	offshore total H	offshore swell H	offshore wind wave H
Thornham	0.02	0.00	0.03
Brancaster	0.20	0.12	0.15
Blakeney	0.14	0.04	0.11

Figure 2.6 shows the time series of 3-hourly offshore wave heights for January 1995 and the corresponding wave heights at the three coastal stations. The four data sets agree well with respect to some individual exceptionally large events, such as on the 1st, 6th, 10th, and 27th of January when large wave heights were observed at all stations. This figure also supports the suggestion that offshore swell contributes relatively little to onshore wave heights.

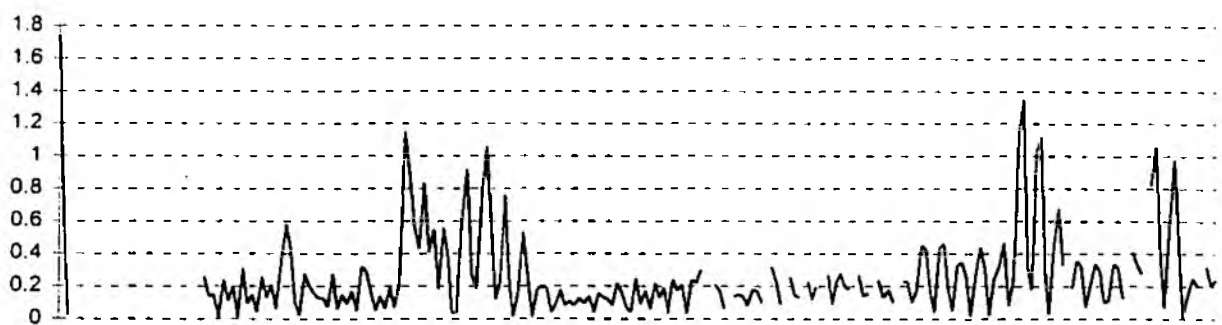
a) offshore



b) Thornham



c) Brancaster



d) Blakeney

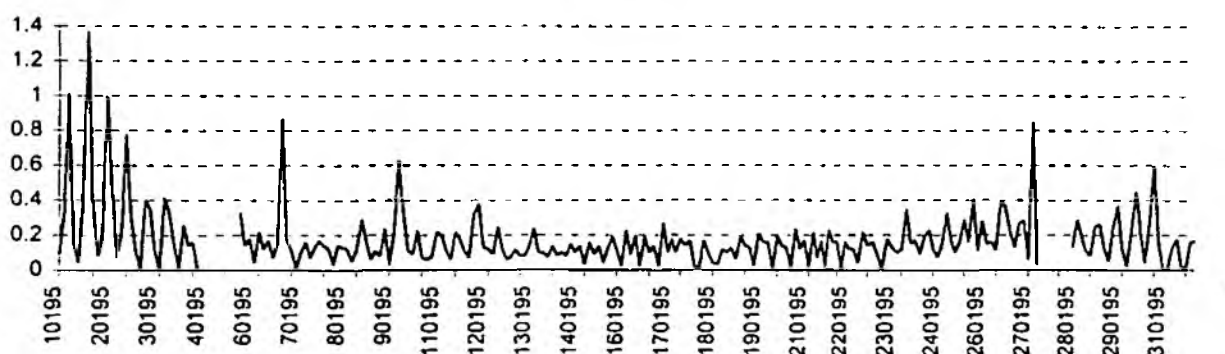


(Fig)

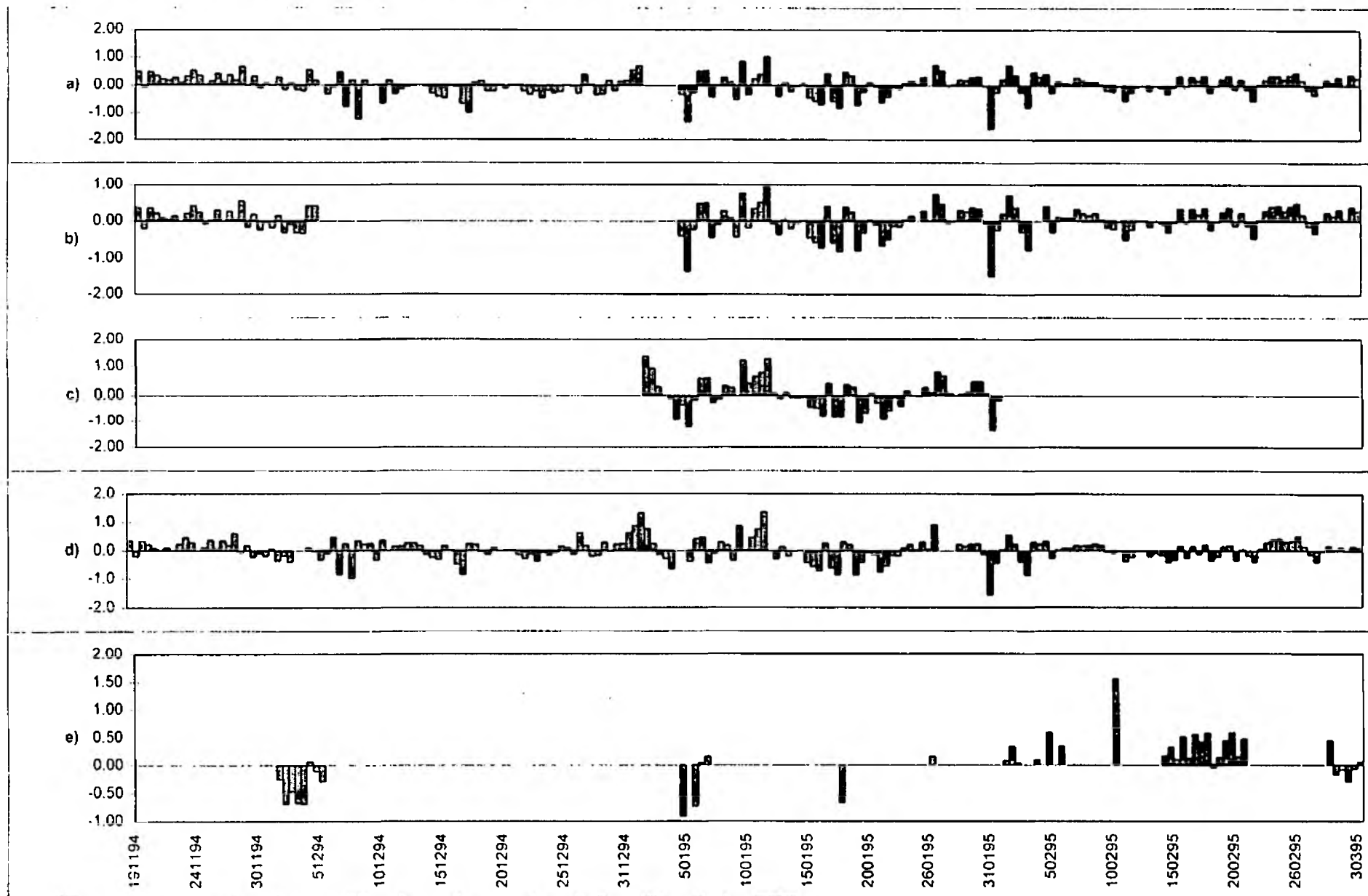
2.6: Three-hourly wave heights offshore (spectral peak height) and at coastal stations (Hs), January 1995 (note: different y-axis scales) (coastal records incomplete)

As mentioned above, the North Sea is particularly susceptible to meteorological influences on tidal elevations. The analysis of observed tidal HWs at five coastal stations compared to predicted HW (Figure 2.7) showed that positive and negative residual water level elevations between -1.0m and 1.0m are common on the north Norfolk coast. As well as influencing tidal residuals, wind speed and direction also determine the wave climate to be expected on the north Norfolk coast.

## 2.2 Environmental synthesis

From the analysis of local tide gauge records, meteorological data, offshore and coastal wave records emerges the picture of a highly dynamic tidal, meteorological, and wave regime which characterises the Norfolk coast in general and the Stiffkey marshes in particular. Data from field stations confirms the classification of this coast as a meso to macro tidal environment. Spring tidal ranges of approximately 5m at Brancaster observed in the winter months of 1994/95 agree well with the spring tidal range of between 5 and 6m mentioned by Pearson (1986). The neap tidal ranges of between 1 and 2m observed in the winter of 1994/95, however, were slightly lower than those cited in the literature (1.5 to 3m (Pearson, 1986) and 2 to 3m (Bayliss-Smith *et al.* (1979))). Attenuation of the tidal wave amplitude from west to east (7.4 m spring tidal range at Hunstanton (v) 4.4 m at Cromer (The Hydrographer of the Navy, 1996)) and the lag in HW times between western and eastern coastal stations corresponds to the movement of the tidal wave from west to east along the Norfolk coast around the offshore amphidromic point.

Large variations in tidal range and a shallow water depth in the southern North Sea combined with the frequent occurrence of cyclones tracking across the North Sea basin, gives rise to a large short term variability in actual water levels. The high frequency of both positive and negative non-tidal water level residuals observed in the north Norfolk water level records testifies to the dominant influence of meteorological conditions. The correlation between wind direction and water level residuals at Thornham, Brancaster, Stiffkey, and Blakeney shows that onshore winds significantly raise water levels above predicted tidal levels, whereas offshore winds lead to lowered water levels. During the winter of 1994/95, extreme water levels occurred on the 1st of January, when observed tidal levels at Wells and Blakeney (the only two gauges operational on this date) reached 4.25 and 3.77m OD. Assuming a mean difference in HW elevations between Wells and Brancaster of 0.6m and between Wells and Stiffkey of 0.8m, it is likely that elevations at Brancaster and Stiffkey on this date were approximately 4.85m OD (4.25m + 0.6m) and 5.05m OD (4.25m + 0.8m) respectively. After the surge of 1978, Steers *et al.* (1979) observed flood level elevations of 5.55m OD at Stiffkey. This suggests, that the surge of the 1st of January 1995 reached elevations at Stiffkey only slightly



Fig

2.7: Normalised non-tidal water elevation residuals for 5 Norfolk stations (November 1994 - March 1995)  
a) Thornham, b) Brancaster, c) Wells, d) Blakeney, e) Stiffkey.

lower than the surge of 1978. Over the whole period of tidal data (November 1994 to March 1995), however, the mean negative residuals at all stations (with the exception of Brancaster) reflect the dominance of offshore winds.

Evidence for an increased storm frequency over the North Sea in recent years has been presented by Schinke (1992) and an increased frequency in extremely high water levels has been suggested by Jenkins (in Steers *et al.*, 1979) who stated that tides exceeding 4.98m OD were observed in only 5 years between 1860 and 1948, but occurred in 6 years between 1949 and 1978. Steers *et al.* (1979) also state that between 1954 and 1978 only 5 tides exceeded 4.0m OD at Wells. During the winter of 1994/95, when the tide gauge at Wells was operational in January only, one tide (that of the 1st of January) exceeded this level by 0.25m. Other than the distinct seasonal variation in wind velocities, no clear trend could be observed in the record of monthly means of offshore wind velocities from 1991 to 1995. A more detailed analysis of longer meteorological and tide gauge records would be needed to establish, whether the occurrence of storms and water elevations of this magnitude is in fact increasing.

In Norfolk, the shallow offshore topography and the presence of offshore sandbars (e.g. at Stiffkey) and barrier islands (e.g. at Brancaster) results in a general wave climate characterised by relatively high frequency, low amplitude waves. Average wave heights observed at the three coastal locations of Thornham, Brancaster, and Blakeney between November 1994 and March 1995 lie below the average value of 0.46m suggested by Pearson (1986). The average peak wave periods of the Environment Agency records, at 11 to 29s, are larger than the typical 6s wave period suggested by Pearson (1986). The Agency records seem unrealistic given the limited water depth and fetch conditions at the coastal locations. It is likely, therefore, that these peak wave periods are an artefact of the signal processing procedures used. The average zero-upcrossing periods of approximately 8s are more realistic and only slightly exceed Pearson's (1986) estimate. Although wave heights are small throughout most of the year, storm surges and the associated high water levels and high onshore wind velocities may alter the wave climate significantly during individual tidal high waters. The occurrence of such high magnitude/low frequency wave events is well illustrated in the record of wave heights at Blakeney, where the average wave height between November and March was 0.16m, but wave heights increased to just under 1.4m on the exceptionally high tide of the 1st of January 1995. Such events, however, occur infrequently - only on 8 tides during a three month period did wave heights at Blakeney exceed 0.6m.

The data presented suggests that swell waves contribute little to overall wave heights offshore and onshore. Even in conditions of high water depths, such as on the 1st of January 1995, when swell waves would be expected to be present and to propagate into the shallower regions of the coast, the times of high waves at the coastal stations do not generally coincide with or

follow upon periods of high modelled offshore swell heights. It appears that, at these particular locations in Norfolk, the high magnitude/low frequency wave events are caused by large water depths in combination with onshore winds which allow the (local) development of wind waves with exceptional heights, rather than by the propagation of swell waves into coastal waters. As all three of the Environment Agency wave recording stations were located in relatively sheltered locations (within creeks or behind barrier islands/spits), however, it may be possible, that the more exposed location of the Stiffkey marshes allows the propagation of swell waves into shallow coastal waters at extreme tidal levels.

### **2.3 Conclusions**

Although no background information on waves at Stiffkey itself was available, the analysis of the wave and tide data of locations in the vicinity of Stiffkey suggests that:

- i) tide tables based on astronomical HW predictions (such as the Immingham tables) will be of little use for the prediction of actual tide levels at Stiffkey, and
- ii) actual tidal HW elevations are, to some extent, dependent on meteorological conditions (atmospheric pressure, wind speed and direction, in particular).
- iii) as a result, wave predictions, which depend on a knowledge of water depths, can only be made over the short term (several hours or days), and
- iv) under most circumstances, wave conditions at Stiffkey cannot be inferred from knowledge on offshore wave conditions, as coastal waves tend to be locally generated and influenced by local wind direction and velocity. Due to the relatively exposed location of the Stiffkey marshes, however, swell waves may well propagate across the Stiffkey sandflat and reach the salt marsh in conditions of extreme tidal levels (due to storm surges).



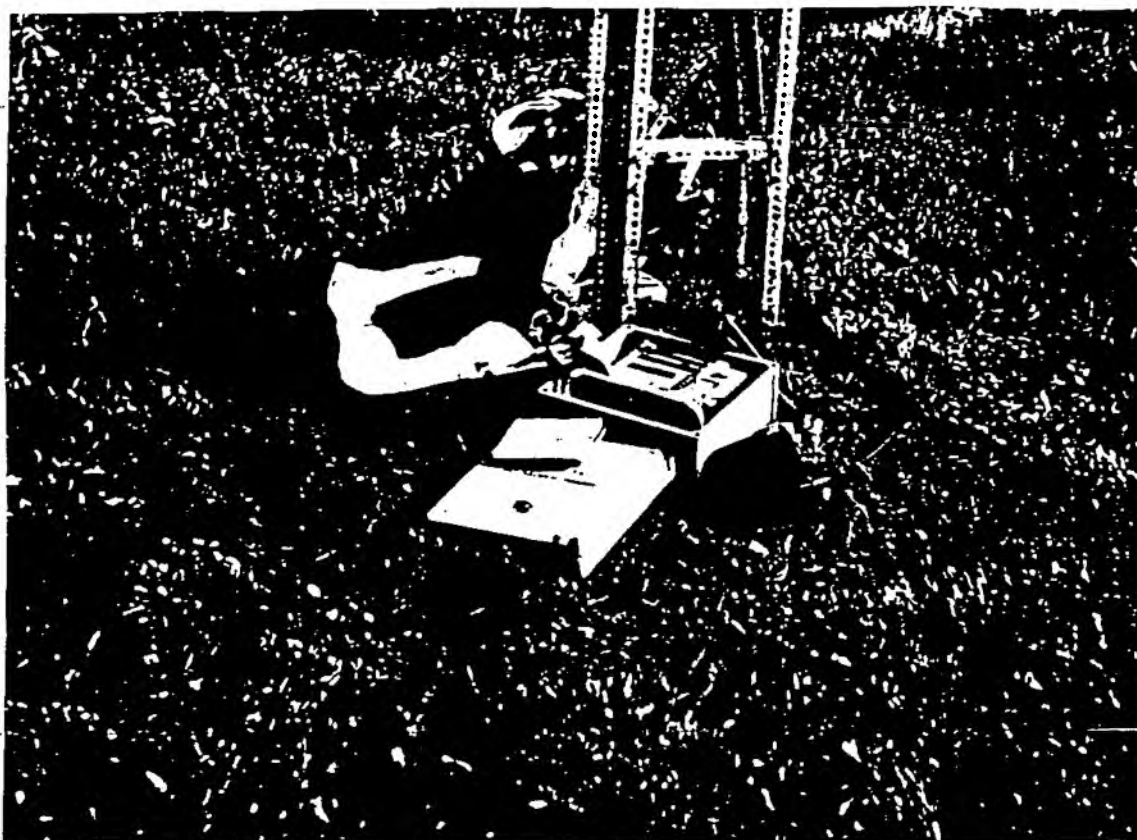


Fig. 3.1: Photograph of dataloggers in casing

### 3. DATA COLLECTION AND PROCESSING

#### 3.1 Field Experimental Design

Information on wave periods, wave heights and mean water level was obtained at three locations along a transect (orientated  $44.5^\circ$  from N) from the shingle ridge across the 'low' marsh and the unvegetated sandflat at Stiffkey (see Figures 1.1 and 1.2). The distance between the outermost (sandflat) and the middle (marsh edge) recording station was 197m and the innermost (marsh) recording station was located 180m inland from the middle (marsh edge) station. Each of the wave recording units consisted of a bottom-mounted 'Druck' pressure transducer (series PDCR380) wired into a ('Campbell Scientific 21X') data logger which was placed on top of a 4 to 5 meter high 'Dexion' tower to protect the electronic logging equipment from salt-water inundation and wave splash. The height of the sensors above the sand/marsh surface varied between 5 and 10cm. Dataloggers were housed in casings protected to IP64 standard against rain and sea water splash (see Figure 3.1). Towers were located 2 to 3m landward of the sensor so as to prevent interference of the structure with approaching waves. To allow for time-efficient downloading of data from the datalogger mounted on the top of the wave-recording station, special 2 to 3 meter long data transfer cables with waterproof connectors were manufactured which remained permanently attached to the datalogger and could easily be accessed without having to remove the datalogger from its mounting. Data was transferred to a standard 286 notebook PC using 'Campbell Scientific's' 'PC208' software and was subsequently imported into an MS Excell spreadsheet for a preliminary analysis and the splitting of the datafiles into files containing the individual 'bursts'. These ASCII files contained two columns: the time of measurement (hour and minute) and the voltage output of the pressure sensor. The time series were subsequently analysed using the 'trafo.m' program written in 'Matlab'. This program converts the voltage output to pressure, de-trends the time series to remove the low frequency tidal components, and applies a frequency-dependent correction to the raw pressure fluctuations to offset the attenuation with depth of the high frequency end of the wave spectrum. It uses the same spectral FFT method to derive the wave parameters ( $H_{rms}$ ,  $T_w$ ,  $E$ , and  $E_{int}$ ) as the 'wave.m' function which was used to process the laboratory wave tank time series described above. In addition, significant wave heights,  $H_s$ , are derived from information on the wave spectrum (see Appendix 4).

### 3.2 Field calibration

Although linear wave theory is strictly applicable only in deep water, the results from the laboratory wave tank experiments have shown that equations used for the calculation of wave height, period and energy parameters from wave spectra ( $H_{rms}$ ,  $T_w$ ,  $E$ , and  $E_{tot}$ ) are a reasonable approximation for shallow water conditions (see also CERC 1984). Some of the inaccuracies of the wave parameters calculated from the laboratory pressure time-series were due to low record length to wave length ratios (record lengths in the laboratory were limited to approximately 44s). Longer records and therefore reduced wavelength to record length ratios are likely to reduce errors in the calculation of wave parameters from wave spectra. However, there are also practical difficulties associated with the recovery of surface wave information from corrected subsurface pressure measurements, with linear transfer functions of the type employed here tending to slightly underestimate the energy in the lower frequency range, whilst overestimating the higher frequency contributions (see above and, for example, Lee and Wang 1984). To establish whether surface waves computed from near-bed pressure records corresponded to actual water surface fluctuations, a video camera was used on a selected tide to record water level fluctuations visually at a frequency of 25 frames per second against a calibrated staff. The video camera was mounted on and operated from a 'Dexion' platform situated approximately 2 to 3m away from the calibrated wave staff. Accurate simultaneous timing of the video record and the datalogger mounted on the wave recording tower was achieved by filming the logger display showing the internal logger time before and after the experiment. The actual free surface record was obtained by visual analysis of the water level record on the individual computer frames at the video editing suite of the Audio Visual Aids Unit, University of Cambridge. This directly observed free surface record was then compared with that computed from simultaneous near-bed pressure measurements derived from the data logger output. Figure 3.2 shows a portion of the observed and calculated free-surface record for 22 September 1994 at the middle station. Statistical analysis of the two time series resulted in a correlation coefficient,  $r$ , of 0.85 (statistically significant the 95% confidence level ( $p = 0.05$ )). This significant correlation between actual and re-constructed water level fluctuations means that if wave length to record length ratios are low (ie. lower than 0.33 (see above)) and wave frequencies are smaller than the Nyquist frequency (ie. smaller than half the sampling frequency) computed spectral wave parameters will be an accurate estimate of actual spectral wave parameters.

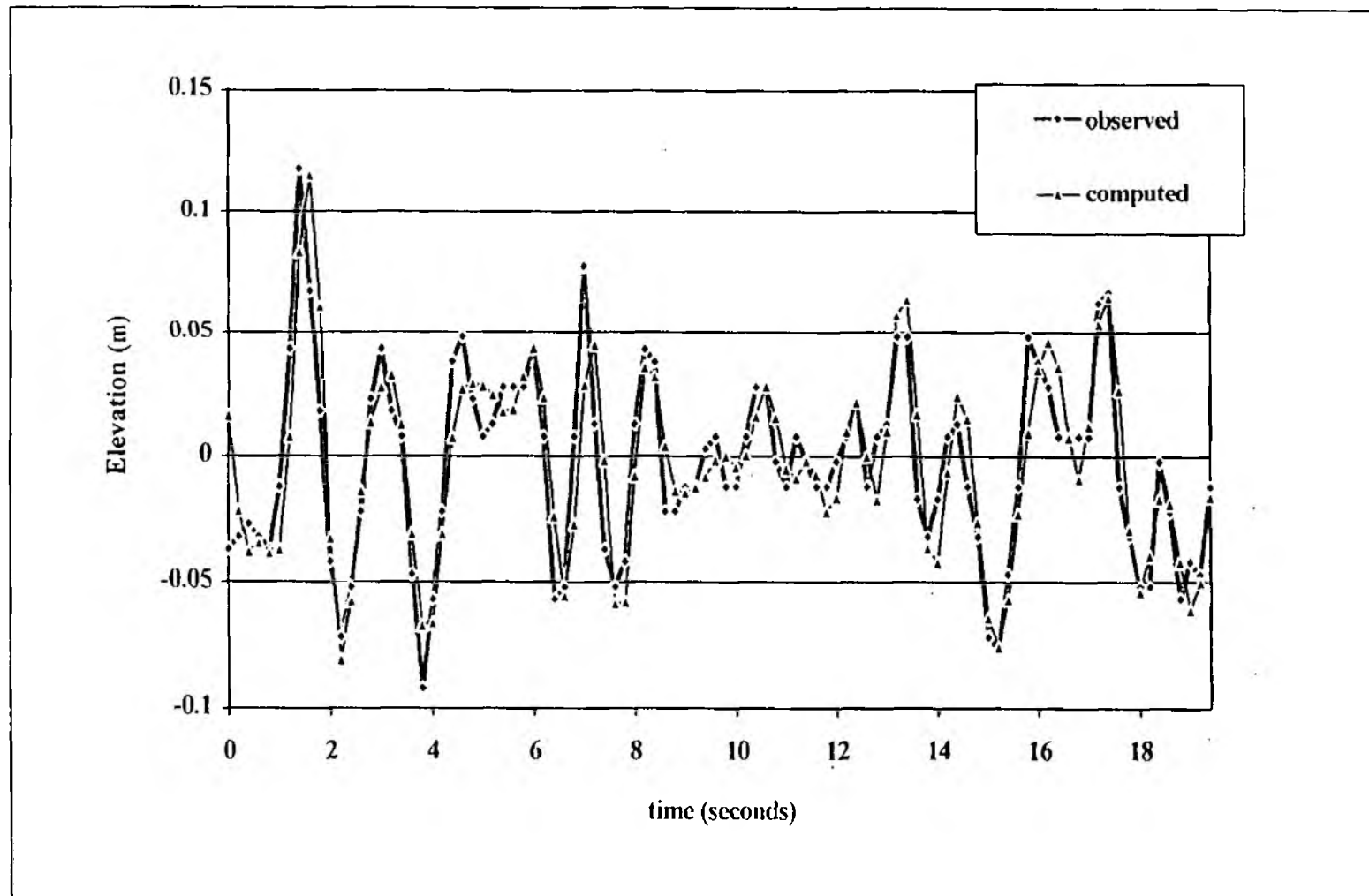


Fig. 3.2: Observed and videoed time series of water surface at the middle station, 22 Sept 1994

### 3.3 Timing and duration of wave measurements

Wave recording was carried out over a range of spring tides during the winter season, between September 1994 and May 1995. The time required to take an individual pressure reading and the limited internal logger memory capacity of the '21X' dataloggers (40,960 bytes random access memory (RAM) with 12,296 locations available for final storage) limited the sampling frequency to 5Hz and the overall duration of wave recording (before downloading of the data was necessary) to 19 minutes. Three values (the logger identifier, time (hour and minute), and water pressure) were stored every 0.2 seconds.

Maximum wave activity at coastal locations occurs close to or during the high water stage of the tidal cycle (as is illustrated by the wave records for the Environment Agency stations (see Figure 6). As the tidal records of Norfolk stations show, however, the prediction of the timing and heights of tidal HW is only possible over a time span of several hours, which was too short to allow for the setting up of the data loggers in the field. To increase the chance of recording waves at a time close to the time of tidal HW (while still allowing enough time for the installation of the equipment) and to obtain information on wave conditions at slightly different stages of the tidal cycle, the 19 minutes available were divided into two 7-minute (ie. 2100 values) and one 5-minute (ie. 1500 values) record. These three time-series were collected either (a) at the time of predicted high water on three consecutive tides or, more usually (b) on individual tides 20 to 30 minutes before predicted high water, at predicted high water, and 20 to 30 minutes after predicted high water.

Downloading took place either after every sampled tide (if the time-series were collected as described in (b) above), or after three consecutive tides (if data collection took place as described in (a)). As only the higher spring tides flood the Stiffkey marshes sufficiently to allow for wave action across the marsh surface, fieldwork coincided with periods of high spring tides. In addition, storm surge forecasts for the Norfolk coast (from the Proudman Oceanographic Laboratory's surge model, supplied through the Environment Agency) were used in the short term to determine the timing of wave-record collection. Out of all wave 'bursts' recorded between September 1994 and May 1995, 54 were complete wave records for all three stations (i.e. tides which actually inundated the marsh surface). Dates and times of the 54 complete sets of wave records at the Stiffkey transect are listed in Table 1.

## **4. RESULTS: WAVE ATTENUATION OVER THE STIFFKEY SANDFLAT/SALT MARSH**

### **4.1 Introduction**

The analysis of the 54 complete transect wave records collected between September 1994 and May 1995 was carried out in two stages. Initially, all records were spectrally analysed using the 'trafo.m' function. The resulting wave parameters of all records were used to obtain information about the distribution and variability of wave heights, periods, and energy dissipation across the sandflat and salt marsh throughout the winter. This allowed individual parameters to be compared to those obtained at the three Environment Agency-maintained wave stations. A subsequent, more detailed, analysis addressed the relationship between wave attenuation at Stiffkey and tidal and meteorological conditions.

### **4.2 General wave conditions at Stiffkey during the field monitoring period**

Table 4 lists the mean, median, and range of wave heights, spectral energy and periods measured during the field monitoring period at Stiffkey (the complete table of wave parameters as calculated for each station and all individual 54 recording times is included in Appendix 4). Frequency distributions for wave heights, periods, and spectral energy observed at the outer (sandflat) station are illustrated in Figure 4.1.

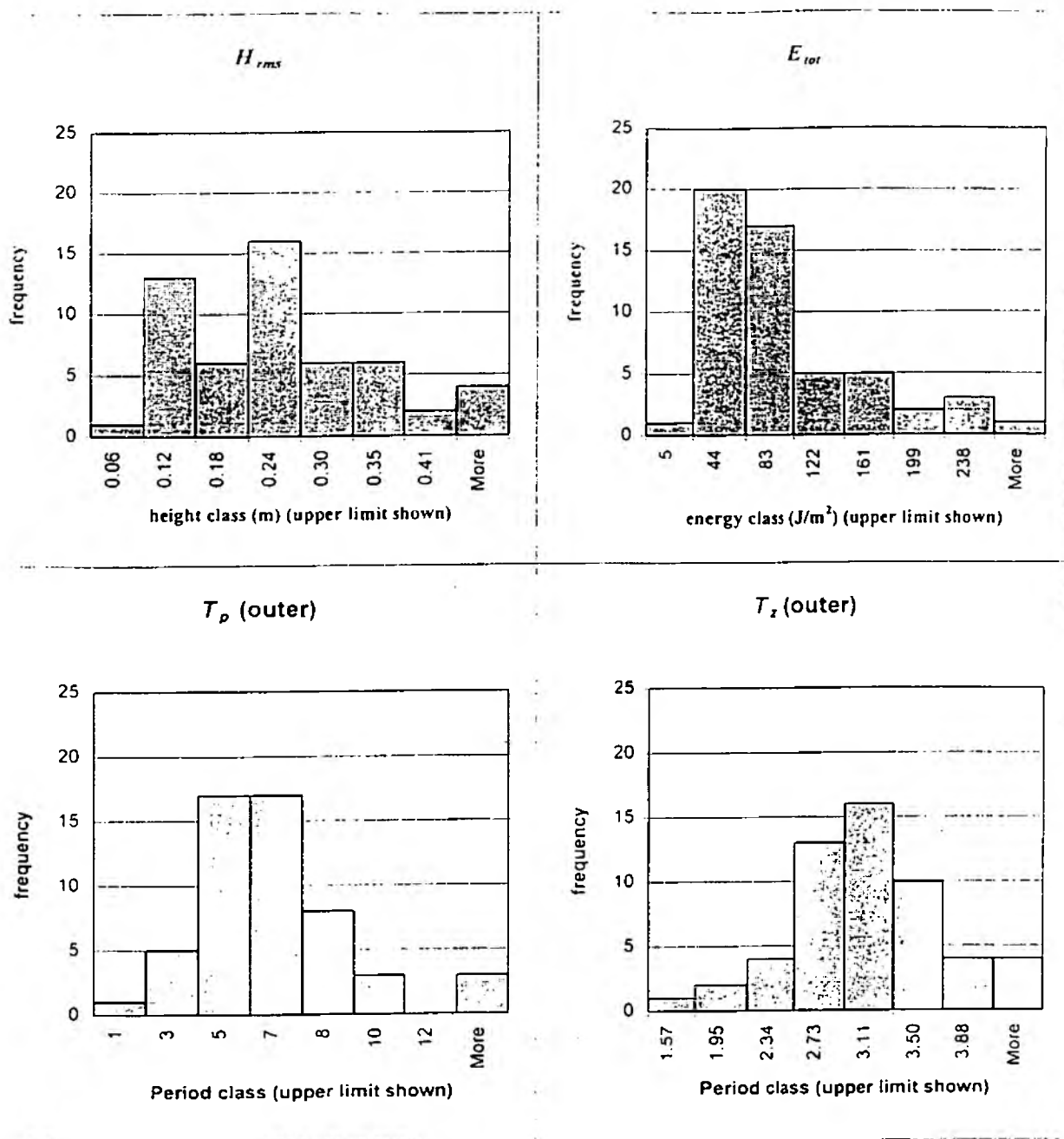


Fig. 4.1: Frequency distributions of  $H_{rms}$ ,  $E_{tot}$ ,  $T_p$ , and  $T_z$  at the outer station. Stiffkey (54 records, 21.9.94 to 17.5.95)

Table 4.1: Summary statistics of main wave parameters calculated from all 54 'burst' records, September 1994 - March 1995.

	$H_{rms}$ (m)	$H_s$ (m)	$E_{tot}$ ( $Jm^{-2}$ )	$T_z$ (seconds)	$T_p$ (seconds)	$L_{outer}$ (m)*
maximum	0.47	0.67	277.09	4.27	13.65	51.88
date of max	20/3am	20/3am	20/3am	4/11pm 5/11am	8/10am	17/3pm
minimum	0.06	0.09	5.16	1.57	1.34	2.78
mean	0.21	0.30	70.72	2.92	5.67	20.40
st. deviat.	0.11	0.15	66.82	0.60	2.70	10.56
median	0.20	0.29	51.38	3.00	5.54	20.20

\* note: wave lengths calculated from wave period,  $T_p$ , and water depth,  $h$ .

#### 4.2.1 Incident wave heights and energy

The frequency distribution of wave heights appears to be bi-modal, with the most frequent wave heights around 0.13m or 0.30m. Median significant wave heights (0.29m) at the outer (sandflat) station were high compared to those measured at Blakeney (0.16m), Brancaster (0.21m), and Thornham (0.12m) between November 94 and March 95. The maximum significant wave height measured at Stiffkey on the 20th March 1995 (0.67m), however, is only half the maximum value observed at Blakeney on the 1st of January 1995 (1.37m). As wave energy is directly proportional to the square of the wave height, the difference between the maximum total spectral energy observed at Stiffkey ( $277Jm^{-2}$ ) and the mean ( $51Jm^{-2}$ ) is much larger than in the case of wave heights and the distribution of wave energy is negatively skewed (Figure 4.1). Comparative wave heights at the Environment Agency-maintained coastal stations were only available for the time period between 19th November and 4th of March and as records were only obtained 3-hourly at the Environment Agency stations, the time difference between these and the Stiffkey records can be up to 1.5 hours. This time difference may explain some of the variability in the differences between  $H_s$  at Blakeney and Stiffkey and at Brancaster and Stiffkey shown in Figure 4.2 (note that the records at Blakeney and Brancaster were incomplete so that Blakeney and Brancaster wave heights are available for only 18 and 12 of the 54 Stiffkey records respectively). Wave heights at Brancaster were highly correlated with but generally higher than those at Stiffkey ( $r^2 = 0.93$ ). A similar pattern can be observed with respect to waves at Blakeney and Stiffkey, although wave heights at Stiffkey did exceed those at Blakeney on 4 occasions resulting in a very low correlation coefficient ( $r^2 = 0.07$ ).



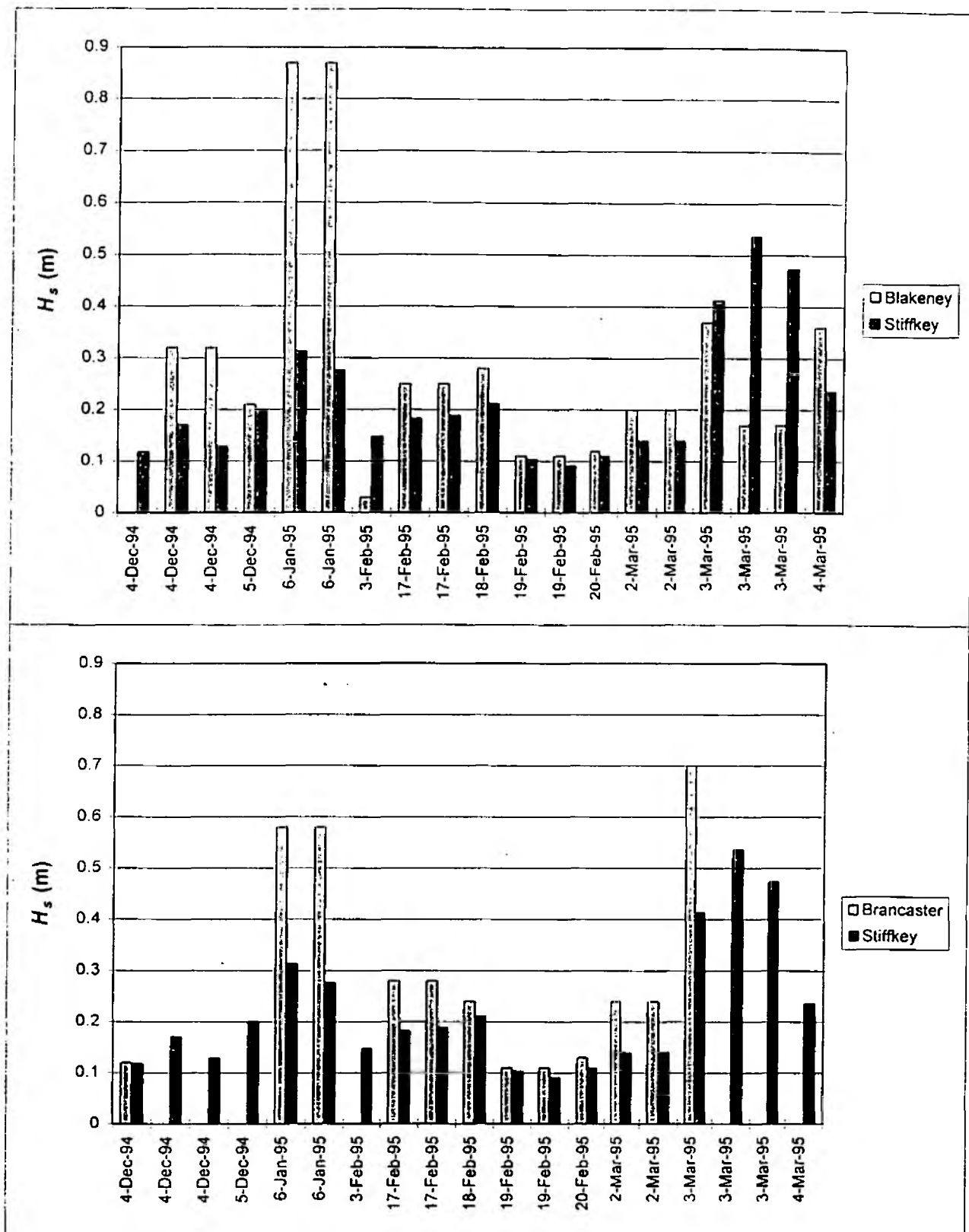


Fig. 4.2: Significant wave heights at (a) Stiffkey and Blakeney, and (b) Stiffkey and Brancaster (3-hourly value closest to Stiffkey recording value) (note: for some Stiffkey records, no matching data was available for Brancaster).

#### 4.2.2 Wave periods

At the sandflat station, average dominant spectral wave periods,  $T_p$ , (mean = 5.7s, standard deviation = 2.70s) were almost twice as high and almost four times as variable as average zero-upcrossing-periods,  $T_z$ , (mean = 2.9s, standard deviation = 0.60s); both period parameters appear to be normally distributed (Figure 4.1).

#### 4.2.3 Influence of tidal, wind and offshore wave conditions

Wave heights at Stiffkey are expected to be determined by tidal conditions (water depths), wind and offshore wave conditions. The analysis of wave records from Thornham, Brancaster, and Blakeney (see above) confirmed the important influence of water depth and wind conditions, but suggests that offshore wave conditions only have a very limited effect on coastal waves. Bivariate linear regression analysis was used in the first instance to obtain information on possible links between tidal and meteorological variables and wave characteristics at Stiffkey.

Table 4.2: Water depth ( $h$ ), offshore wind speeds ( $U_o$ ), and offshore wave (total, wind, and swell wave) conditions during wave recording at Stiffkey

	HW (m OD)	$h$ (m)	$U_o$ ( $\text{ms}^{-1}$ )	$H_{tot}$ (m)	$H_{wind}$ (m)	$H_{swell}$ (m)
min	2.71	0.91	4.12	0.40	0.00	0.00
max	3.92	1.75	21.11	3.40	3.00	1.70
date of	20/3am	19/3pm	17/3pm	17/3pm	17/3pm	17/3pm
max		20/3am				
mean	3.32	1.35	9.51	1.66	1.55	0.46
median	3.29	1.38	9.52	1.70	1.60	0.30
st. dev.	0.28	0.20	3.43	0.69	0.69	0.42

High water elevations during wave recording ranged from 2.71 to 3.92m OD with water elevations above the sandflat surface at the outer station, derived from the time series analysis of underwater pressures, ranging from 0.91 to 1.75m. Maximum elevations occurred on the evening tide of the 19th and the morning tide of the 20th of March. The average HW height over all wave records (3.32m) lies above the mean of the 112 tidal maxima observed during the field season at Stiffkey.  $H_{rms}$  values measured at the outer station were not significantly correlated with water depth at the same location ( $r^2 = 0.04$ ).

During periods of wave recording at Stiffkey, winds were most frequently of a south to southwesterly direction (see Figure 4.3). Offshore wind velocities during any of the wave recording times were generally lower than  $15\text{ms}^{-1}$ . This value was only slightly exceeded on the 3rd and 17th of March (morning tides), when winds were from a west-southwest and west-northwest direction (Figure 4.3).

Wind velocities recorded offshore did not in themselves explain the variation in incident wave heights at the outer (sandflat) station ( $r^2 = 0.07$ ), but when those occasions of offshore winds were removed and only those with onshore winds were analysed, wind velocities appear to influence incident wave heights significantly (see Figure 4.4).

Table 4.3: Water depth ( $h$ ), offshore wind speeds ( $U_o$ ) and offshore wave (total, wind, and swell wave) conditions for wave records obtained in onshore wind conditions.

	HW (m OD)	$h$ (m)	$U_o$ ( $\text{ms}^{-1}$ )	$H_{tot}$ (m)	$H_{wind}$ (m)	$H_{swell}$ (m)
<b>min</b>	2.71	0.91	5.15	0.60	0.50	0.00
<b>max</b>	3.92	1.75	15.44	2.90	2.90	1.30
<b>date of</b>	20/3am	19/3pm	3/3am	20/3am	20/3am	21/3am
<b>max</b>		20/3am				
<b>mean</b>	3.24	1.31	9.37	1.75	1.63	0.51
<b>median</b>	3.23	1.29	9.27	1.80	1.70	0.60
<b>st. dev.</b>	0.32	0.24	2.56	0.62	0.65	0.36

Table 4.3 illustrates the wind velocity, water depth, and offshore wave conditions that were experienced during the 24 wave records obtained in conditions of onshore winds. Mean offshore wave heights for all Stiffkey wave recording times (1.66m) were high compared to the average wave height of 1.43m over the whole offshore record from April 1991 to September 1995. Offshore waves were highest during wave recording on the 17th of March, when offshore swell and wind waves reached a height of 1.7 and 3.0m respectively. Wave heights at the outer (sandflat) station at Stiffkey were only weakly (but, at the 95% confidence level, still significantly) correlated with offshore wave heights computed for times within three hours before the Stiffkey wave recording time ( $r^2 = 0.26$ ). Offshore swell waves did not seem to have any influence on Stiffkey wave heights ( $r^2 = 0.08$ ).

Water depth did not have a strong influence on incident wave periods ( $T_p$  and  $T_s$ ) ( $r = 0.17$  and  $0.41$  respectively, the former was not significant at the 95% confidence level). Similarly,

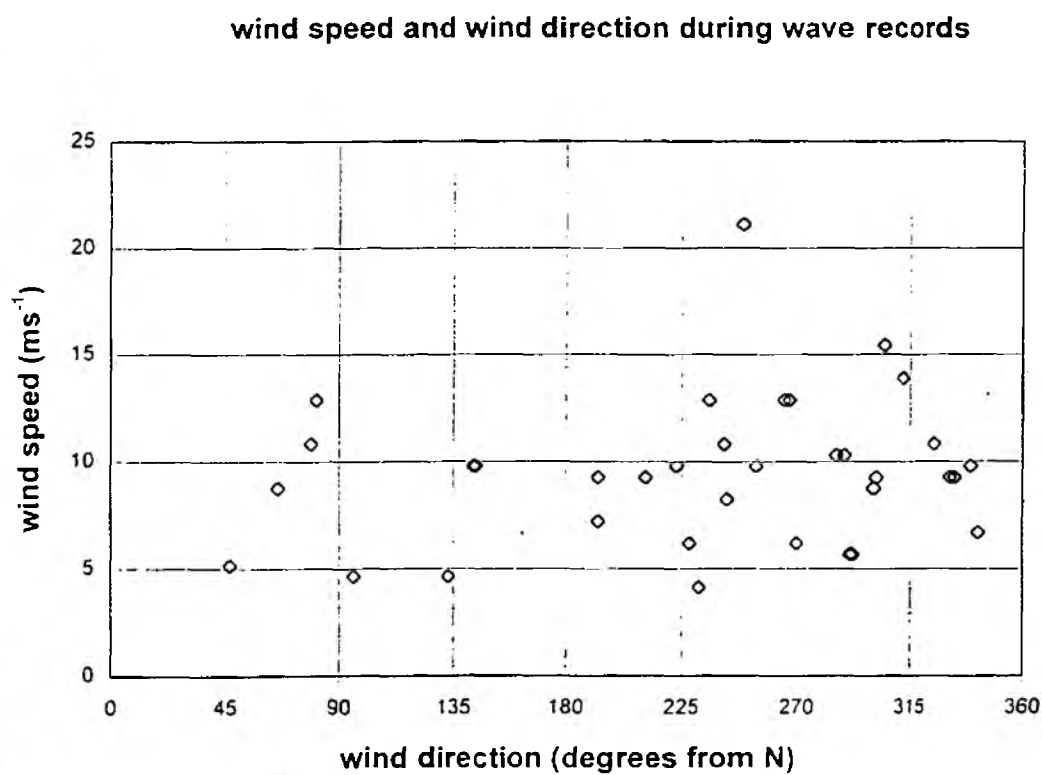
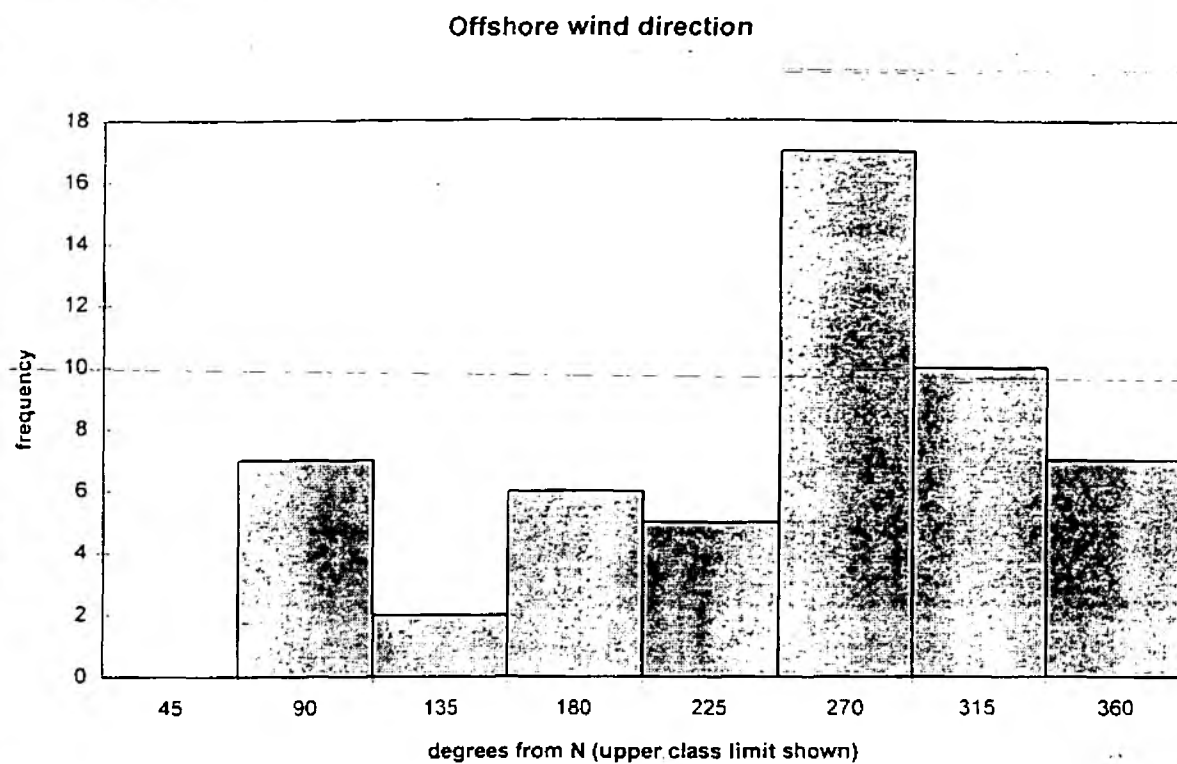


Fig. 4.3: Offshore wind speed and direction during 54 wave records

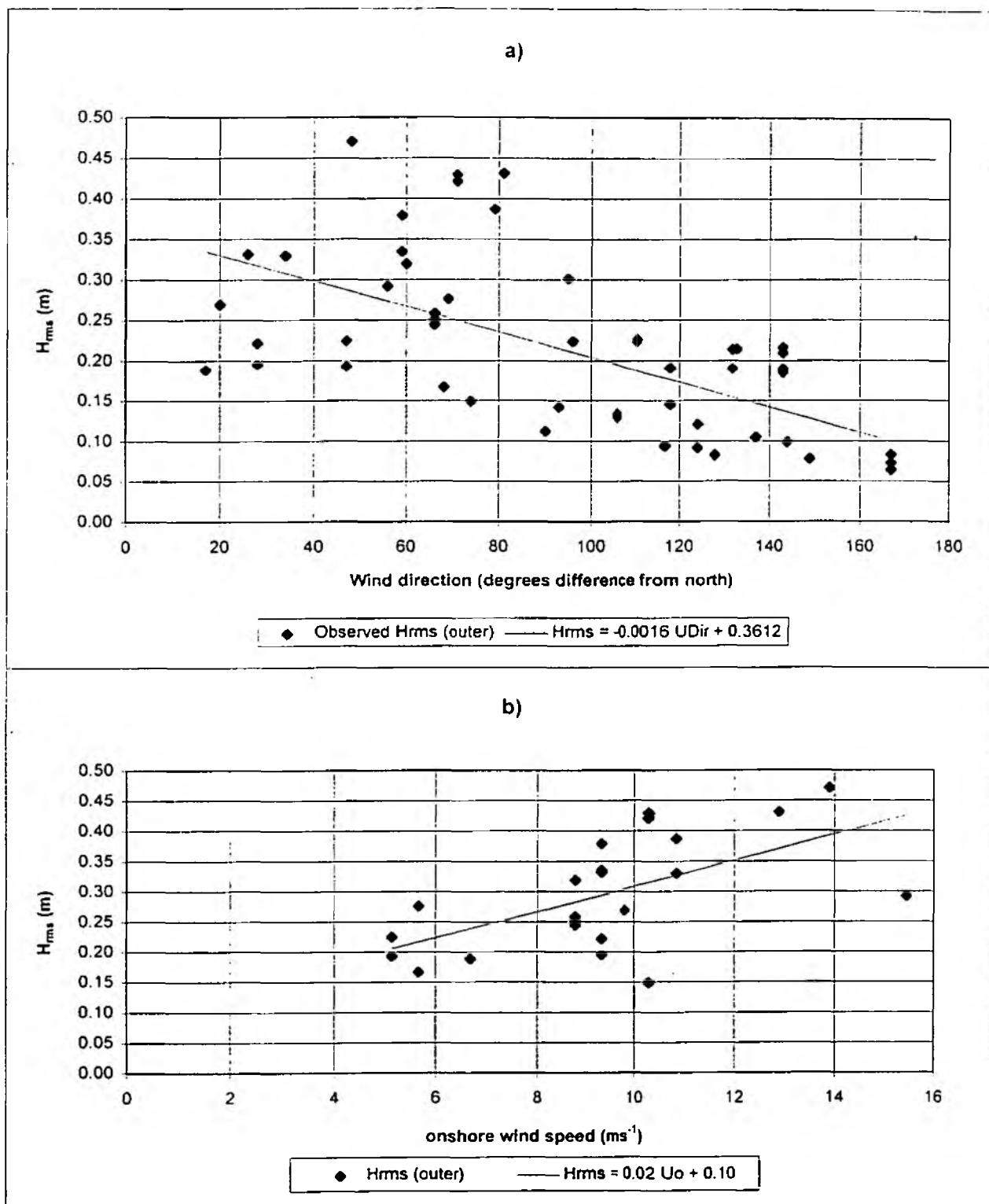


Fig. 4.4: a) Relationship between wind direction (as deviation from N) measured offshore and incident wave height at Stiffkey (least squares regression line shown) ( $r = 0.63$ ), and b) Relationship between velocity of onshore winds and incident wave height at Stiffkey ( $r = 0.60$ ).

onshore wind velocities (encountered in 24 cases) were not significantly correlated with either of the two wave period parameters ( $r = -0.067$  and  $-0.109$  in the case of  $T_z$  and  $T_p$  respectively). Wind velocities in offshore directions (encountered on 30 occasions), however, were significantly (and negatively) correlated with both  $T_z$  and  $T_p$  ( $r = -0.53$  and  $-0.67$  respectively).

#### 4.2.4 Conclusions

As illustrated by Table 4.3, the set of wave records obtained at Stiffkey covers a wide range of water depth, offshore wave, and wind conditions. Tidal elevations for those tides during which wave recording took place were at the high end of the spectrum of tidal HWs recorded during the field season. Similarly, wind velocities and offshore wave heights were high compared to longer term average conditions. Contrary to what was expected from the analysis of other coastal wave records, incident wave heights at Stiffkey were not significantly correlated with water depth. This low correlation may be due to the significant effect of meteorological conditions on wave generation over the Stiffkey sandflat. The meteorological influence possibly overrules the effect of water depth (within the range of depths - 0.91 to 1.75m - observed here), with northerly winds of relatively high velocity resulting in increased incident wave heights. The link between wave height and wind speed/direction and the lack of statistical evidence for the influence of offshore swell supports the idea that waves at Stiffkey are predominantly locally generated. Wave heights recorded at Stiffkey, however, do seem to be linked to total offshore (wind and swell) waves to some extent. In addition, the fact that the maximum wave height recorded at the outer station (see Table 4.2) occurred when i) the water was deepest, ii) tidal elevation was largest, iii) winds were in an onshore direction, and iv) offshore waves were largest amongst those that occurred during onshore wind conditions (see Table 4.3), however, does support the hypothesis that, especially in conditions of high water depths, waves generated offshore may propagate further inshore and contribute to local wave heights. The significant negative correlation between offshore wind velocities and wave periods at the outer (sandflat) station suggests that offshore winds may cause small waves with low wave periods (high frequency) to form over the relatively short fetch distance across the salt marsh and the sandflat. In these wind conditions, it appears that these waves dominate the wave spectra due to the lack of longer period onshore waves.

### 4.3 Wave attenuation over sandflat and salt marsh

Wave characteristics (height, energy, and period) were expected to change significantly over the length of the wave recording transect. Wave shoaling, percolation into the sand/mud surface, and friction due to the presence of ripples or vegetation are some processes which result in

wave energy dissipation (Horikawa, 1978). Over the salt marsh part of the transect, however, the shallower water depths, increased micro-topography, altered surface sediments, and the presence of vegetation are likely to influence approaching waves differently and lead to an increased wave height, energy, and period change. To assess these differences in wave transformation over the sandflat and salt marsh, differences in spectral wave height, energy, period, and zero-upcrossing period between the three stations were computed and are summarised in Table 4.4. The transformation of wave height, energy, and period, and the possible influence of environmental conditions on these transformations is discussed in turn below.

Table 4.4: Wave parameter changes between the three stations at Stiffkey - summary statistics

	Change in $E_{tot}$			Change in $H_s$		
	outer-mid.	mid.-inner	outer- inner	outer-mid.	mid.-inner	outer- inner
max neg change	-55.27	-99.98	-99.99	-33.10	-98.37	-99.15
max pos change*	10.86	-47.36	-49.21	5.25	-27.45	-28.72
mean	-26.34	-79.64	-83.80	-14.65	-58.33	-63.53
median	-27.06	-82.39	-86.98	-14.59	-58.02	-63.92
st. deviat.	15.59	14.57	13.22	9.08	17.48	17.18

Table 4.4 continued

	Change in $H_{rms}$		Change in $T_p$			
	outer-mid.	mid.-inner	outer- inner	outer- mid.	mid.- inner	outer- inner
max neg change	-33.09	-98.75	-99.16	-1.32	-1.86	-2.25
max pos change*	5.30	-27.46	-28.77	0.29	-4.82	4.46
mean	-14.64	-58.34	-63.54	-0.18	0.05	-0.14
median	-14.58	-58.06	-63.94	-0.16	-0.04	-0.24
st. deviat.	9.10	17.47	17.17	1.23	0.33	1.07

	Change in $T_p$		
	outer-mid.	mid.-inner	outer- inner
max neg change	-11.40	-4.75	-4.75
max pos change	3.30	202.07	203.41
mean	-1.2	60.47	59.28
median	-0.18	63.91	58.71
st. deviat.	2.78	66.32	66.40

\* note: Height and energy change between middle and inner station was never positive, i.e. the value given here is the smallest negative change

#### 4.3.1 Wave height and energy

Frequency distributions of percent spectral energy and wave height change over the sandflat (i.e. between the outer and middle station), over the salt marsh (i.e. between middle and inner station), and over the whole transect (i.e. between outer and inner station) are shown in Figure 4.5.

Taking all 54 data series into account, wave height ( $H_{rms}$ ) decreased on average over the sandflat by approximately 15%. On individual occasions an increase in wave heights was observed over the sandflat which, however, never exceeded 6%. Over the salt marsh, in contrast, average wave height reduction was almost four times higher at a value of just over 58%. On no occasion was an increase in wave heights observed over the salt marsh, but the degree of wave height reduction varied from just over 27% to just under 99%. The difference between sandflat and salt marsh wave attenuation was significant at the 95% confidence level.



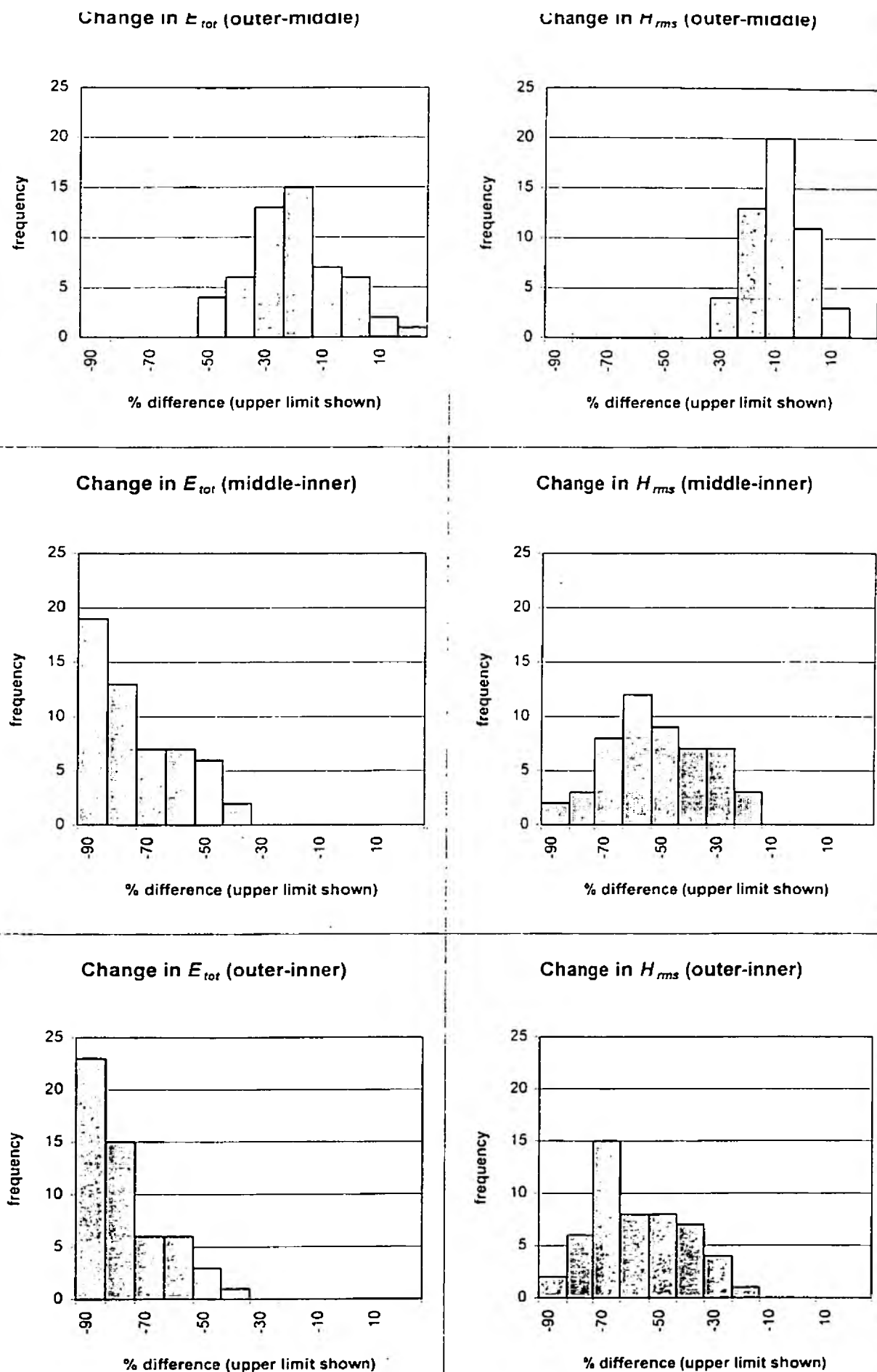


Fig. 4.5: Frequency distribution of change in  $E_{tot}$  and  $H_{rms}$  between stations at Stiffkey

With respect to total spectral energy loss, a similar picture emerged with a mean loss of approximately 26% over the sandflat but a significantly higher loss of 80% over the salt marsh. An occasional spectral energy increase up to 11% was observed over the sandflat, whereas spectral energy always decreased over the salt marsh.

#### 4.3.2 Wave periods

Whereas both frequency distributions of  $T_p$  and  $T_z$  reflect a period shift towards higher average wave frequencies from the outer to the middle station, the frequency distribution of  $T_p$  at the inner station (Figure 4.6) suggests the dominance of very low frequency waves ( $> 12s$ ). The distribution of  $T_z$  at the inner station shows a much more even spread of wave periods with a modal class of 2.7s to 3.1s. Possible reasons for this discrepancy will be discussed below.

#### 4.3.3 Influence of water depth

Water depth,  $h$ , in relation to wave length,  $L$ , plays an important role in influencing wave transformation due to shoaling, percolation, and friction. The difference in wave attenuation over the sandflat and the salt marsh may, therefore, be the result of lower water depths over the salt marsh compared to the sandflat rather than being caused by differences in surface roughness or percolation. Results from the regression analysis of wave height,  $H_{rms}$ , change and water depth,  $h$ , at the outer and the middle transect station (Figure 4.7) suggest that water depth itself did influence wave attenuation: an increase in water depth resulted in reduced wave height attenuation, whereas waves tended to be increasingly attenuated in shallow water. Although the relationship between wave attenuation and water depth was significant in the case of both the sandflat ( $r = 0.47$ ) and the salt marsh ( $r = 0.79$ ) section of the transect, the characteristics of this relationship differ; the least-squares regression lines (see Figure 4.7) differ significantly with respect to line slope ( $21.1 \pm 5.5$  and  $63.5 \pm 7.4$  for sandflat and salt marsh sections respectively) and intercept ( $-43.2 \pm 7.5$  and  $-120.8 \pm 7.4$  respectively). Total spectral wave energy, through being related to the square of wave height, is thus also significantly correlated with water depth ( $r = 0.46$  and  $0.73$  over sandflat and salt marsh respectively). Information on wavelengths,  $L$ , was only available indirectly (as calculated from wave period). The ratio  $h/L$  was not significantly correlated with either wave height,  $H_{rms}$ , change or with change in the energy,  $E$ , of the spectrally dominant wave over the sandflat ( $r = 0.12$  and  $0.18$ ) or the salt marsh ( $r = 0.17$  and  $0.05$ , respectively).

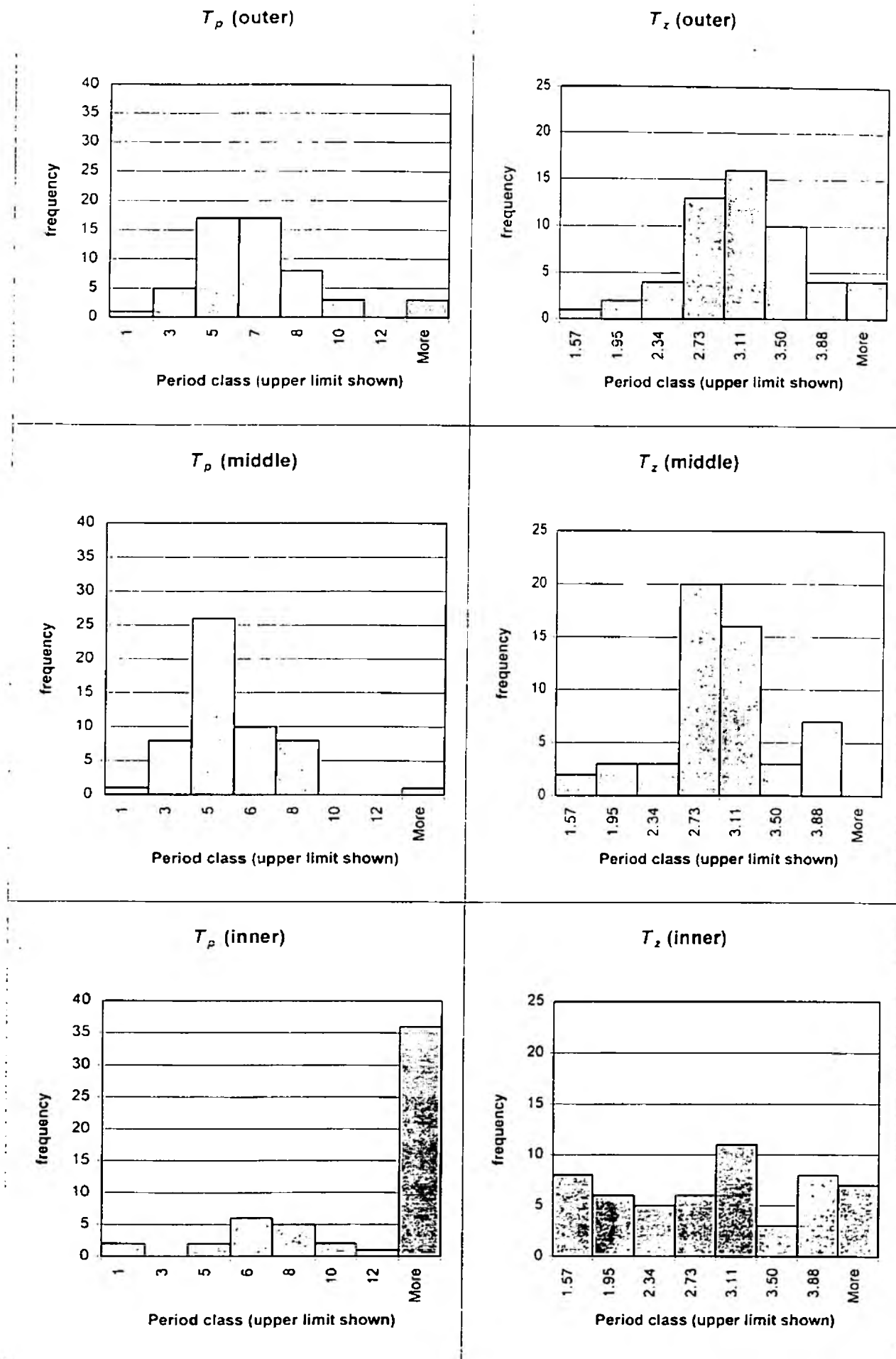


Fig. 4.6: Frequency distribution of  $T_p$  and  $T_z$  (seconds) at the three stations at Stiffkey (54 records, 21.9.94 to 17.5.95).

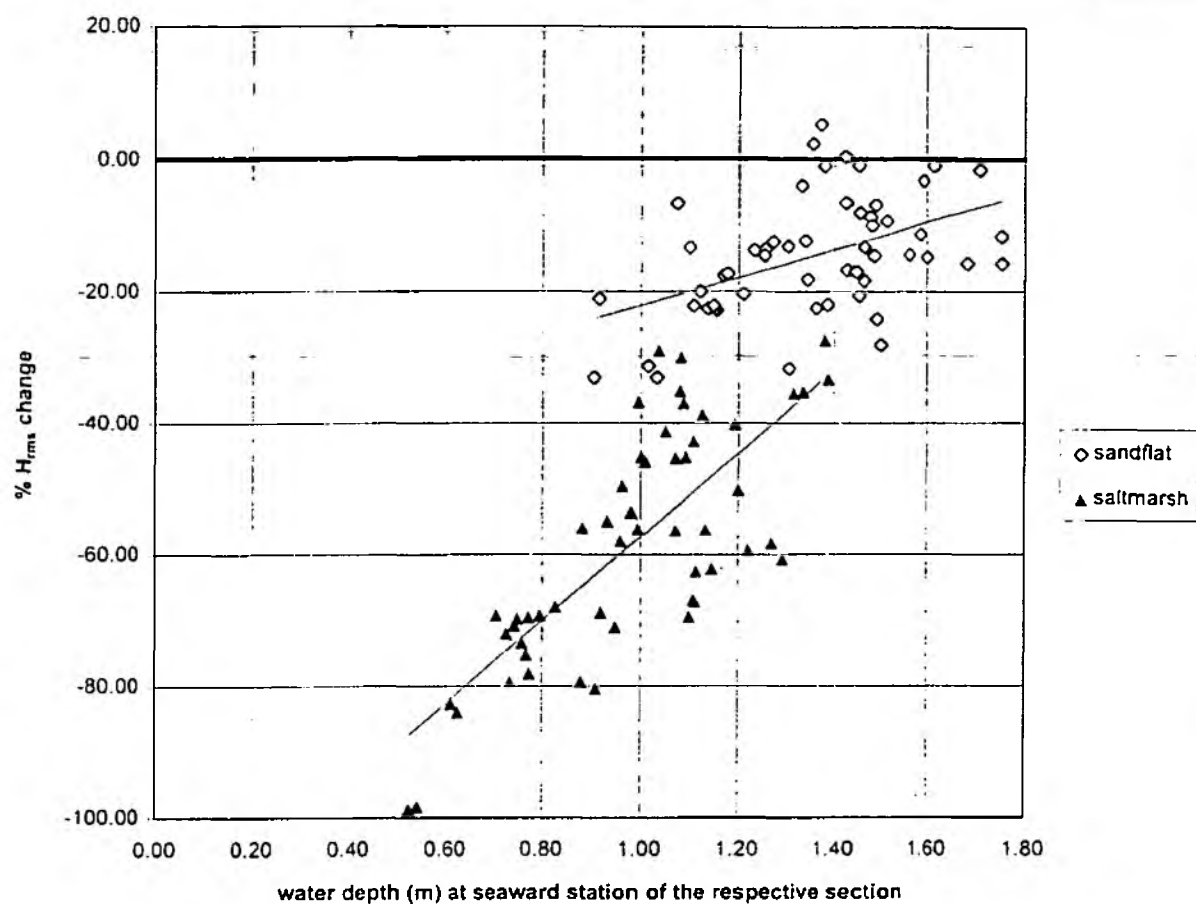


Fig. 4.7: Relationship between water depth at seaward station of section and  $H_{rms}$  change over the respective sections ( $r = 0.47$  over sandflat,  $r = 0.77$  over salt marsh)

The characteristic decrease in wave periods across the sandflat and the subsequent increase in periods across the salt marsh does not seem to be linked to differences in water depth (all  $r$  values  $< 0.2$ ).

#### **4.3.4 Influence of wind speed and direction**

The pressure transducers used for wave recording at Stiffkey do not provide any information on wave directions. Although wave refraction immediately offshore and along the transect is negligible due to the shallow sloping nature of the sandflat, the high variability of wind velocity and direction throughout the field monitoring period may well have caused variations in the dominant direction of wave travel on individual occasions. Such variation in the direction of wave approach would result in different fetch distances and therefore different wave spectra at individual wave recording stations. It has already been shown that wind direction had a significant effect on wave heights at the outer wave recording station and that high onshore wind velocities tend to result in increased incident wave heights.

In general, northerly winds tended to coincide with relatively low wave height attenuation over the sandflat and the salt marsh, but correlation coefficients were small ( $r = 0.44$  and  $0.23$  respectively). Wind velocity itself did not seem to have any influence on wave attenuation ( $r < 0.1$ ). When considering those wave records obtained in onshore wind conditions, however, high wind velocities tended to decrease wave attenuation (Figure 4.8). The effect of wind speed on wave attenuation appears to be stronger over the salt marsh than over the sandflat. With respect to winds from offshore directions, in contrast, high velocities tended to increase attenuation, but correlation coefficients were not significant ( $r = -0.26$  and  $-0.22$  for sandflat and salt marsh attenuation respectively).

Whereas wind direction, expressed in degree difference from north, did not have any significant influence on changes in wave periods over the sandflat ( $r = 0.07$  with respect  $T_p$ ), winds from southerly direction appear to have resulted in smaller wave period shifts over the salt marsh ( $r = 0.42$  with respect to  $T_p$ ). The influence of wind direction on peak spectral wave periods,  $T_p$ , was negligible ( $r < 0.25$ ).

#### **4.3.5 Combined influence of tidal and meteorological factors**

The above bi-variate regression analysis allows only limited inferences to be made about the linkages between individual tidal and meteorological variables influencing wave heights,

periods, and attenuation. From the results presented above it is not possible to determine whether the influence of one variable on another is direct or indirect (i.e. through the influence on a second variable which then influences the dependent variable). To determine the more detailed structure of relationships between variables, multiple correlation and regression techniques were used. Figure 4.9 illustrates the relative influence of incident wave periods, heights, water depth, local wind speed, and wind direction on each other and on wave attenuation across the sandflat and the salt marsh. The proportion of the variability in wave attenuation over the sandflat explained by the variability in wave periods only, for example, is obtained by regressing the residual variability of wave attenuation (not explained by any of the other four variables) on the residual variability in wave periods (not explained by any of the other four variables).

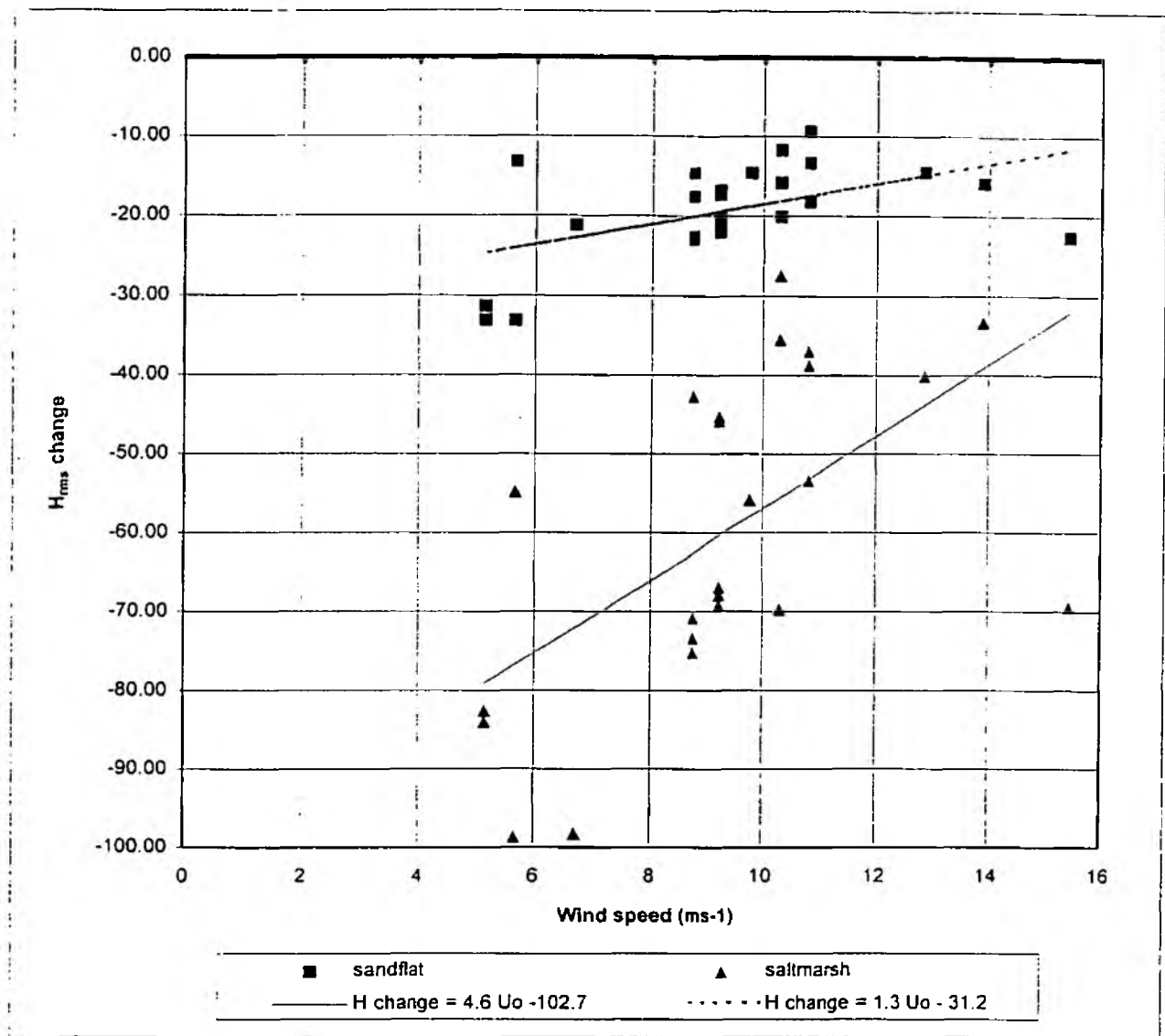
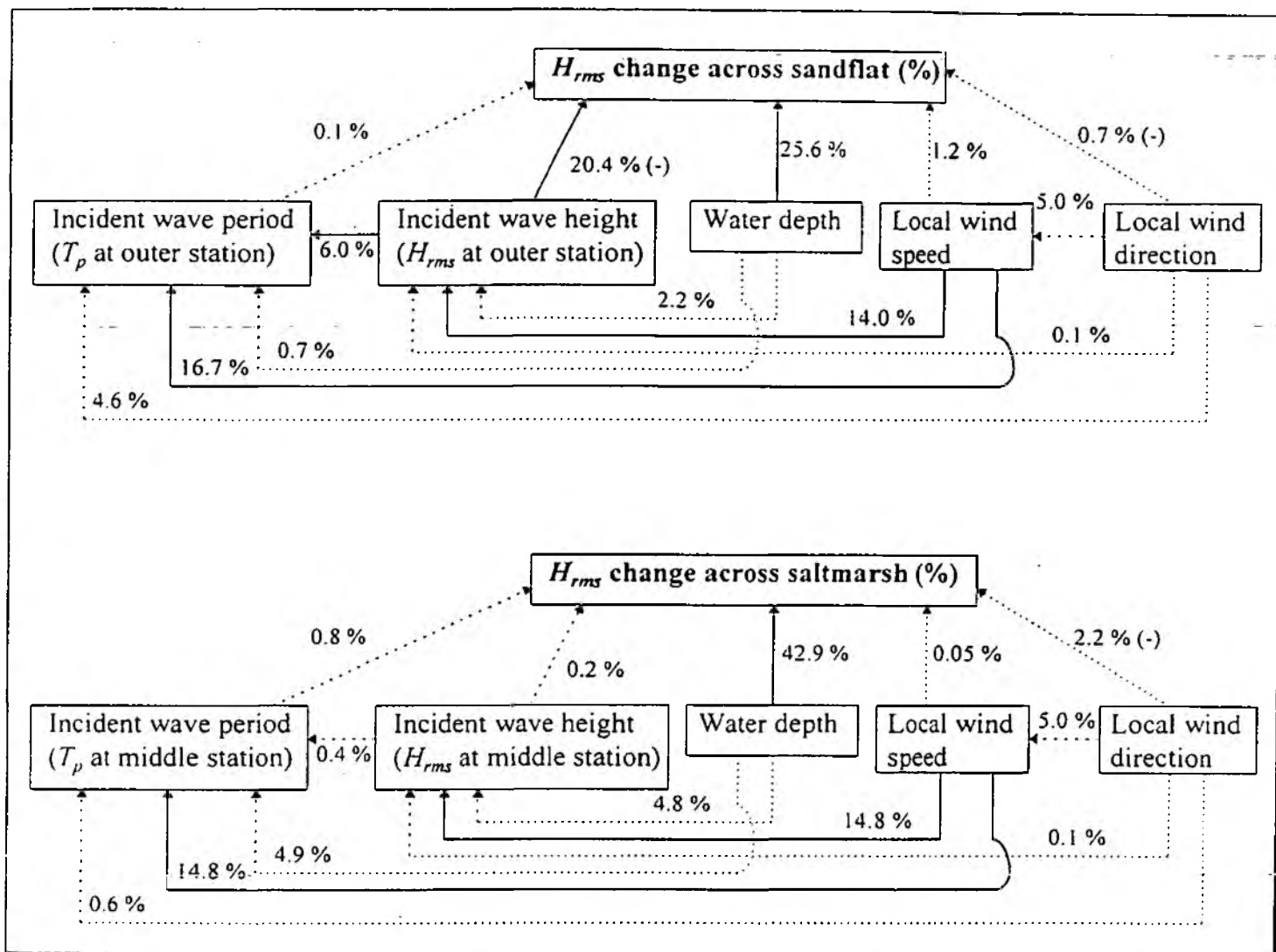


Fig. 4.8: Relationship between onshore wind velocity and  $H_{rms}$  change across sandflat ( $r = 0.52$ ) and salt marsh ( $r = 0.58$ )



Multiple regression of  $H_{rms}$  change over sandflat ( $\Delta H_{rms}(sfl)$ ) saltmarsh ( $\Delta H_{rms}(sm)$ ) on incident wave height residuals,  $H_{ou}$  and  $H_{mi}$ , (after removal of influence of water depth, wind speed, and direction on incident wave heights), water depth,  $h_{ou}$  and  $h_{mi}$ , local wind speed,  $U_s$ , and local wind direction,  $U_{dir}$ :

$$\Delta H_{rms}(sm) = 0.74 T_p + 10.22 H_{ou} + 68.55 h_{ou} + 0.42 U_s - 0.08 U_{dir} - 120.79 \quad r = 0.79$$

$$\Delta H_{rms}(sfl) = 0.13 T_p - 43.07 H_{ou} + 23.14 h_{ou} - 0.27 U_s - 0.03 U_{dir} - 41.59 \quad r = 0.66$$

Fig. 4.9: Graphical representation of results from regression analysis showing percentage of total variance in each variable accounted for directly by other variables (based on 54 wave records at Stiffkey) (stippled lines indicate relationships not significant at the 95% confidence level).



## 5. MODELLING WAVE ATTENUATION

### 5.1 Introduction

The reduction of wave energy in shallow water results from a large number of individual factors. Some controls on wave attenuation (for example water depth, wind direction and speed) have been discussed with reference to the Stiffkey marsh environment in the previous sections. However, additional influences are likely from sandflat and salt marsh surface characteristics. When waves reach shallow water, the orbital water particle motion beneath the waves is increasingly influenced by the sea bed and becomes elliptical. As a result, wave height and energy changes. Individual laboratory experiments and theoretical analysis has provided equations for an estimation of wave height or energy dissipation over areas of known surface characteristics as a result of shoaling, friction, or percolation. Few of these theoretical equations, however, have been validated by observations in the field. This lack of field validation is to a large extent due to the difficulties associated with the quantification of the complex surface characteristics of intertidal, vegetated, areas (such as, for example, surface roughness). Although physical laboratory experiments have proved useful for the understanding of isolated hydrodynamic processes and for the development of individual hydrodynamic equations, when used for the simulation of field conditions such experiments are often restricted by problems of scale.

A mathematical modelling approach provides a means to visualize, understand, and simulate the complex non-linear relationships between the large number of individual parameters which influence wave transformations in shallow water. Mathematical models generally do not have the scaling problems associated with laboratory experiments and allow the study of the controlled interaction of a number of forcing mechanisms on a particular process. With regard to wave attenuation, such an approach serves the dual purpose of i) illustrating the combined effect of shoaling, percolation, and friction on wave damping, and ii) providing a basis on which to assess the importance of individual surface parameters on wave damping in a particular environmental setting. Furthermore, once the model has been calibrated with field observations, the controlled variation of input parameters can be used to assess the possible outcome of changing conditions in particular field settings. Furthermore, the comparison of expected and observed wave height reduction, provides an opportunity to estimate quantities (such as surface friction) which can not be directly determined in the field.

Attempts to dynamically simulate the nearshore environment have only been made since the use of computers allowed the development and implementation of complex numerical models. A detailed review of physical, statistical, deterministic and probabilistic models is provided in Fox (1985) and Horikawa (1988) and a recent example of models developed for the simulation of wave propagation and nearshore sediment transport by waves and rivers is that described by Milbradt and Holz (1992) and Martinez and Harbaugh (1993).

The mathematical model described below was developed specifically for simulating wave attenuation along the Stiffkey sandflat-to-salt marsh transect. Model development followed the 'five-step method' (Meerschaert, 1993) which is summarised in Figure 5.1. The structure of this chapter reflects this five-stage development procedure of the model: i) the initial formulation of the problem, ii) the identification of parameters and relevant theoretical/semi-empirical equations and inherent assumptions, iii) the formulation of the model, iv) the description of model behaviour (sensitivity to changing boundary conditions) and the application of the model to a particular 'problem' (i.e. the Stiffkey field setting), and v) the interpretation of the model results.

Step 1. Ask the question.

- (a) Make a list of all the variables in the problem, including appropriate units.
- (b) Be careful not to confuse variables and constants.
- (c) State any assumptions you are making about these variables, including equations and inequalities.
- (d) Check units to make sure that your assumptions make sense.
- (e) State the objective of the problem in precise mathematical terms.

Step 2. Select the modeling approach.

- (a) Choose a general solution procedure to be followed in solving this problem.
- (b) Generally speaking, success in this step requires experience, skill, and familiarity with the relevant literature.
- (c) In this book we will usually specify the modeling approach to be used.

Step 3. Formulate the model.

- (a) Restate the question posed in step 1 in the terms of the modeling approach specified in step 2.
- (b) You may need to relabel some of the variables specified in step 1 in order to agree with the notation used in step 2.
- (c) Note any additional assumptions made in order to fit the problem described in step 1 into the mathematical structure specified in step 2.

Step 4. Solve the model.

- (a) Apply the general solution procedure specified in step 2 to the specific problem formulated in step 3.
- (b) Be careful in your mathematics. Check your work for math errors. Does your answer make sense?
- (c) Use appropriate technology. Computer algebra systems, graphics, and numerical software will increase the range of problems within your grasp, and they also help reduce math errors.

Step 5. Answer the question.

- (a) Rephrase the results of step 4 in nontechnical terms.
- (b) Avoid mathematical symbols and jargon.
- (c) Anyone who can understand the statement of the question as it was presented to you should be able to understand your answer.

Fig. 5.1: Meerschaert's (1993) 5-step approach towards mathematical modelling

## 5.2. Wave attenuation: formulating the problem

Wave attenuation due to bottom friction (caused, for example, by the presence of vegetation) and/or percolation has been investigated to a large extent theoretically (e.g. Putman and Johnson (1949), Bretschneider and Reid (1954), Dalrymple *et al.* (1984), Camfield (1983), Kobayashi *et al.* (1993)). The theoretically developed equations, however, have been validated by only a limited number of laboratory experiments (see e.g. Fonseca *et al.* (1982), Pethick *et al.* (1990), and Fonseca and Cahalan (1992), and Kobayashi *et al.* (1993)) and field studies (e.g. Price *et al.* (1968), Knutson *et al.* (1982), Knutson (1988)). The standard theoretical approach for predicting wave energy dissipation (and therefore wave height reduction) due to surface friction and/or percolation treats wave transformation as a vertically two-dimensional problem based on the time-averaged conservation of energy equation from linear wave theory. As such, the change in the average wave energy transported through a vertical section with unit crest width per unit time,  $d(\bar{E}cn)$ , per unit surface area can be expressed as:

$$\frac{d(\bar{E}cn)}{dx} = -D_e \quad (2)$$

where 
$$n = 0.5 \left[ 1 + \frac{4\pi \frac{h}{L}}{\sinh\left(\frac{4\pi h}{L}\right)} \right] \text{ and } c = \frac{gT}{2\pi} \tanh\left(\frac{2\pi h}{L}\right) \quad (\text{Horikawa, 1978})$$

The relationship between incident wave height,  $H_1$ , and the wave height at a distance  $Dx$  along the wave ray,  $H_2$ , can be expressed as

$$H_2 = H_1 e^{-a_0 \Delta x} \quad (3)$$

which assumes that the small-amplitude monochromatic wave propagates in still water in the positive  $x$ -direction and that the local wave height decays exponentially (Kobayashi *et al.* (1993)). For some types of wave damping (such as for example the coastal flooding of trees due to storms (see Dalrymple *et al.*, 1984)) it has been shown that wave height decay is not exponential but varies according to

$$H_2 = H_1 \left( \frac{1}{1 + b \Delta x} \right) \quad (4)$$

where  $b$  = a damping factor. For small values of  $bDx$  or  $aDx$  (less than 0.1), the functions expressed in equations 6.2 and 6.3, however, behave alike, so that

$$H_2 = H_1 e^{-a_0 \Delta x} \approx H_1 \left( \frac{1}{1 + b \Delta x} \right) = H_1 K \quad (5)$$

where

$b = a_0$  and  $K$  = the decay factor.

The most important processes causing wave height changes along the wave ray are shoaling (due to changing water depth), friction (due to a viscous bottom boundary layer and surface roughness), and percolation (due to surface permeability). Although the effect of each of these processes can be calculated from equation 6.4 (once the decay factor  $K$  is known), the combined effect of all four processes in a variety of morphological and tidal conditions can best be assessed through mathematical modelling and simulation. The problem of wave height change due to the combination of processes can be expressed mathematically as

$$H_2 = H_1 K_s K_v K_f K_p \quad (6)$$

where the subscripts  $s$ ,  $v$ ,  $f$ , and  $p$  denote the shoaling, viscous friction, bottom friction, and percolation transformation factors, respectively. This equation forms the basis of the mathematical model developed below to predict wave heights along the wave ray from incident wave heights measured at a known distance offshore.

### **5.3 Theoretical and semi-empirical equations**

The following section introduces the theoretical basis and mathematical equations from which the model is developed. In some cases several equations exist to describe a particular process (for example energy dissipation due to percolation). The model was formulated using the most recently developed equations.

### 5.3.1 Shoaling

Over an impermeable, smooth surface, wave shoaling due to a decrease in water depth causes wave heights to increase and waves to steepen. Assuming the energy transmitted shorewards between two wave rays remains constant, i.e.:

$$E_1 n_1 c_1 = E_2 n_2 c_2 \quad (7)$$

where

$$n = \frac{1}{2} \left( 1 + \frac{4\pi h / L}{\sinh(4\pi h / L)} \right) \text{ and the subscripts indicate station number,}$$

the following equation is used to determine consecutive wave heights along a wave ray:

$$H_2 = H_1 \sqrt{\frac{n_1 c_1}{n_2 c_2}} = H_1 K_s \quad (8)$$

where  $K_s$  is called the 'shoaling coefficient' (CERC, 1984).

### 4.3.2 Viscous boundary layer friction

Whereas the effect of shoaling over an impermeable, frictionless surface is to increase wave height (i.e.  $K_s > 1.0$ ), friction due to a viscous layer at the bottom and surface roughness leads to energy loss in the form of heat and therefore a reduction in wave height (i.e.  $K_f < 1.0$ ). The effect of the viscous boundary layer at the sea bed-water interface over a smooth impermeable surface can be quantified using the following equation (Sleath, 1984):

$$H_2 = H_1 e^{-a_1 \Delta x} \quad \text{where} \quad e^{-a_1 \Delta x} \approx [1 + a_1 \Delta x]^{-1} = K_v \quad (9)$$

where  $a_1$  can be approximated

$$a_1 = \frac{(2\pi / L)^2}{\left( \frac{4\pi h}{L} + \sinh\left(\frac{4\pi h}{L}\right) \right) \sqrt{\frac{\pi}{Tv}}}$$

which provided a good agreement between theory and experiment (see Figure 5.2 (Sleath, 1984)) and will be used in the model developed here.

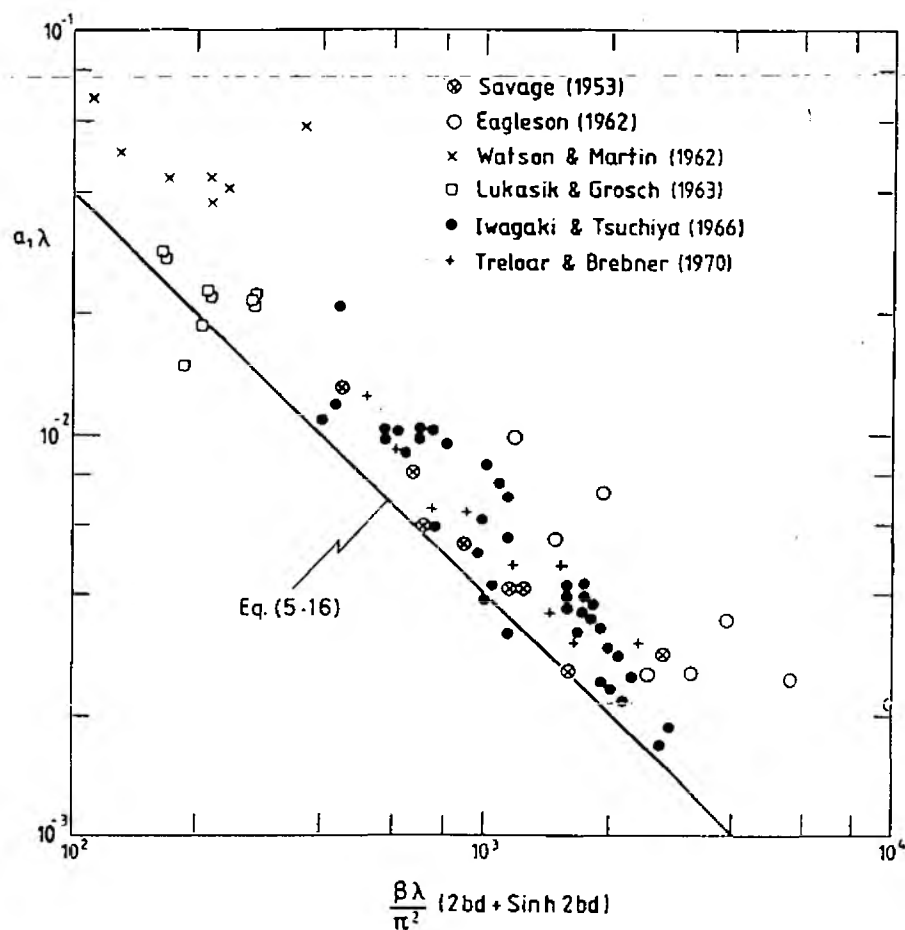


Fig. 5.2: Viscous friction factors, theory and experiment (Sleath, 1984)

### 5.3.3 Bottom surface friction

In addition to the viscous boundary layer, bottom roughness will cause friction. The effect of this friction on wave energy is incorporated as a friction factor  $f$ . According to CERC (1984) and Horikawa (1978), who bases his equation on Putman and Johnson (1949) and Bretschneider and Reid (1954), consecutive wave heights (in uniform water depth) are related to each other by:

$$H_2 = H_1 \left[ 1 + \frac{64\pi^3}{3g^2} \frac{fH_1\Delta x}{h^2} \frac{h^2}{T^4} \frac{K_s^2}{\sinh^3(2\pi h/L)} \right]^{-1} \quad (10)$$

where the expression in brackets is the friction coefficient,  $K_f$ . This equation includes the friction factor,  $f$ , which is defined by Sleath (1984) as:

$$f = \frac{\tau_v}{\frac{1}{2}\rho U_\infty^2} \quad (11(a))$$

or, for small amplitude waves:

$$f = \frac{2}{\sqrt{R}} \quad \text{where} \quad R = U_\infty \frac{a}{\nu} \quad (11(b))$$

Several attempts have been made at estimating  $f$  directly from surface characteristics. Such relationships between values of  $f$  and surface bedforms have mainly been determined experimentally under controlled laboratory conditions. Figure 6.3 shows approximate values of  $f$  for four different surfaces (CERC, 1984). With regard to sandflat roughness, Bagnold (see Putman and Johnson (1949)) found that for low Reynolds numbers ( $Re$ ),  $f$  is related to the spacing of ripples on sand,  $L_r$ , and the half-amplitude of the horizontal displacement of water particles at the bottom,  $0.5a$ :

$$f = 0.072 \left( \frac{0.5a}{p} \right)^{-0.75} \quad (12)$$

for low  $Re$ , where  $Re = \frac{\rho h U}{\eta}$ ,



$U$  is the overall mean velocity of the flow,  $h$  is the flow depth, and  $\eta$  is the viscosity of water. This relationship, however, is only valid if  $0.5a/L_r > 1$ . When  $0.5a/L_r < 1$ , then  $f$  is constant at a value of 0.08.

Experimental results have also shown that  $f$  is related to ripple dimensions and grain size. Sleath (1982) suggests values of around 0.22 for ripple steepness ( $h_r/L_r$ ) of 0.17. Sleath (1984) suggests the use of a formula developed by Swart in 1976:

$$f = 0.00251e^{5.21\left(\frac{a}{k_s}\right)^{-0.19}} \quad \text{for } \frac{a}{k_s} > 1.57$$

and

(13)

$$f = 0.3 \quad \text{for } \frac{a}{k_s} \leq 1.57$$

where  $k_s$  is the Nikuradse grain roughness, which can be taken as  $2D_{90}$  for these approximations (or  $k_s/h_r = 25(h_r/L_r)$ , where  $h_r$  = ripple height,  $L_r$  = ripple length).

Others (Denny (1989), Vogel (1981), and Kobayashi *et al.* (1993)) relate the friction coefficient to the drag coefficient,  $C_D$ :

$$C_D \equiv \frac{2f_d}{\rho S_p u^2}$$

(14)

where  $f_d$  refers to the friction factor associated with this drag on the surface/object,  $S_p$  refers to the area of the object projected into the direction of the flow, and  $u$  is the horizontal fluid velocity. This relationship has been developed for unidirectional flow, so that its validity for circulatory flow under waves is limited. For a given shape and size of object, the drag coefficient depends only on the Reynold's number of the flow,  $Re$ . For an upright circular cylinder, for example, Reynold's numbers between 20,000 and 50,000 result in a drag coefficient  $C_D$  of 0.74 (Vogel (1981) and Denny (1989)). This means, that if the Reynold's number for the flow around a given cylindrical shaped object is known, the friction factor can be estimated from the knowledge of  $S_p$  and  $u$ . With regard to vegetation, however, horizontal single cylinders are a poor approximation of the complex morphology of individual plants. It is therefore not possible to estimate drag coefficients directly from morphological plant characteristics such as height and diameter. For the purpose of this model, therefore,  $f$  will be estimated from equation 13 for the sandflat surface and from Figure 5.2 for the salt marsh surface.

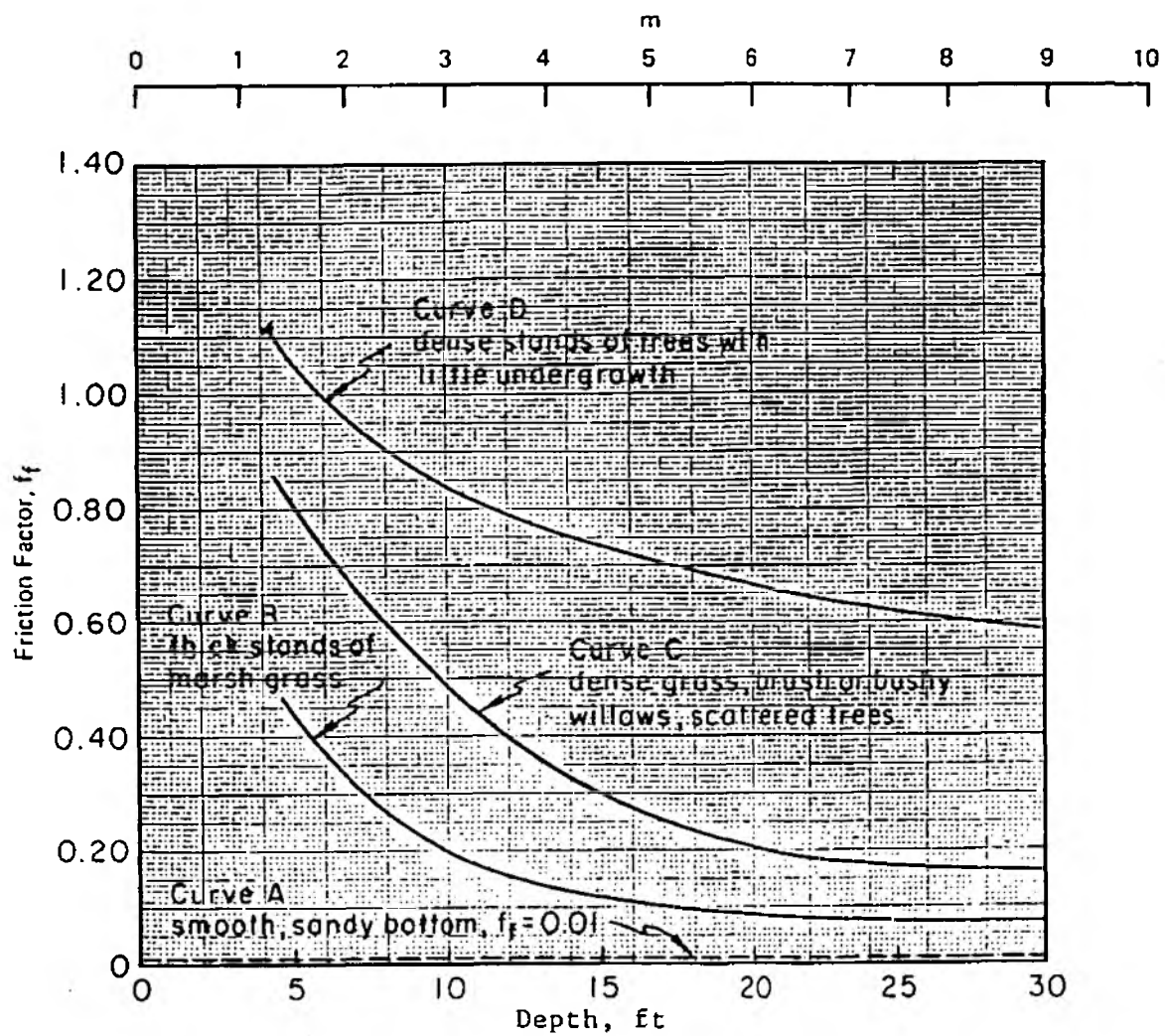


Fig. 5.3: The variation of friction factors for a range of surfaces with water depth (CERC 1984)

### 5.3.4 Percolation

The amount of energy dissipated due to the movement of water into and out of the surface sediment layer in response to the pressure gradient underneath the waves depends on the permeability of the surface material. Assuming that the permeable surface material does not move, the rate at which this movement of water occurs follows Darcy's law which states that:

$$Q = -\frac{KA}{\nu} \frac{\Delta p}{d} \quad (15)$$

where  $K$  is the specific permeability of the surface layer (given in  $\text{m}^2$ ),  $d$  is the layer depth,  $\Delta p$  is the pressure drop through the layer ( $\text{Nm}^{-2}$ ),  $A$  is the surface area considered, and  $\nu$  is the dynamic viscosity of water ( $\text{Nsm}^{-2}$ ) (Allen, 1985). Sleath (1984) states, that the permeability of the sediment layer can be estimated from:

$$K = \left[ A \left( \frac{(1 - n_p)^2}{n_p^3} (B \sum \frac{P}{100 D_{gm}})^2 \right) \right]^{-1} \quad (16)$$

where  $n_p$  is the porosity of the sediment (0.3 to 0.4 for uniform sand),  $A$  is a packing factor (usually around 5.0),  $B$  is the sand shape factor (ranging from 6.0 for spherical grains to 7.7 for angular grains),  $P$  is the percentage of sand held between two adjacent sieves, and  $D_{gm}$  is the geometric mean of the two mesh sizes.

Allen (1985) also mentions that at low  $Re$ ,  $k$ , the permeability coefficient, can be approximated by:

$$k = \frac{1}{18} \frac{(1 - C_{lim})^n D_s^2}{C_{lim}} \quad (17)$$

where  $C_{lim}$  is the upper limit of volume concentration of particles (i.e. 'packing density'),  $D_s$  is the sediment particle diameter, and  $n$  ranges from 2.33 to 4.65 depending on  $Re$ .  $k$  is expressed in  $\text{ms}^{-1}$  and is related to the specific permeability  $K$  by:

$$k = \frac{Kg}{\nu} \quad (18)$$

Once the permeability is known, the rate of energy dissipation per unit surface area for sandy substrates can be calculated by using a formula developed by Putman (1949) and corrected by Reid and Kajiura (1957):

$$\frac{d(\bar{Enc})}{dx} = -D_p = -\frac{\pi k \rho g H^2}{4L \cosh^2(2\pi h/L)} \quad (19)$$

which is based on the assumption that the sand at the sand/water interface does not move. Assuming a uniform water depth between the stations, substituting wave energy by wave height, and transforming equation 19 (see equation 2 and 5) one obtains

$$H_2 = H_1 \left[ 1 + \frac{16\pi^2 k \Delta x K_p^2}{4LgT \cosh^2(2\pi \frac{h}{L})} \right]^{-1} \quad (20)$$

where the expression in brackets is the percolation coefficient,  $K_p$ . According to Bretschneider and Reid (1954), percolation loss can also be calculated from:

$$K_p = \frac{c_2}{c_1} \left[ \frac{\tanh(2\frac{\pi h_2}{L_2})}{\tanh(2\frac{\pi h_1}{L_1})} \right]^B \quad \text{where} \quad B = \frac{8\pi p}{vmT}, \quad (21)$$

$p$  is the permeability coefficient,  $v$  the kinematic viscosity, and  $m$  the slope ( $-dh/dx$ ) for a permeable bed whose depth is  $>0.3$ . More recently, Sleath (1984) has provided an equation for rigid, permeable, surfaces, which includes the depth,  $d$ , of the permeable layer and which will be used for modelling wave attenuation over the sandflat:

$$H_2 = H_1 e^{-a_2 \Delta x} \approx H_1 [1 + a_2 \Delta x]^{-1} = K_p H_1 \quad (22)$$

where  $a_2$  can be approximated by:

$$a_2 = \frac{K(\frac{2\pi}{T})}{v} \frac{\frac{4\pi}{L}}{\left( \frac{4\pi h}{L} + \sinh\left(\frac{4\pi h}{L}\right) \right)} \tanh\left(\frac{2\pi d}{L}\right)$$

When  $d$  is infinite, this equation is the same as that given by Reid and Kajiura (1957), provided the value of  $Kw/v$  is small.

### 5.3.5 Wave breaking

As deep water waves approach shallow water, their height increases (due to shoaling), increasing their steepness. If wave height reduction due to energy dissipation is comparatively small, waves eventually reach a critical steepness which results in wave breaking. At the Stiffkey sandflat, breaking of deep water waves occurs at a distance several hundred meters offshore from the outer wave recording station. Waves at the outer wave recording station can therefore be assumed to have reached their breaking steepness already or are locally generated or reformed after breaking. The limiting steepness for waves travelling in depths,  $h$ , less than  $0.5L$  without a change in form is given by Miche's formula (CERC, 1984):

$$\left(\frac{H}{L}\right)_{\max} = 0.142 \tanh\left(\frac{2\pi h}{L}\right)$$

and therefore:

(23)

$$H_{\max} = L 0.142 \tanh\left(\frac{2\pi h}{L}\right)$$

In this study,  $h$  is known from observation and  $L$  is calculated according to linear wave theory from  $T$  and  $h$ , so that the condition above can be applied as a limiting conditions to wave heights predicted from the model.

### 5.3.6 Assumptions

The theoretical formulae for determining wave height change in response to shoaling, friction, and percolation, are based on a set of assumptions which should be kept in mind when evaluating and interpreting the numerical model results based on these equations:

1) Theoretical models developed for the calculation of wave attenuation across a given surface and slope are based on linear wave theory and should therefore be regarded as no more than approximations of a complex set of interacting shallow-water processes. However, although these approximations do not provide accurately reconstructed wave profiles, Dean (1970) has shown that they are able to provide an accurate assessment of relative differences in single parameters, such as wave heights and periods. Furthermore, Kobayashi *et al.* (1993) showed that when using the alternative approach of continuity and linearized momentum equations for flow within and above vegetation, the expressions for the wave number and the exponential decay coefficient reduce to those based on linear wave theory if damping is small.

2) Most analytical solutions obtained for the small-amplitude monochromatic waves, therefore assume that wave height decays exponentially (equation 5) along the wave ray or that damping is small ( $aDx < 0.1$ , i.e.  $K > 0.9091$  in equation 5).

3) All equations assume that the consecutive locations for which wave height and energy are being calculated are located on the path of the approaching waves. In the case of the Stiffkey shoreline, refraction can be assumed to be negligible along the measurement transect. The very extensive shallow sloping sandflat ensures that wave crests are approximately parallel to the shoreline by the time they reach the outermost wave recording station (see section 2). The line defined by the three wave recording stations can therefore be assumed to be parallel to the wave ray.

4) The interaction of tidal currents with waves is assumed to be insignificant. Wave heights can decrease significantly through the influence of horizontal currents (Sleath (1984) provides an equation which allows the calculation of the height decay factor from information on mean current, wave celerity, period, and water depth. The influence of currents on waves is only significant, however, when waves propagate from a region of no mean current into a region in which there is a mean current. With regard to this study, currents can be assumed to remain relatively constant along the wave recording transect and over the 5 to 7 minute wave recording period.

5) The equations apply to monochromatic waves only. The transformation of the whole spectrum is not considered. Calculation of spectral changes is complicated by the fact that the individual component waves interact along the wave path and may each be influenced by different processes. The wave which contains the dominant proportion of the spectral energy (i.e. the wave with period  $T_{max}$ ), however, can be used to give a reasonable approximation of the shoaling experienced by the spectrum. Silvester (1974) points out that "by the time shallow water is reached the shoaling of a spectrum is essentially the same as that of a monochromatic wave with period  $T_{max}$ ".

6) All equations require knowledge of the incident wave length,  $L$ . In the case of single point measurements,  $L$  can only be approximated from wave period, using Eckart's equation developed in the 1950s (CERC (1984), Dean and Dalrymple (1984)) (see above) which is based on linear wave theory and is accurate to within 5%. The maximum error of 5% occurs when  $\frac{H}{L} = 0.159$ . As it is unclear whether this error significantly alters the resulting wave height estimate, the sensitivity of the model to changes in  $L$  needs to be determined.

7) The model equations do not take into account the fluid nature (viscosity) of the sand/mud substrate. The equations describing energy dissipation due to percolation assume a permeable substrate but do not include the effect of the deformation of the sand/mud surface due to the pressure change beneath waves. Dalrymple and Liu (1978) developed an equation for viscous mud surfaces of known thickness, viscosity, and density and, more recently, Macpherson (1980) used a viscoelastic model to predict wave height attenuation by mud surfaces. In addition to mud viscosity and density, Macpherson's model requires knowledge of the elasticity of the bed. As a result of i) the difficulty of determining these variables in advance for any given bed of mud, and ii) the limited number of laboratory results that might provide guidance, the above equation can only give an indication of the possible attenuation. It is assumed here that the vegetated mud surfaces which provide the focus of this study behave very different to bare mud beds, as the root system of the vegetation strengthens the substrate and reduces its elasticity and its viscous fluid nature. The effect of the marsh surface roughness due to the vegetation cover can therefore be assumed to overrule any effect of mud elasticity or viscosity.

8) Lastly, and possibly most importantly, the modelling approach expressed in equation 6 assumes that the individual energy dissipation mechanisms can be separated and vary independently. With the exception of the equation for the calculation of viscous boundary layer friction which includes the shoaling coefficient, the model does not allow for an interaction between the different mechanisms. Such an interaction may well exist (for example in the case of an increased surface roughness altering the wave motion and therefore changing the response of the wave to decreased water depth). As there are currently no detailed studies investigating

such interactions, however, their effect can not be included in the model. It is hoped, that the model results will help to identify water depth/wave conditions in which such interactions may be of importance.

## **5.4 Model formulation and sensitivity analysis**

Equations 6, 8, 9, 10, 16, 22 and 23 were used to formulate a model for the computation of wave attenuation due to shoaling, viscous friction, friction due to surface roughness, and percolation, respectively. Several versions of the model were written as Matlab programs. The purpose of the initial version was to assess the sensitivity of the model results to changes in initial conditions (such as water depth, wave, and surface characteristics). The response of each of the above equations to the independent variables will be discussed in turn below, before assessing the combined influence of the individual decay factors.

### **5.4.1. Input parameters**

To compute the decay factors of the attenuation model, a set of independent variables need to be specified. Table 5.1 lists the model input variables, including the source of information on the particular variables for the Stiffkey model simulation.

Table 5.1: Model input variables

Variable	Notation	Units	Source
Incident wave period	$T$	s	Estimate from spectra
Incident wave length	$L$	m	Estimate from wave period (error $\pm 5\%$ )
Incident wave height	$H_i$	m	Estimate from spectra
Water depth at seaward station	$h$ or $h_i$	m	Field measurement
Distance along wave path	$Dx$	m	Field measurement
Surface slope	$dh$	nd	Field measurement
Dynamic viscosity of water	$\nu$	$m^2s^{-1}$	Estimate from literature
Friction factor	$f$	nd	Estimate from literature
Permeability coefficient	$k$	$ms^{-1}$	Estimate from equations 6.15 and 6.17
Mud thickness	$d$	m	Estimate from literature

nd = non-dimensional



#### 5.4.2 Model output - sensitivity to input variables

Before applying the model to the field data obtained at Stiffkey, the model was tested for its response to changes in the values of the main input variables above. This kind of sensitivity analysis was used in the first instance to identify any mathematical and/or programming errors, but also i) to assess the relative importance of the individual decay factors, ii) to assess the relative influence of the individual input variables on wave attenuation, and iii) to consider the sensitivity of the model output to possible measurement and/or estimation errors in the input variables.

##### Wave length estimate, $L$ .

All of the above equations for the decay factors include the relative water depth term,  $h/L$ , of which only  $h$  is known a priori and  $L$  is estimated from Eckart's equation (CERC, 1984). It is therefore important to assess the possible error in the calculated decay factors due to an error in the calculated wave length. For this purpose, a set of vectors representing the range of water depths and wave periods to be expected at gently sloping shoreline locations (such as the Stiffkey marshes) were defined as input into the Eckart's wavelength equation (CERC, 1984). Based on results from the above analysis of contextual data and Stiffkey wave records, water depth was defined to vary from 0.5 to 3.0m at 0.1m intervals and wave periods were defined to vary from 0.5 to 30 seconds at 0.5 second intervals (i.e. covering the range of 'ordinary gravity waves' (Horikawa, 1978)). The resulting wave length estimates ranged from 0.4m (in 0.5m depth) to just over 162m (in 3.0m depth) (Figure 5.4) and relative depths,  $h/L$ , for each of the  $T/h$  combinations, ranged from approximately 0.01 to 8 (see Figure 5.5). According to these calculations, waves with periods between approximately 1 and 8 seconds on the given range of water depths classify as 'transitional water waves' with  $h/L$  of between 0.04 and 0.5, longer period waves with  $h/L$  values  $< 0.04$  fall into the category of 'shallow water waves' (CERC, 1984). The maximum error of 5% in the  $L$  estimate results in an error of  $< 5\%$  in the  $h/L$  estimate.

##### Shoaling coefficient, $K_s$ .

Figure 5.6 shows the sensitivity of  $K_s$  to relative depth,  $h/L$ , as computed with the Matlab attenuation model for waves of period  $T = 4s$  in water depths of  $h = 0.5$  to  $3.0$ , and for different values of water depth decrease,  $dh$ , ( $0.25$  to  $0.5m$ ) between consecutive stations. For  $h/L > 0.14$ , shoaling coefficients are  $\leq 1.0$  for the whole simulated range of  $dh$ . Such waves will slightly decrease in height in spite of the decrease in water depth which has little influence on wave motion at high  $h/L$  values. Waves with  $h/L < 0.14$  experience a height increase ( $K_s > 1.0$ ). The pattern displayed in Figure 5.6(a) is similar to that described in the literature (Horikawa, 1978, CERC, 1984). In a water depth of  $1.5m$ , for example, waves with periods exceeding  $3s$  would result in  $h/L$  values  $< 0.14$  and would experience a height increase. All

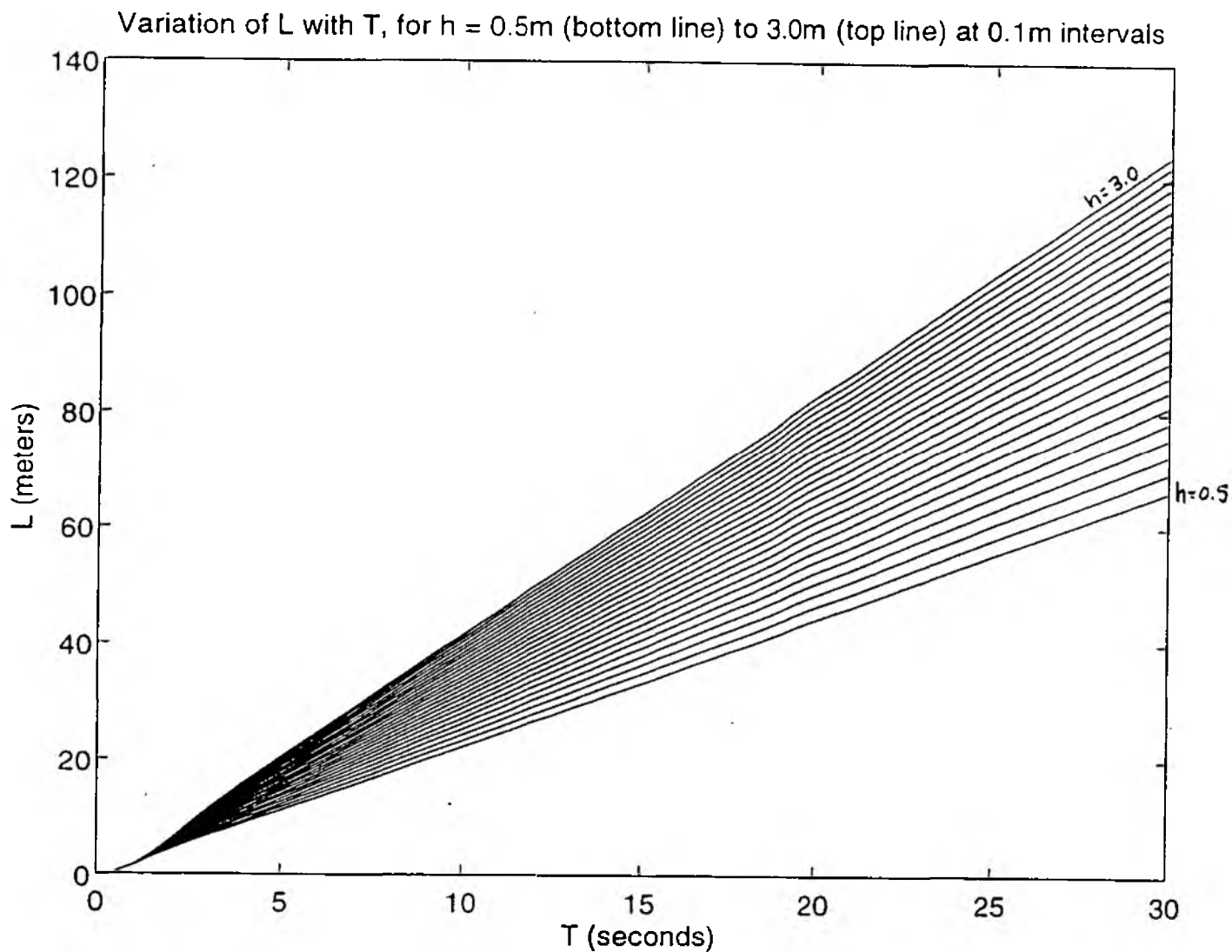


Fig. 5.4: The variation of wave length,  $L$ , with wave period,  $T$ , for varying water depths,  $h$  ( $0.5\text{ m}$  (bottom line) to  $3.0\text{ m}$  (top line) at  $0.1\text{ m}$  intervals), as predicted from the model computations

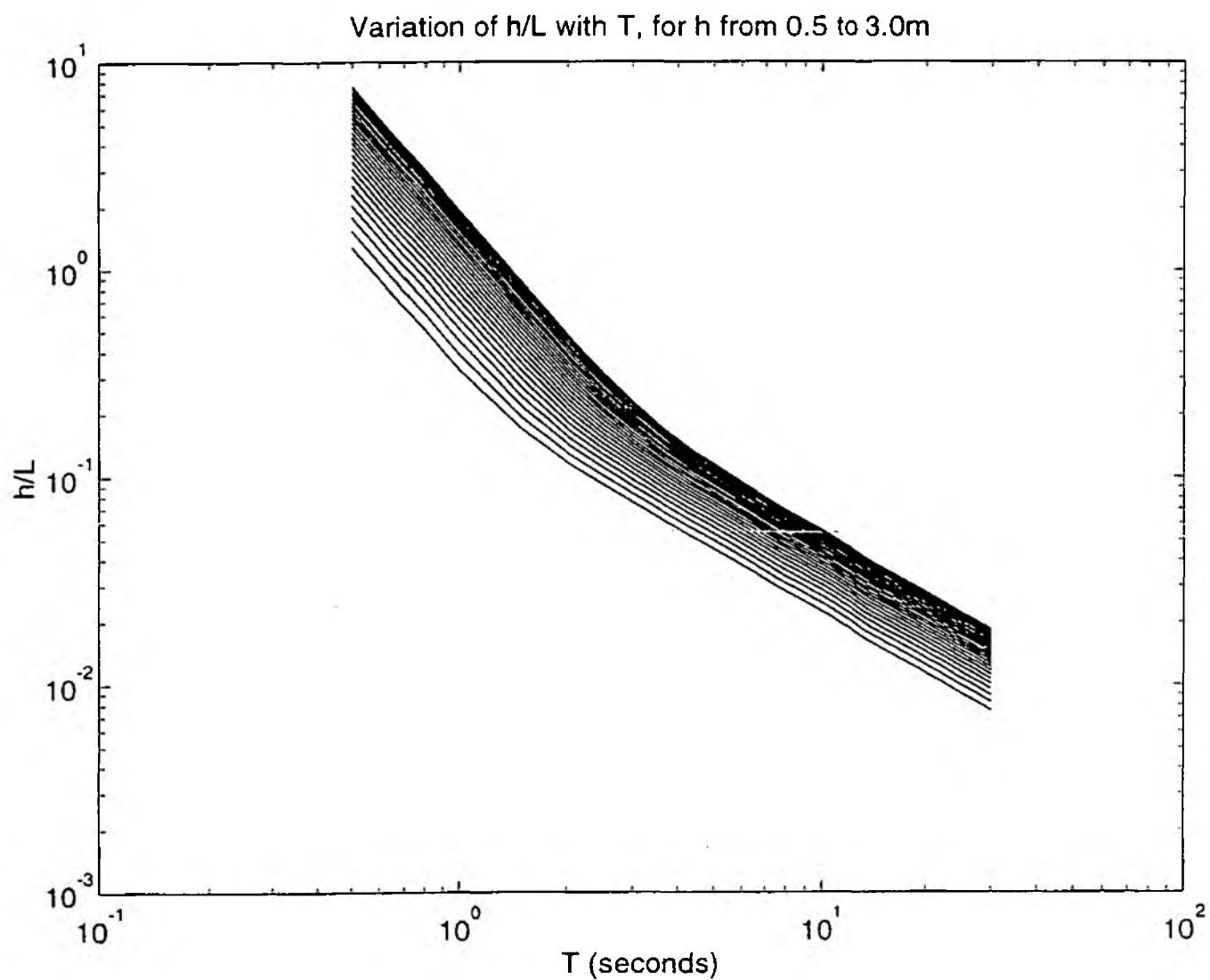
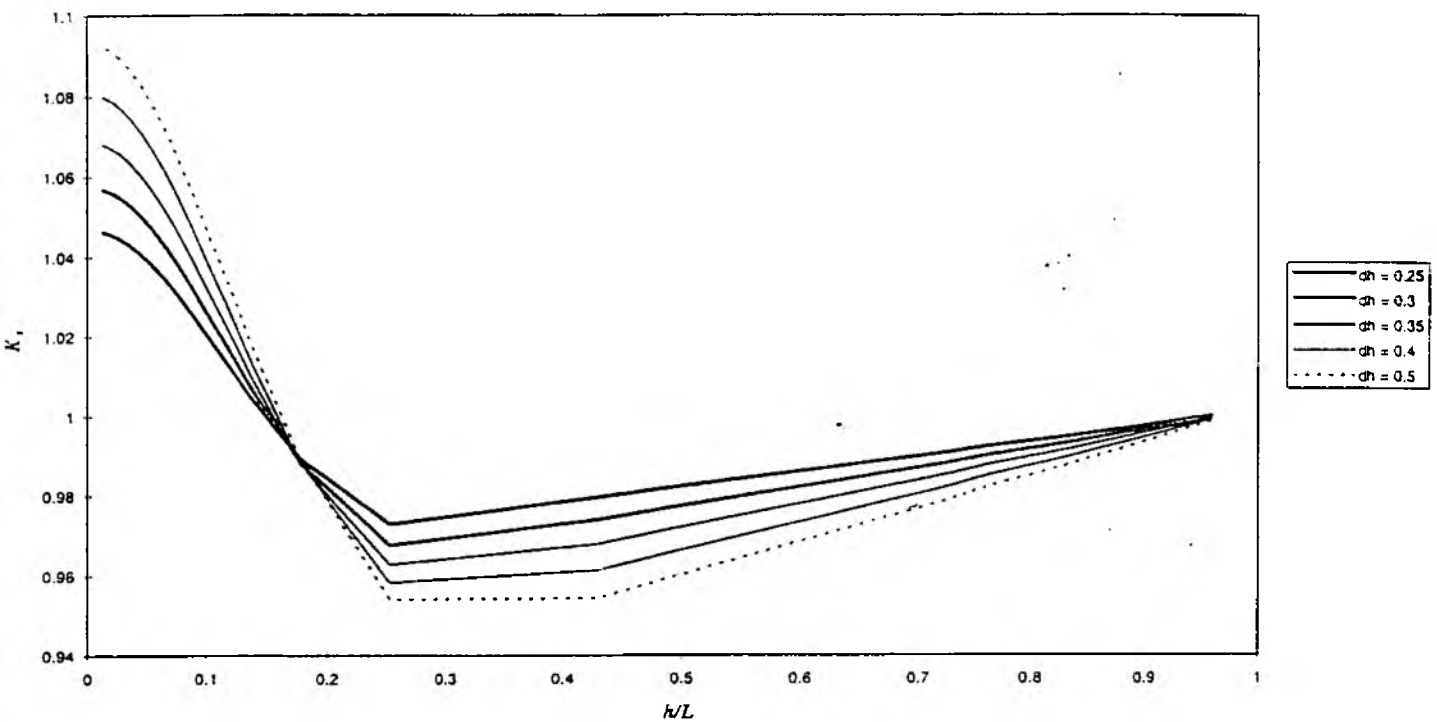


Fig. 5.5: The variation of relative water depth,  $h/L$ , with wave period,  $T$ , for varying water depths,  $h$  (0.5 to 3.0 m), as predicted from the model computations

Variation of  $K_s$  with  $h/L$  ( $T = 0.5$  to  $30s$ )



Variation of  $K_s$  with  $h/L$ , for  $h$  from  $0.5m$  to  $3.0m$

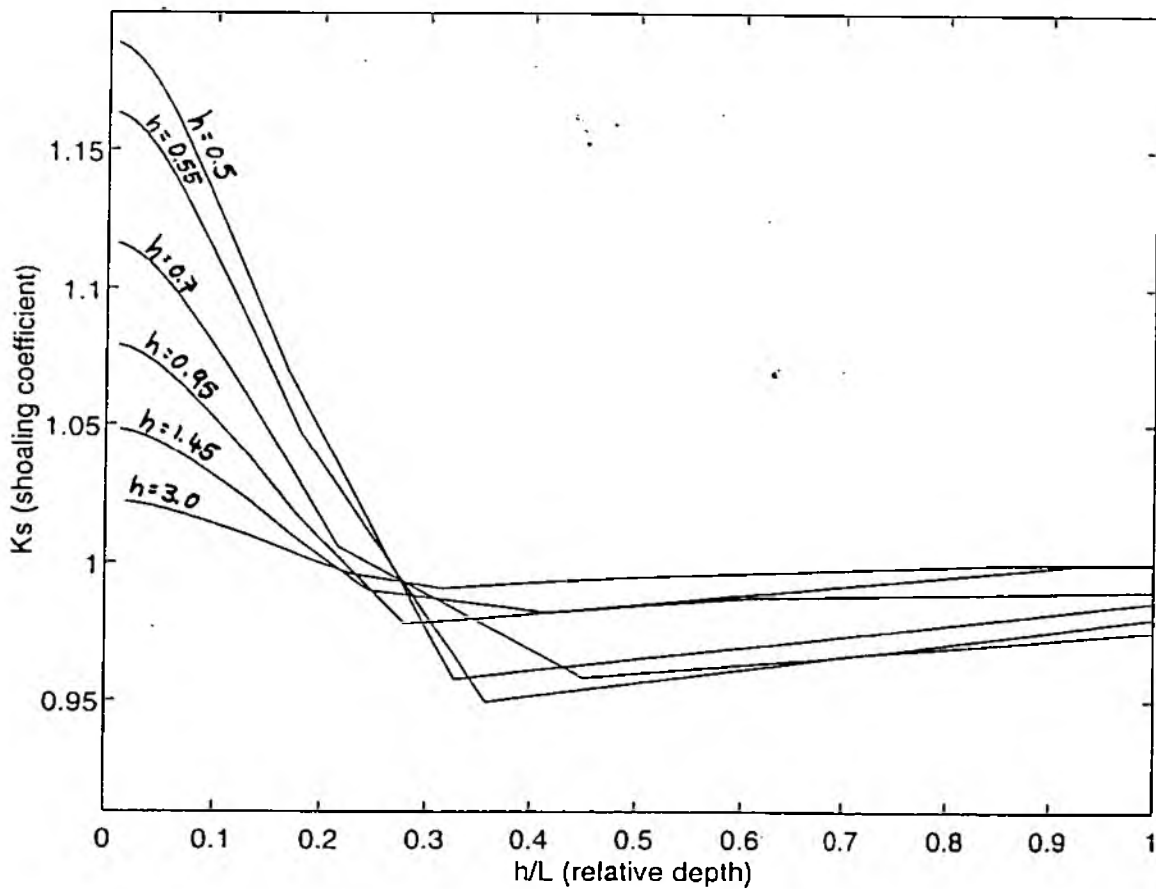


Fig. 5.6: The variation of modelled  $K_s$  with  $h/L$  for (a) varying slopes ( $dh$ ) and (b) varying water depths ( $h$ )

other waves would decrease in height. The variation of  $K_s$  with  $h/L$  for different water depths and wave periods follows a similar pattern (Figure 5.6(b)). At fixed water depths, it is the long period waves that gain most height due to the effect of shoaling. For a given wave period, deeper water results in smaller values of  $K_s$  and a slightly lower  $h/L$  threshold above which  $K_s < 1$ . In a water depth of 3m, for example,  $K_s$  is  $< 1$  for all  $h/L > 0.2$ , whereas in water depths of 0.5m, the respective  $h/L$  threshold is 0.26 (see Figure 5.6(b)). Shoaling coefficients for the wave period/water depth conditions simulated here for a water depth decrease of 0.25m reach a maximum of approximately 1.18 in the case of waves with long periods (30s) in shallow water (0.5m). Shoaling coefficients at Stiffkey are expected to lie below this value, as the water depth decrease over the Stiffkey sandflat and salt marsh is less than 0.25m.

#### **Viscous friction coefficient, $K_v$ .**

The effect of viscous friction is small compared to the effect of shoaling (Figure 5.7). For the  $h/L$  values simulated ( $\nu = 1.36 \cdot 10^{-4} \text{ms}^{-1}$ ,  $dx = 200\text{m}$ ) the decay factor reaches its minimum of just over 0.89 at  $h/L \approx 0.18$  where  $h = 0.5\text{m}$ , and  $T = 1.5\text{s}$ . The variation of  $K_v$  with  $h$  is minimal (the difference in  $K_v$  at  $h/L \approx 0.18$  for  $h = 0.5\text{m}$  and for  $h = 3.0\text{m}$  is approximately 11%). The value of  $h/L$  at which  $K_v$  reaches a minimum, however, decreases slightly with increasing water depth. At a depth of  $h = 0.95\text{m}$ ,  $K_v$  reaches its minimum of 0.96 at  $h/L \approx 0.14$  (22% lower than the respective  $h/L$  threshold for  $h = 0.5\text{m}$ ).

#### **Percolation coefficient, $K_p$ .**

The effect of percolation (calculated using equation 22) for the range of relative depths,  $h/L$ , and percolation coefficients,  $k$ , ( $3.6$  to  $5.6 \cdot 10^{-4} \text{ms}^{-1}$ ) simulated here was negligible (Figure 5.8(a and b)). Although the variation of  $K_p$  followed a similar pattern to that of  $K_v$  with a minimum at  $h/L \approx 0.18$  and a slight increase for increased values of  $k$  and  $d$ , the values of  $K_p$  never decreased below 0.9999. The existence of an intermediate threshold value of  $T$  for which the attenuation reaches a maximum is explained by the fact that the energy dissipation due to percolation is proportional to the product of the pressure on the bed,  $p$ , and the velocity of the flow into and out of the bed,  $u$ . For waves with shorter periods, the pressure on the bed decreases and results in a decrease of  $pu$ . For waves with longer periods,  $p$  tends towards a limiting value and  $u$  decreases due to an increase in the distance between the points of maximum and minimum pressure under the wave (i.e.  $0.5L$ ). As a result  $pu$  also decreases.

#### **Bottom friction, $K_f$ .**

Bottom friction, together with wave shoaling, dominates wave transformation in this model. The maximum effect of surface friction on wave height is reached where  $h/L \approx 0.12$ . This is true for the range of all wave height, period, water depth, and friction coefficients simulated here (Figure 5.9(a to d)). A decrease in the friction factor from  $f = 0.1$  to  $0.5$ , however, increases the minimum value of  $K_f$  by 15% from 0.85 to 0.98 (Figure 5.9(a)). A friction factor of 0.05 has

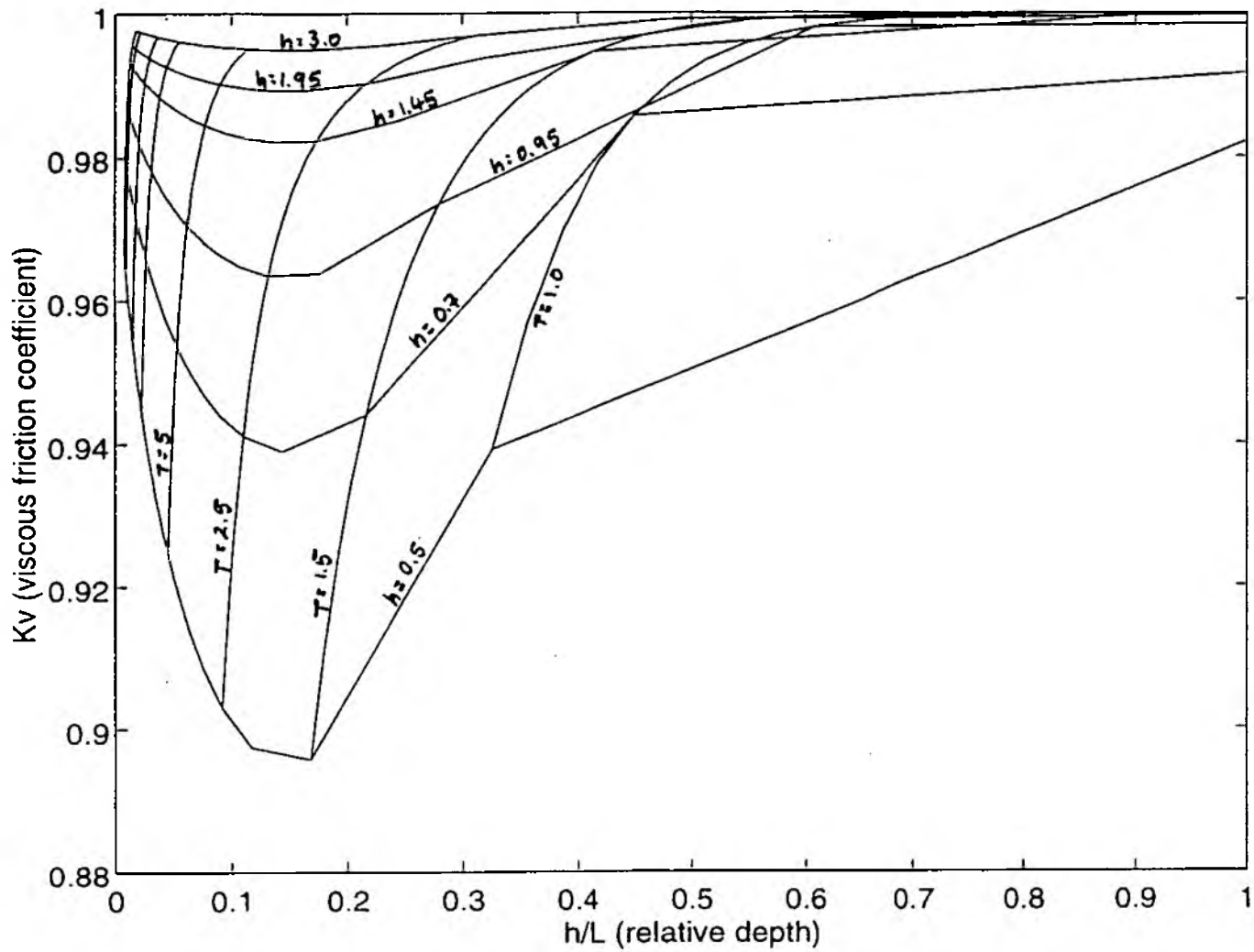


Fig. 5.7: The variation of modelled  $K_v$  with  $h/L$  for varying  $T$  and  $h$

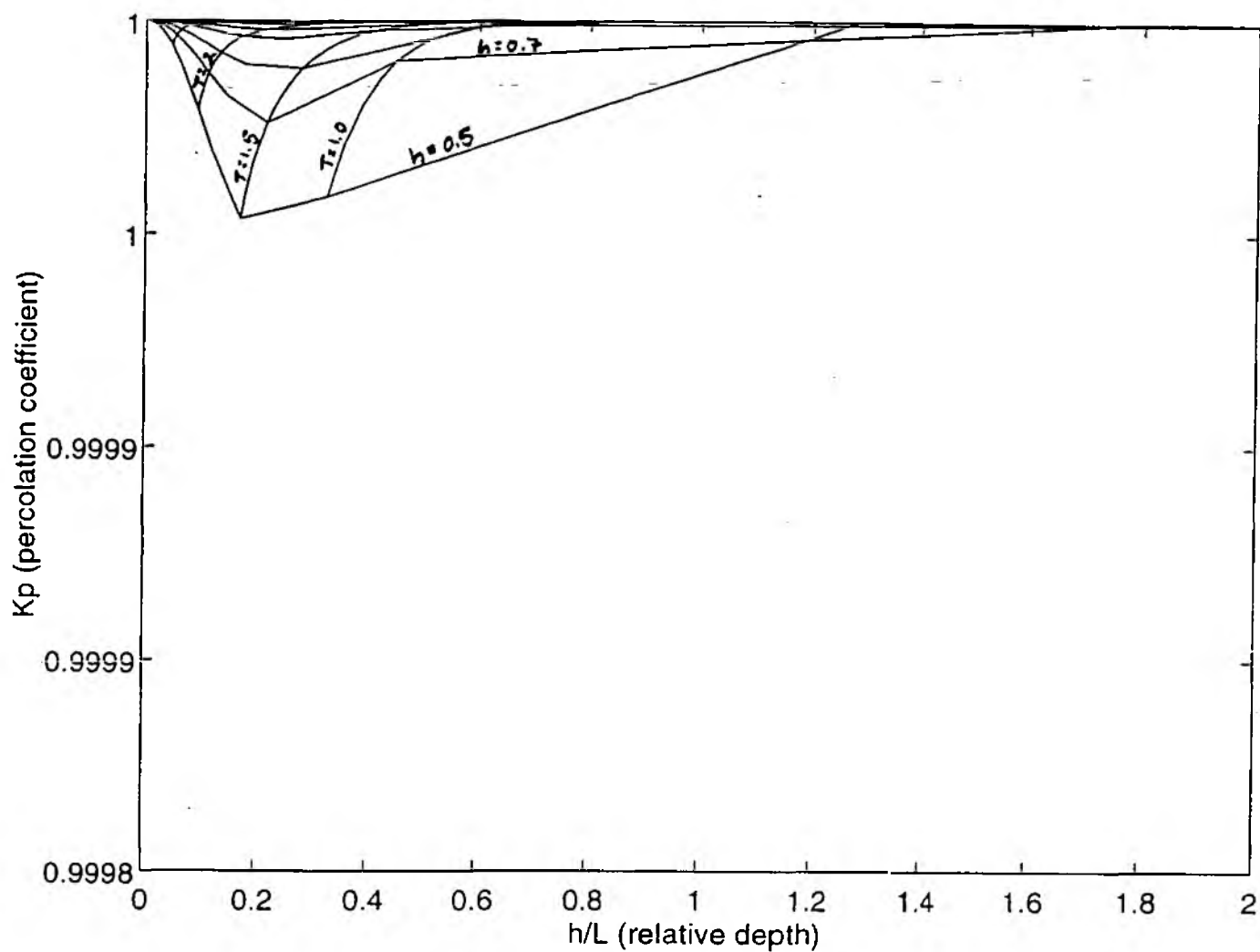


Fig. 5.8: The variation of modelled  $K_p$  with  $h/L$  for varying  $T$  and  $h$ .  
(a)  $d = 0.2$

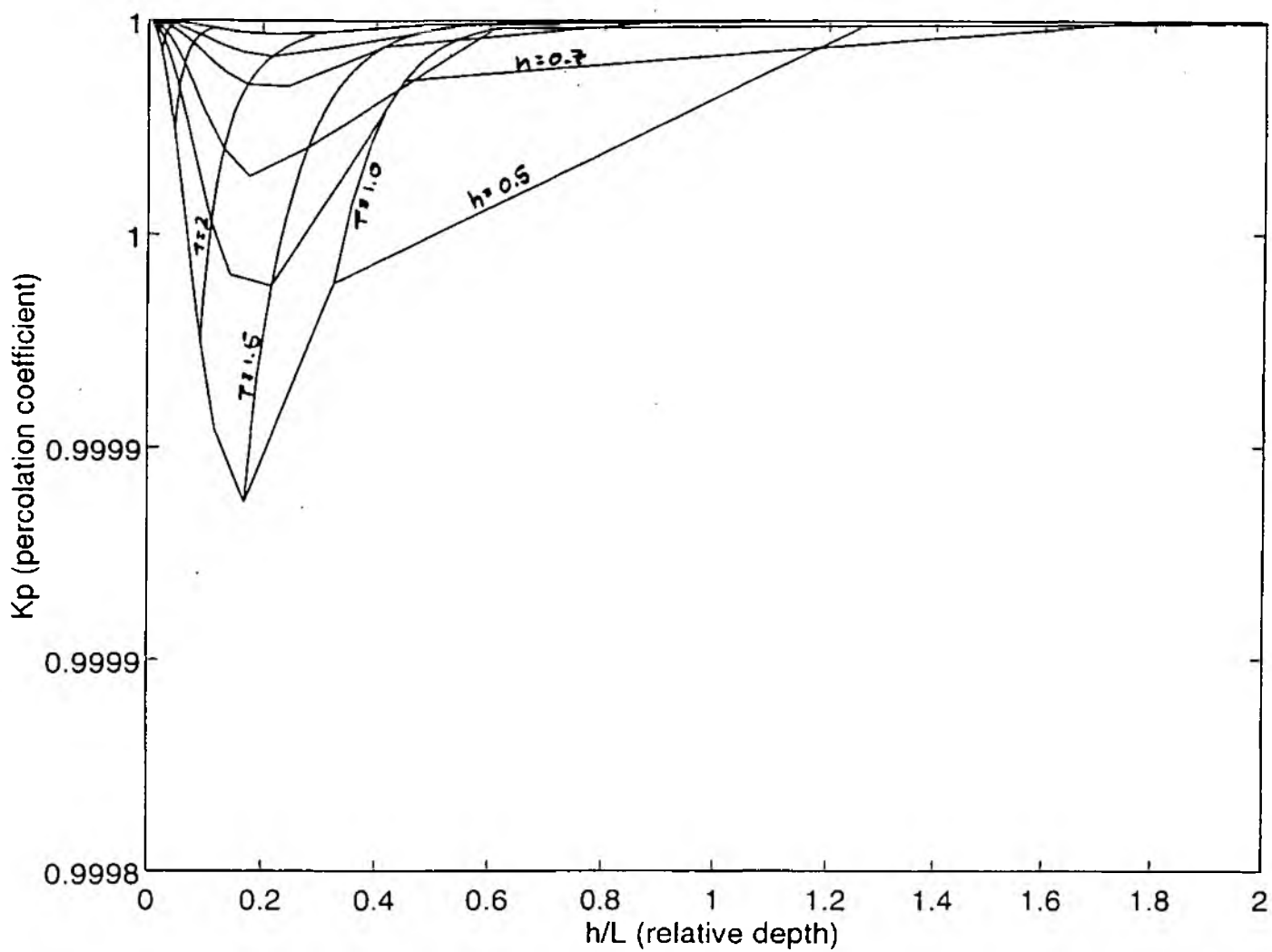


Fig. 5.8: The variation of modelled  $K_p$  with  $h/L$  for varying  $T$  and  $h$ .  
(b)  $d = 1.0$



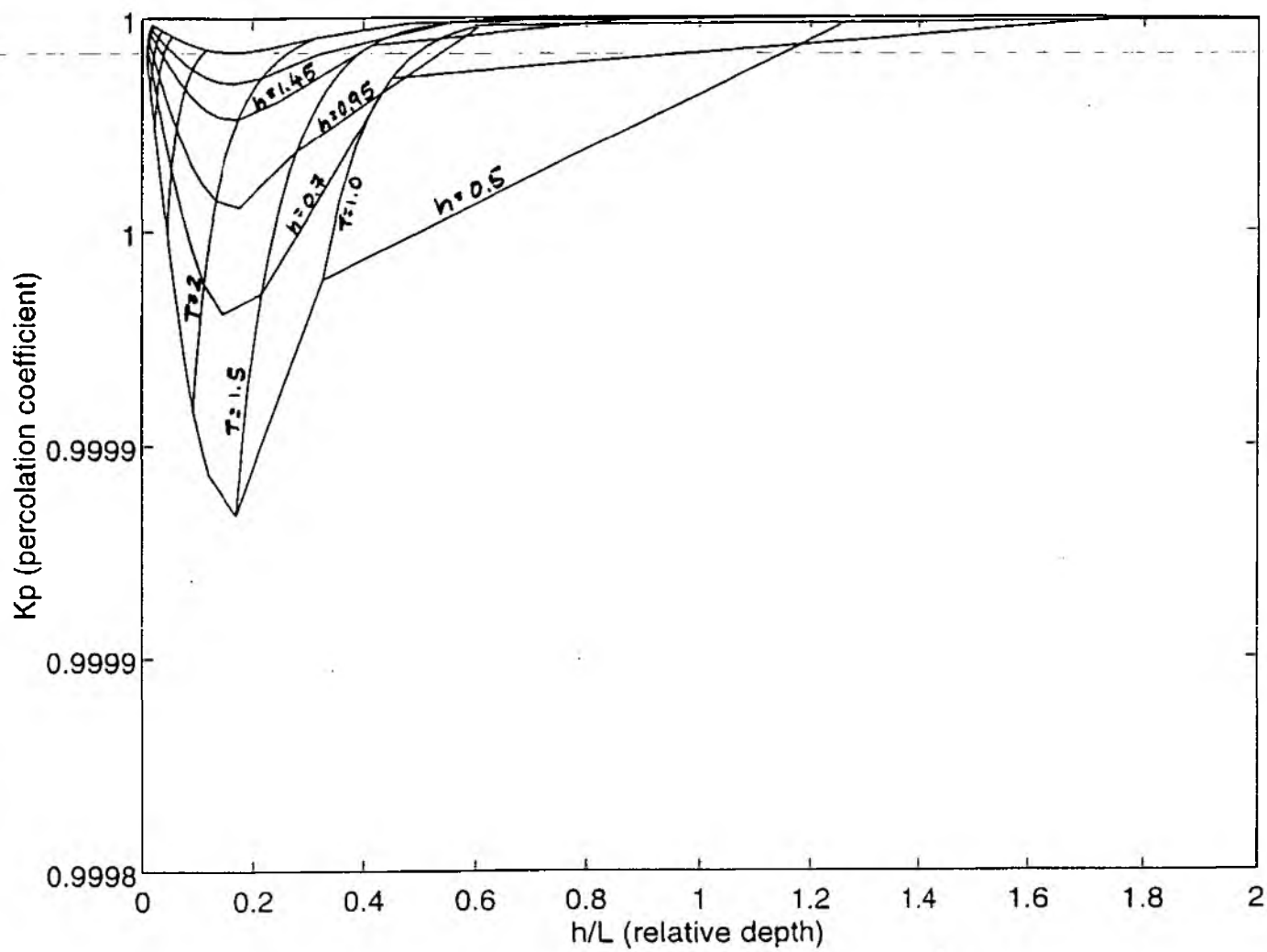


Fig. 5.8: The variation of modelled  $K_p$  with  $h/L$  for varying  $T$  and  $h$ .  
(c)  $d = \bullet$ .

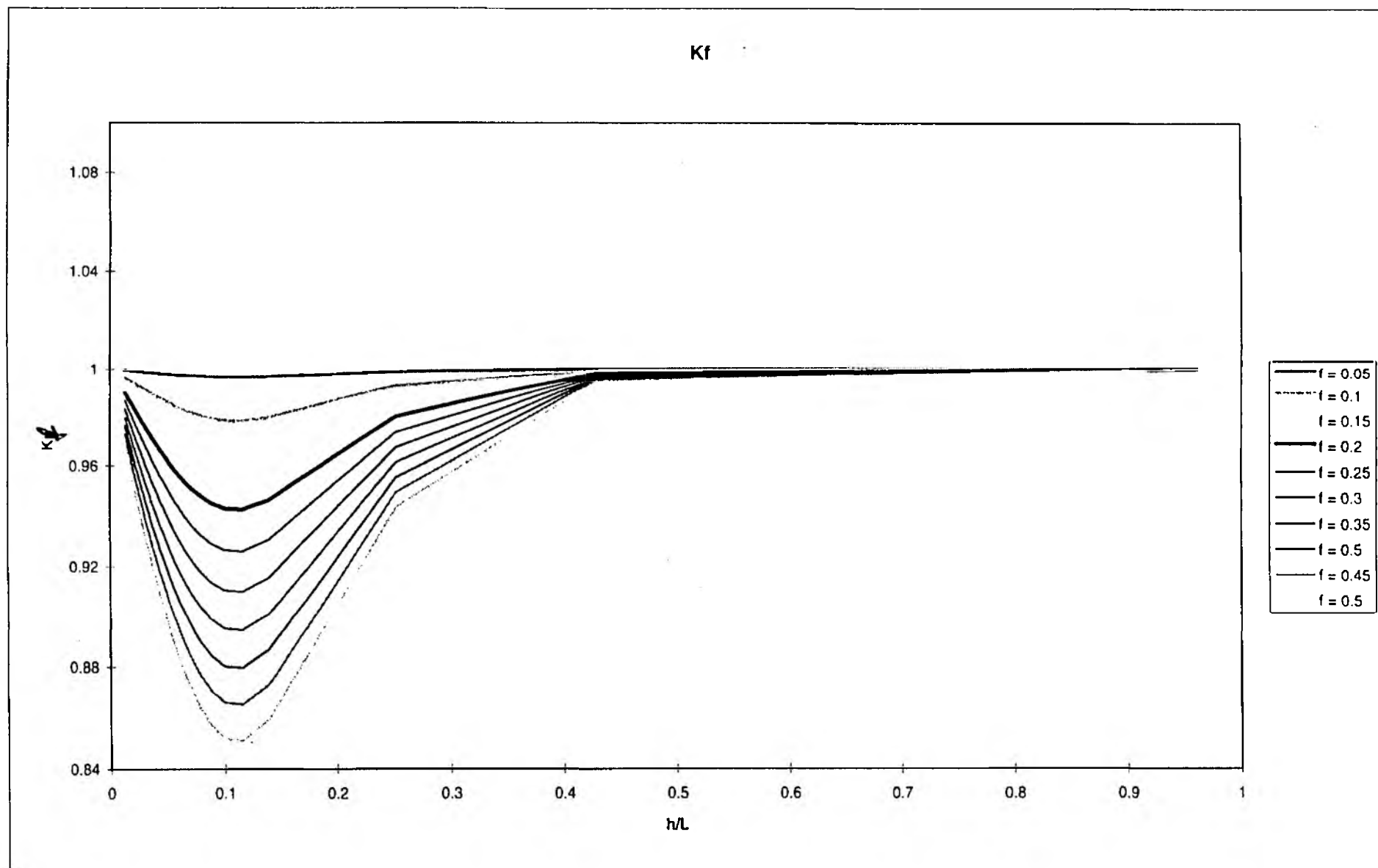


Fig. 5.9: The variation of modelled  $K_f$  with  $h/L$  for (a) varying  $f$  ( $h = 1.5\text{m}$ ,  $H = 0.2\text{m}$ ,  $dh = 0.25\text{m}$ ,  $dx = 200$ )

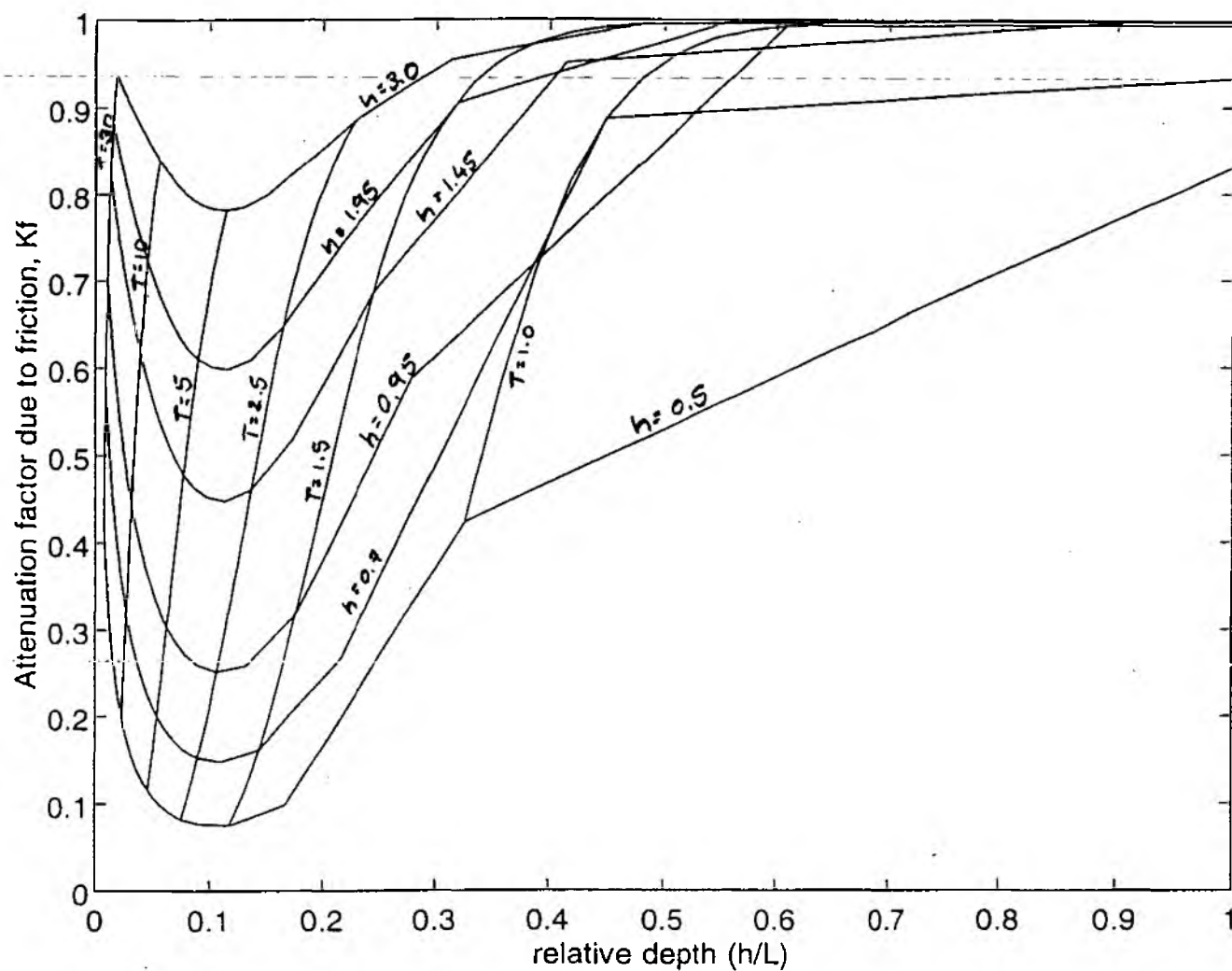


Fig. 5.9: The variation of modelled  $K_f$  with  $h/L$   
 (b) varying  $T$  and  $h$  for  $f = 0.1$ ,  $H = 0.6\text{m}$ ,  $dx = 200$ ,  $dh = 0.25$

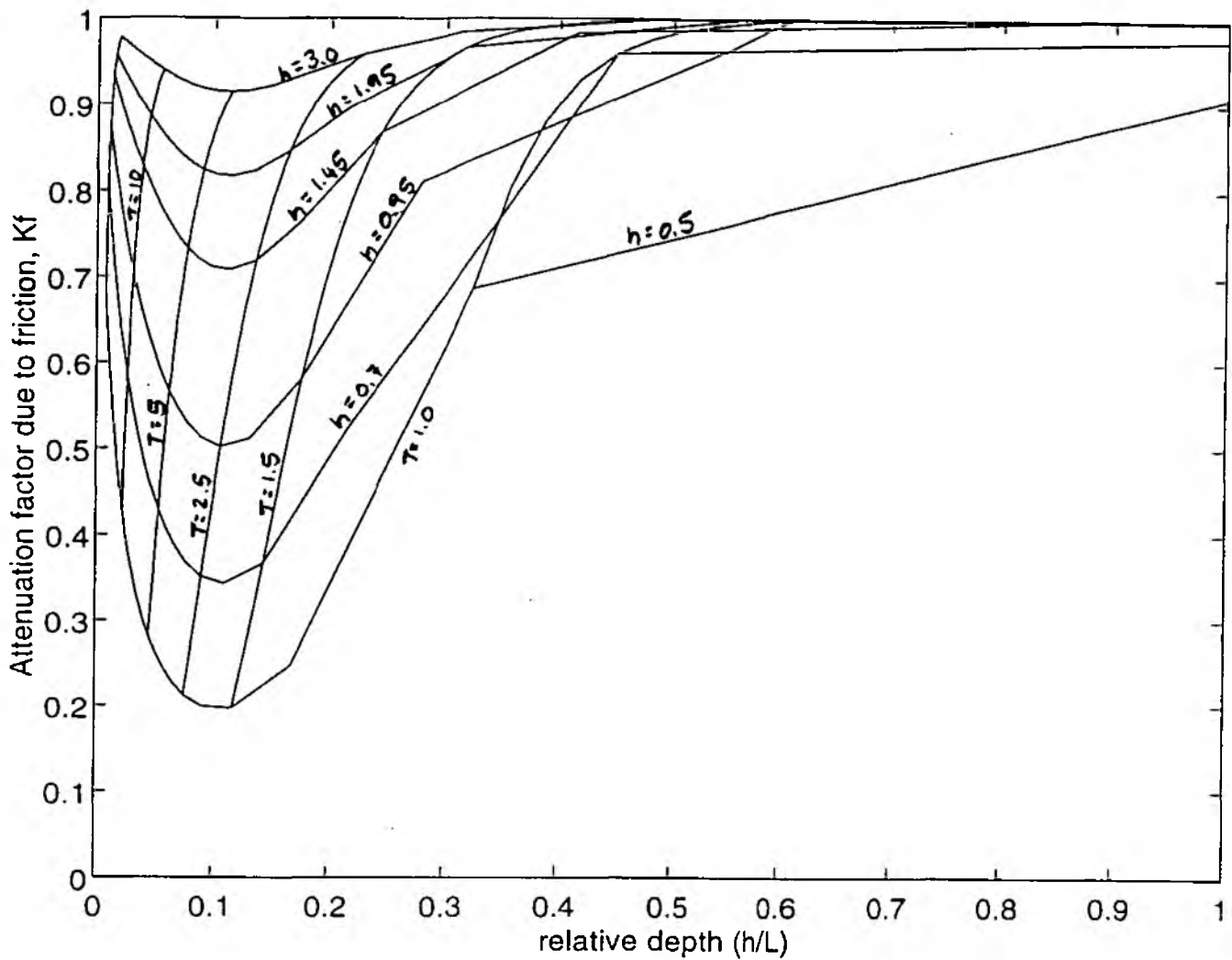


Fig. 5.9: The variation of modelled  $K_f$  with  $h/L$   
(c) varying  $T$  and  $h$  for (c)  $f = 0.1$ ,  $H = 0.2\text{m}$ ,  $dx = 200$ ,  $dh = 0.25$

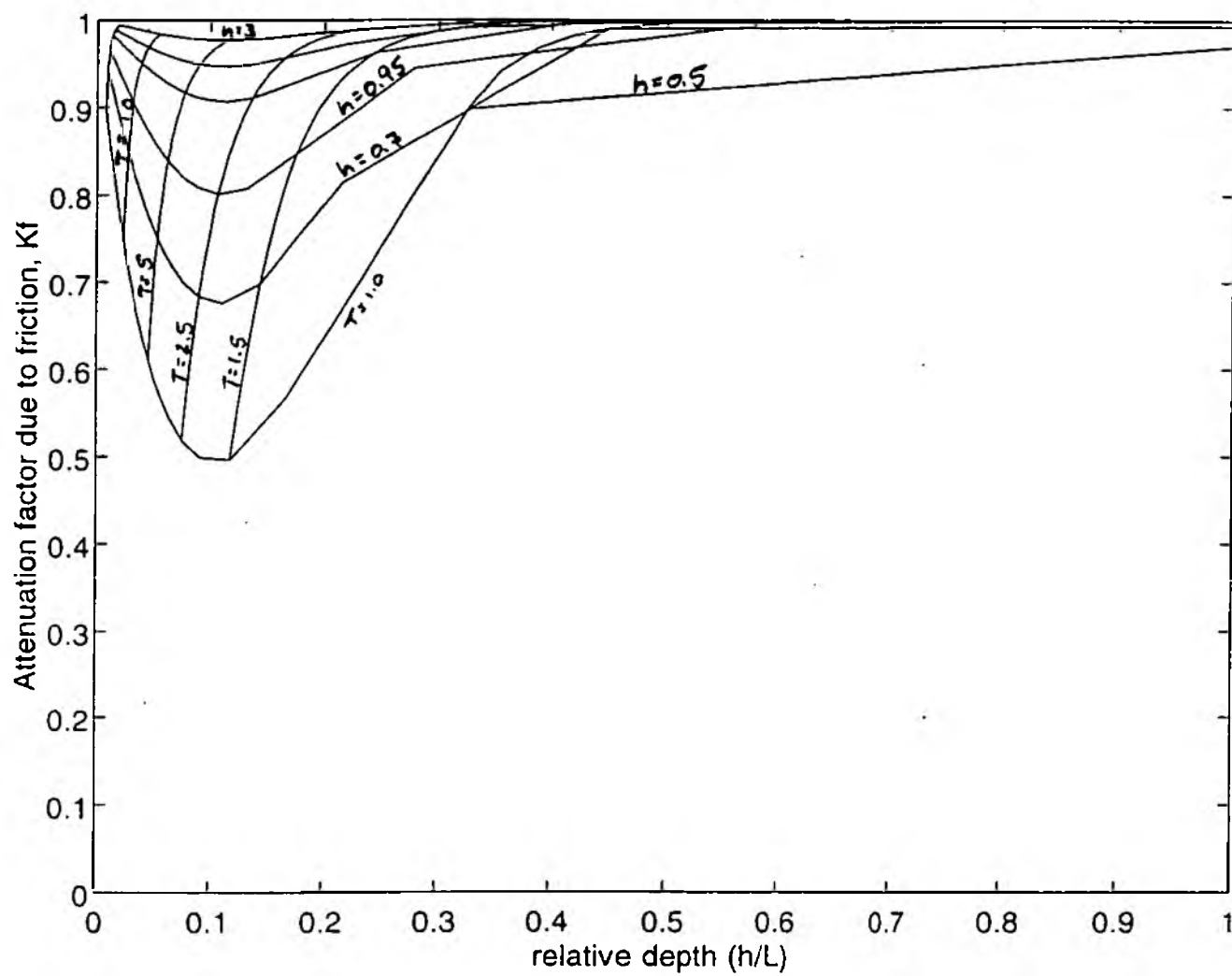


Fig. 5.9: The variation of modelled  $K_f$  with  $h/L$   
 (d) varying  $T$  and  $h$  for  $f = 0.1$ ,  $H = 0.05\text{m}$ ,  $dx = 200$ ,  $dh = 0.25$

no effect on wave heights, as  $K_f$  is approximately equal to 1.0 for this value of  $f$ . The sensitivity of  $K_f$  to wave height can be derived from Figure 5.9b, c, and d: A wave height decrease of 67% from 0.6 to 0.2m results in a 185% increase of  $K_f$  from 0.07 to 0.20. For a further decrease in wave height by 75% to 0.05m,  $K_f$  increases by 145% from 0.20 to 0.49. For values of  $h/L > 0.45$ ,  $K_f$  is negligible for the range of wave periods and water depths simulated. As  $h/L$  decreases below 0.12 in a wave depth of 1.5m,  $K_f$  increases (i.e. wave height attenuation decreases) at a rate of ca 1% for every 10% decrease in  $h/L$ . For a water depth of 1.5m, this means that waves with periods of around 3.5s experience the largest height reduction due to bottom friction and that waves with periods smaller than 1.5s are not influenced by bottom friction. This sensitivity of  $K_f$  to  $h/L$  for  $h/L < 0.12$  increases with decreasing water depth (Figure 5.9(b to d)). The maximum decay at an intermediate value of  $h/L$  for a given water depth occurs for a similar reason as explained in the case of  $K_p$  above: on the one hand, in the case of short waves in relatively deep water, wave motion does not interact with the sea bed; on the other hand, for a given water depth and bottom friction, an increase in wave period and therefore wave length (i.e. an increase in  $h/L$ ) beyond a critical value causes a decrease in the horizontal component of the velocity at the bed and therefore a reduction in the shear stress and in energy dissipation (Sleath, 1984).

#### **Combined effect, $K$ .**

The combined effect of shoaling, viscous and bottom friction, and percolation on wave heights (Figure 5.10) is highly dependent on relative depth,  $h/L$ . The overruling effect of shoaling and bottom friction relative to percolation and viscous friction is apparent in the shape of the curve in Figure 5.10. For the conditions modelled here, the combined decay factor reaches its minimum value of 0.93 at a relative depth of 0.18. In a water depth of 1.5m, this refers to a wave period of 2.5s. Beyond this  $h/L$  threshold,  $K$  increases gradually and reaches a value of 1.0 at  $h/L$  of 0.96. For  $h/L < 0.18$ ,  $K$  increases rapidly and for values of  $h/L < 0.036$ ,  $K > 1.0$  as the effect of shoaling dominates over the effect of energy dissipation. In a water depth of 1.5m this means that waves with periods  $> 1$  s will increase in height, whereas waves with periods  $< 1$  s will decrease in height.

#### **5.4.3 Conclusions**

The wave attenuation model based on equations developed theoretically and in laboratory experiments produced estimates of wave height reduction which seem realistic given the range of input water depth, wave, and surface parameters to be expected at open coast salt marsh sites. The error in the estimate of wave length,  $L$ , from information on wave period and water depth results in an  $h/L$  error of less than 5%. The error in the model simulations is therefore likely to be low ( $< 5\%$ ). The sensitivity of wave attenuation to changes in relative depth varies

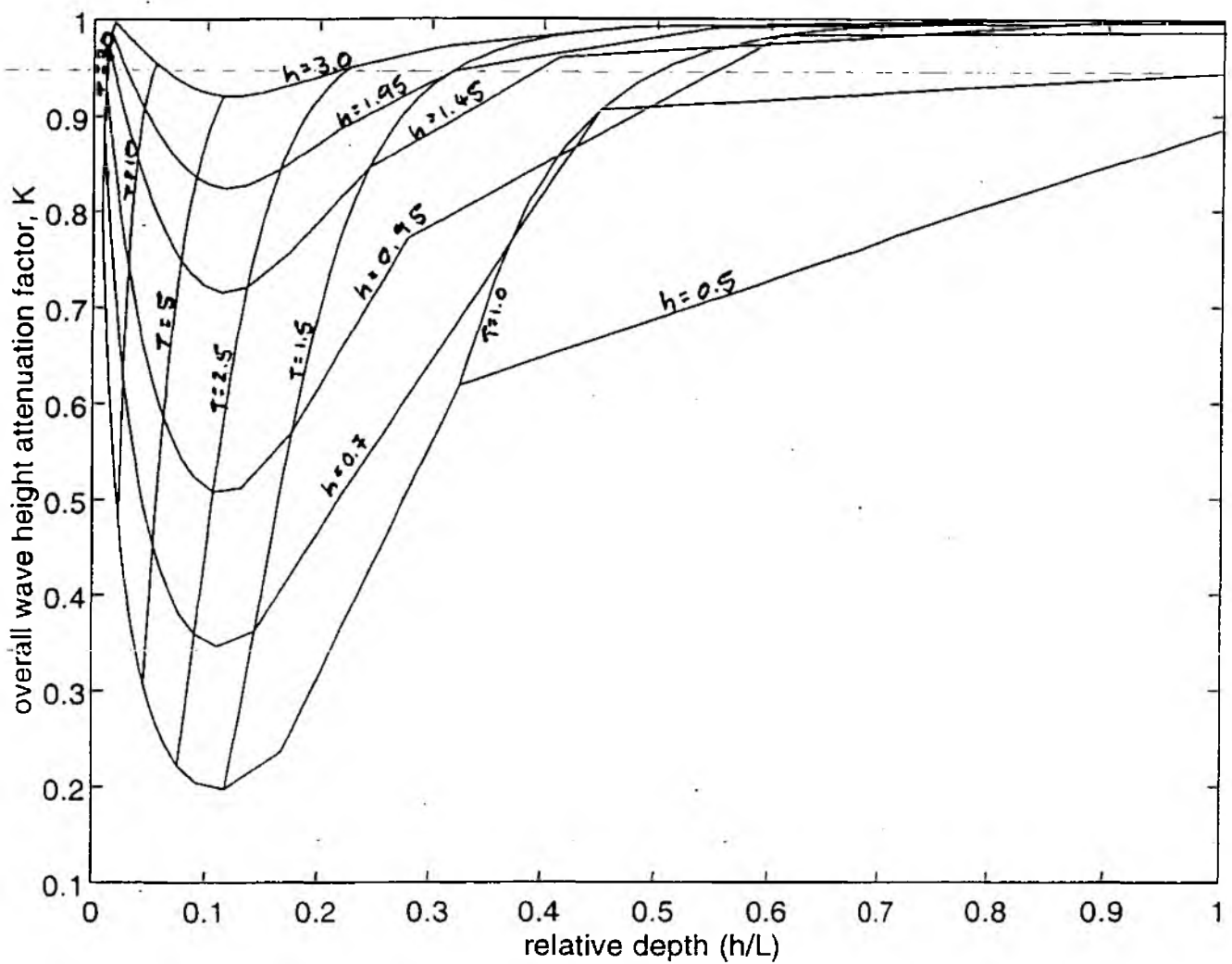


Fig. 5.10: The variation of  $K$  with  $h/L$  ( $\nu = 1.36 \cdot 10^{-6}$ ,  $dx = 200$ ,  $dh = 0.05$ ,  $H = 0.2$ ,  $f = 0.1$ ,  $k = 4 \cdot 10^{-4}$ ,  $d = 1.0$ ,  $T = 0.5\text{s}$  to  $30\text{s}$ ,  $h = 0.5$  to  $3.0$  m).

with respect to the individual energy dissipation processes, with attenuation due to surface friction varying most strongly with changing  $h/L$ . Over the range of water depth and wave conditions simulated and based on the assumptions discussed above, the wave height decay predicted from the model is less than 1% in the case of percolation and less than 10% in the case of viscous friction. Attenuation due to percolation into the sea bed is therefore negligible in all these water depth/wave conditions. The effect of viscous friction can be neglected for water depths  $> 1.5\text{m}$ , for which the wave height decay is less than 1%.

## **5.5 Model application to the Stiffkey sandflat/salt marsh transect**

### **5.5.1 Introduction**

To assess the applicability of the theoretical model to field conditions, the model was used to simulate wave attenuation across the sandflat and the salt marsh surfaces at the Stiffkey field site in Norfolk. As mentioned in section 4.3.6 (assumption 5) above, the spectral wave with maximum energy and period  $T_{max}$  can be used to approximate wave spectrum attenuation. In the case of the Stiffkey field wave spectra, the period of the wave with maximum energy varies between the three transect stations. The theoretical formulae used in the model, however, assume the wave period to remain constant along the shore-normal transect. It was therefore decided to use the zero-upcrossing period,  $T_z$ , for the computation of expected wave attenuation at Stiffkey as  $T_z$  varies little between the stations for a given record. In addition, the wave height parameter  $H_{rms}$  was used, as this parameter most accurately represents the average wave height of a time-series.

For each of the 54  $H_{rms}$  wave heights observed at the outer and the middle station of the Stiffkey transect, the wave heights expected at the following station can be calculated using the equations for the effect of shoaling, friction, and percolation mentioned above. To carry out these calculations, a 'Matlab' program ('attmodel.m') was written. Wave height change due to shoaling is calculated from information on surface slope which can be assumed constant over the period of wave measurement. Similarly, viscous friction and percolation are approximated using values for viscosity stated in the literature and from field data on the grain size distribution of the sand/mud substrate. As viscous friction and percolation play a relatively minor role in wave attenuation, errors in these estimates are unlikely to lead to large errors in the overall attenuation coefficient. The computation of frictional decay, however, is problematic as the surface characteristics which determine the friction factor,  $f$ , (for example sand ripples, distribution and structural properties of vegetation) can vary over small time scales (in response to tidal circulation or seasonal change). The program therefore only calculates  $K_s$ ,  $K_v$ , and  $K_p$ .



On the basis of the observed wave heights at the outer (sandflat) or middle (marsh edge) wave recording station, "attmodel.m" generates values for wave heights to be expected at the next station, i.e. the middle or inner (marsh) station. The breaking criterion (equation 25) is applied to all the calculated wave heights, so that the maximum steepness of the waves satisfies Miche's formula. These expected wave heights can then be compared to those observed and conclusions can be drawn as to the possible causes of wave attenuation in the field. Based on the assumption that the computation of  $K_s$ ,  $K_v$ , and  $K_p$  was accurate, it is then possible to deduce the value of the friction factor,  $f$ , which would be required to explain any discrepancy between expected and observed wave attenuation. Conclusions regarding the validity of the mathematical equations under specific field conditions and the accuracy of the field data can also be drawn.

### 5.5.2. Input variables

Of the input parameters of Table 5.1 required for running the model, the first six are known from field observations and measurements. The remainder of variables was estimated indirectly from field data or was based on values quoted in the literature. The field data used included the recorded wave spectra, field measurements of surface characteristics and sandflat/salt marsh topography:

- 1) Observed  $H_{rms}$  wave heights (termed  $H_1$  and  $H_2$  for the outer and the marsh edge station respectively) at the beginning of each transect section are known. Water depths ( $h_1$  and  $h_2$ ) are the mean water surface elevation measured during wave recording and wave periods ( $T_1$  and  $T_2$ ) are the computed zero-upcrossing periods at the outer and middle station (i.e. the seaward end of the sandflat and salt marsh transect section) respectively. Information on wave lengths is obtained from water depths and wave periods.
- 2) The slope of the sandflat transect ( $dh_1 = 0.00112$ ), the salt marsh transect ( $dh_2 = 0.0196$ ) and the distance across the sandflat ( $dx_1 = 196.72\text{m}$ ) and across the salt marsh ( $dx_2 = 179.82\text{m}$ ) are obtained from field surveys.
- 3) The dynamic viscosity of sea water,  $\nu$ , was assumed to be  $1.36 \cdot 10^{-6} \text{ m}^2\text{s}^{-1}$ , a value quoted in Vogel (1981) and Denny (1989) for seawater at temperatures of around  $10^\circ\text{C}$ .
- 4) The specific permeability,  $K$ , was calculated from the grain size distribution of the sandflat sediment. This was very well sorted with a median size of  $250\mu\text{m}$ . A permeability coefficient,  $k$ , of  $2.42 \cdot 10^{-3} \text{ ms}^{-1}$ , was calculated on the basis of equation (16) and (18) above. Porosity,  $n_p$ , was assumed to be around 0.3, a value given by Sleath (1984) for uniform sand. The sand shape factor,  $B$ , was set to 6.0 (values of 6.0 referring to spherical and 7.7 to completely angular grains). As suggested by Sleath (1984), the packing factor,  $A$ , was set to 5.0.

5) The depth of the permeable layer,  $d$ , is defined to be 2m. For this depth,  $K_p$  behaves approximately the same as for infinite values of  $d$  (see Figure 5.8(c)). This agrees with the assumptions in the literature on energy dissipation over permeable seabeds (for example Macpherson (1980)).

The same assumptions as mentioned above (section 4.3.6) are made with regard to the direction of wave travel and the nature of wave energy dissipation. In addition, the marsh surface is assumed to be smooth, i.e. the effect of any marsh topography other than the general surface slope is ignored.

### 5.5.3 Model results and discussion

The 'attmodel.m' output includes the computed values of  $K_s$ ,  $K_v$ , and  $K_p$  for each of the observed incident wave conditions at the station on the sandflat and at the sandflat/salt marsh transition. When multiplying the incident wave height with the combined decay factor,  $K_{mod}$  ( $=K_s K_v K_p$ ), one obtains the wave height expected at the respective landward station (i.e. at the marsh edge or at the back of the marsh),  $H_{2mod}$ , due to shoaling, viscous friction, and percolation. Below, the modelled values of  $K_s$ ,  $K_v$ ,  $K_p$ , and  $K_{mod}$  and their variation with observed  $h/L$  are discussed with reference to graphical model output shown in Figures 31 to 38.

#### 5.5.3.1. Wave decay due to shoaling, viscous friction, and percolation

##### The sandflat.

Across the sandflat section of the transect, modelled decay factors due to percolation are negligible ( $K_p \approx 1.0$ ) for the given permeability, incident wave heights,  $H_{rms}$ , wave periods,  $T_s$ , and water depths,  $h$ , observed at the outer station. Shoaling coefficients are greater than 1.0 in all but three cases, but all are small ( $< 1.05$ ) (Figure 5.11(a)). Viscous boundary layer friction is small, with  $0.96 < K_v < 0.99$ . As expected from the sensitivity analysis (see Figure 5.6),  $K_s$  decreases with increasing relative depth,  $h/L$ , (Figure 5.12(a)). Over the relative water depths encountered at the Stiffkey sandflat, this relationship appears to be linear. The three cases where  $K_s < 1.0$ , i.e. where there is no increase in wave height due to shoaling, occurred when relative depth was largest ( $h/L > 0.2$ ). The maximum value of  $K_s = 1.04$  occurred at the lowest relative depth of 0.116. The two decay factors,  $K_p$  and  $K_v$ , in contrast, show no relationship to observed  $h/L$ . As a result of the dominant dependence of shoaling on  $h/L$  and the much smaller influence of viscous friction and percolation, the combined decay factor,  $K_{mod}$ , also decreases linearly with relative depth (Figure 5.13) and is smaller than 1.0 for  $h/L$  values in excess of approximately 0.13. None of the values of  $H_{2mod}$  exceed the respective critical breaking height

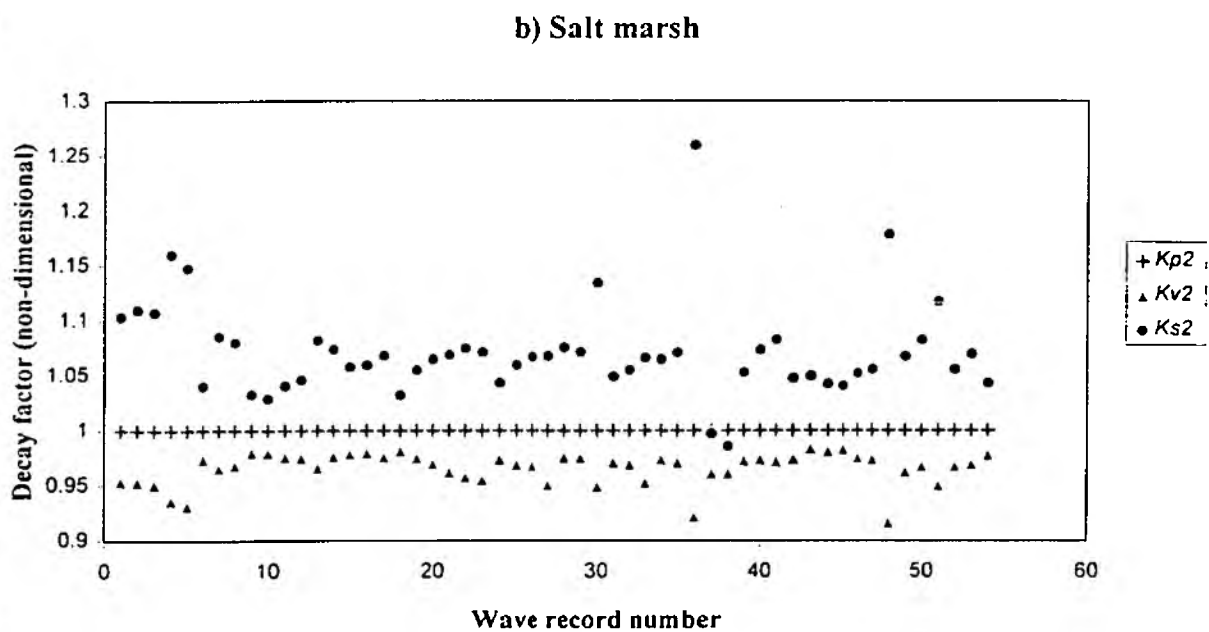
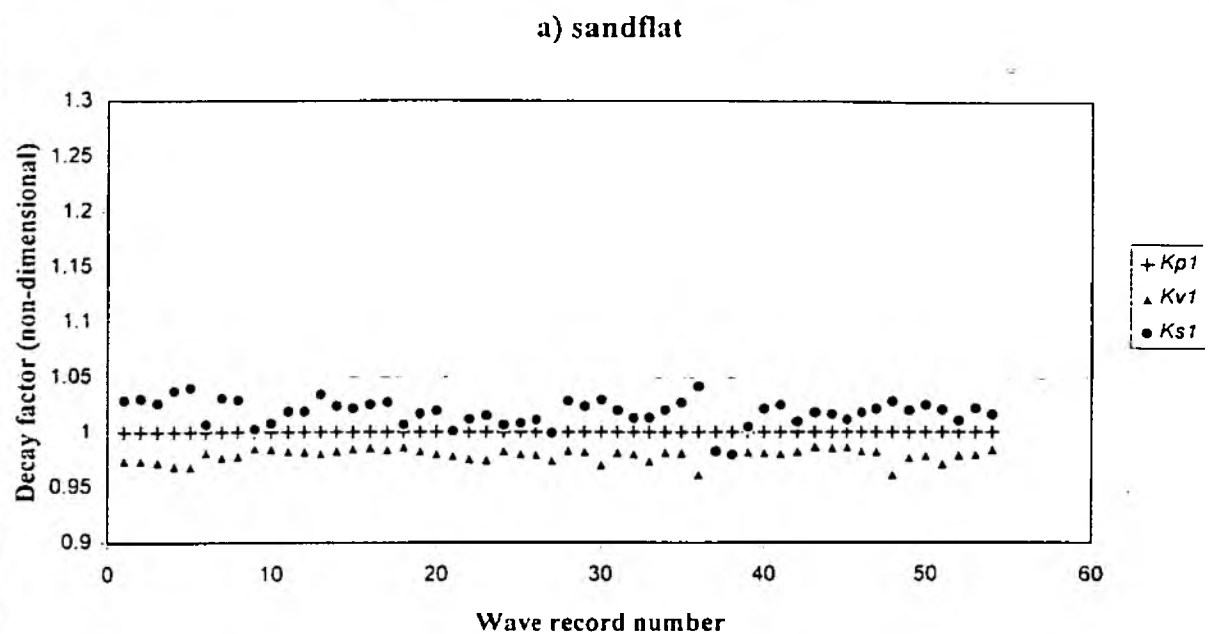


Fig. 5.11: Variation of  $K_S$   $K_P$   $K_V$  for the 54 records for (a) the sandflat, (b) the salt marsh

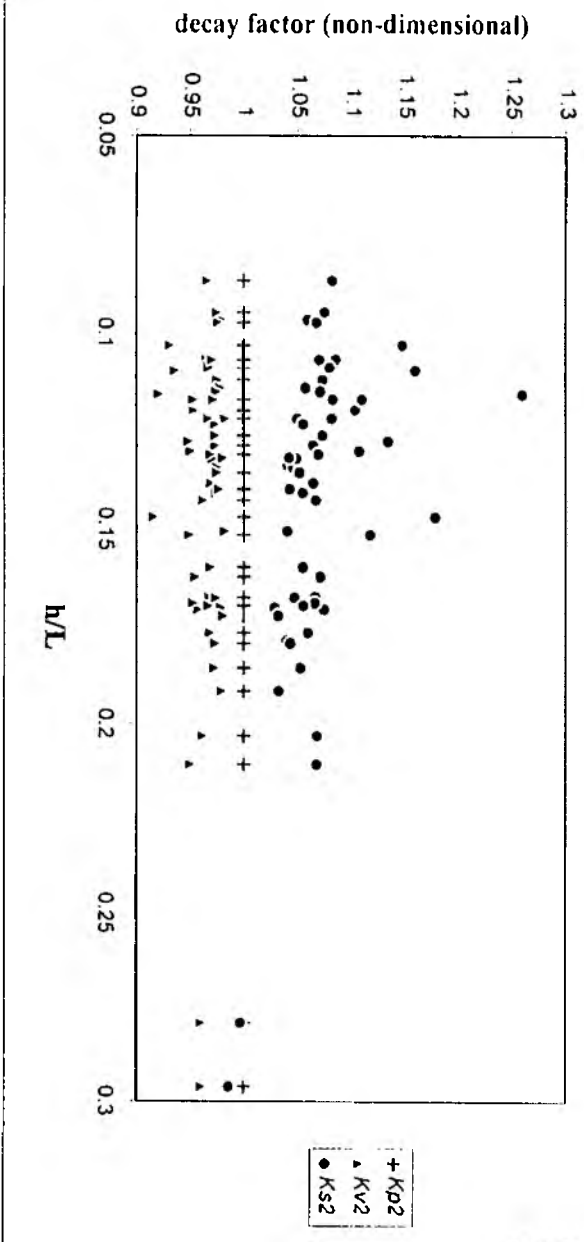
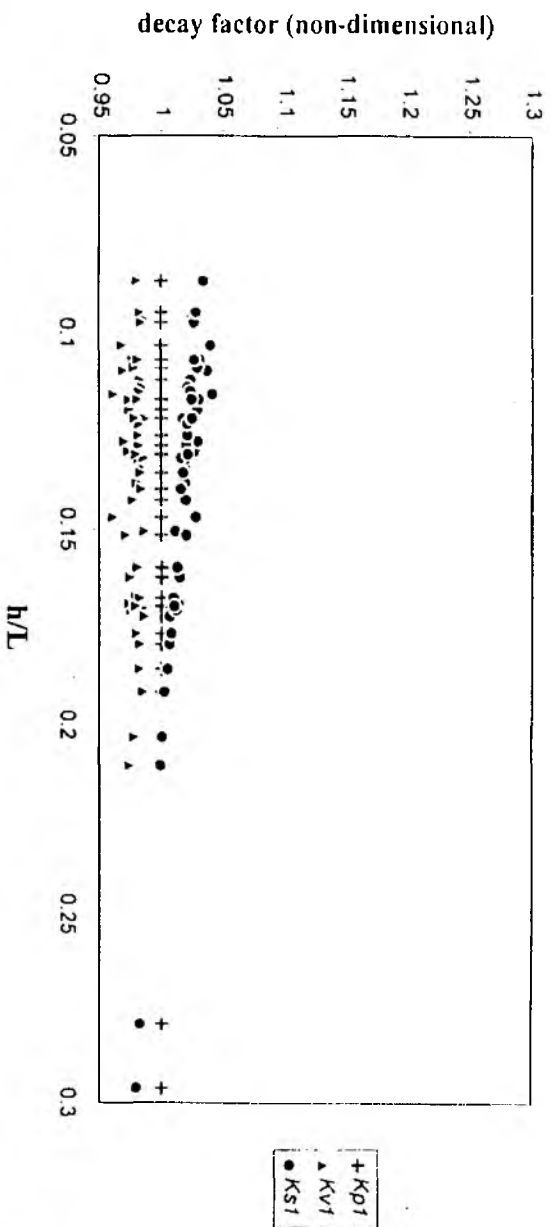


Fig. 5.12: Variation of  $K_s$   $K_p$   $K_v$  with  $h/L$  for (a) the sandflat, (b) the salt marsh

### a) Sandflat



### b) Salt marsh

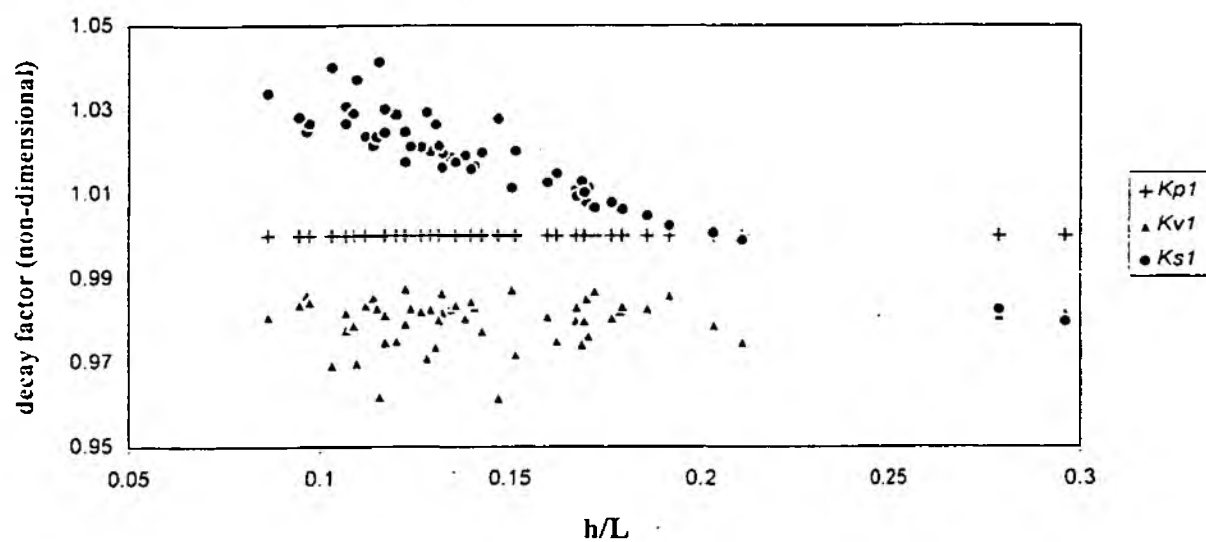


Fig. 5.13: Variation of  $K_S K_P K_V$  with  $h/L$  for sandflat (note: y-axis scaled different to Figure 5.12)

defined by equation 23. This suggests that no wave breaking occurs between the outer and middle station.

### The salt marsh.

The relative influence of modelled percolation, shoaling, and viscous friction on wave heights across the salt marsh is similar to that across the sandflat (Figure 5.11(b)). In absolute terms, however, the effect of shoaling and viscous friction is significantly larger across the salt marsh, with  $K_v$  varying from 0.92 to 0.98, and  $K_s$  as high as 1.26. Furthermore, although still present in Figure 5.12(b), the decrease of  $K_s$  with increasing  $h/L$  is less well defined over the salt marsh section compared to the sandflat. It appears from Figure 5.12(b), that the critical value of  $h/L$  beyond which  $K_s$  is smaller than 1.0 is larger over the salt marsh (where the critical value of  $h/L \approx 0.25$ ) than over the sandflat (where the critical value of  $h/L \approx 0.2$ ). The combined decay factor,  $K_{mod}$ , decreases with increasing relative water depth,  $h/L$ , as it does over the sandflat transect (Figure 5.13). The relationship between  $K_{mod}$  and  $h/L$ , however, breaks down for  $h/L < 0.13$ . Above this value,  $K_{mod}$  decreases faster in the case of the salt marsh than it does in the case of the sandflat transect. The critical relative depth beyond which  $K_{mod} < 1.0$  is larger in the case of the salt marsh transect (approximately 0.18 compared to 0.13, Figure 5.13). This shift towards a higher  $h/L$  threshold reflects the effect of the slightly higher slope across the salt marsh which leads to an increased effect of wave shoaling (i.e. an increase in wave height) at any given relative depth compared to the sandflat transect. The apparently random variation of  $K_{mod}$  for low relative depths is caused by the random variation of shoaling and percolation coefficients (see Figure 5.12(b)) which may, in turn, result from an interference of the vegetation cover with the shoaling and/or percolation processes as described by equations 8 and 22 above. As a result of the larger values of  $K_f$  (mean = 1.03), the model predicts an increase of  $H_{2mod}$  above the critical breaking height in two cases. Wave breaking is most likely in conditions of low relative depth (i.e. maximum shoaling) and/or high incident wave heights. The results from the model confirm this theory, as both cases of modelled wave height breaking occurred for the lowest values of  $h/L$  in the 54 records.

#### 5.5.3.2 Wave decay unexplained by viscous friction, percolation and shoaling

The ratio of the actual  $H_{rms}$  decay ( $K_{obs}$ ) to the modelled decay due to shoaling, viscous friction, and percolation ( $K_{mod}$ ) is smaller than unity for both salt marsh and sandflat (Figure 5.14) indicating that the model underestimates wave attenuation in both cases. For the salt marsh transect, however, this wave decay underestimation is greater, as  $K_{obs}/K_{mod}$  is significantly smaller than in the case of the sandflat transect (both distributions appear to be normal (mean  $\approx$  median) and the difference between the means of all  $K_{obs}/K_{mod}$  is significant at the 95% level, see Table 5.2). On average, modelled percentage wave attenuation is more than 98% smaller

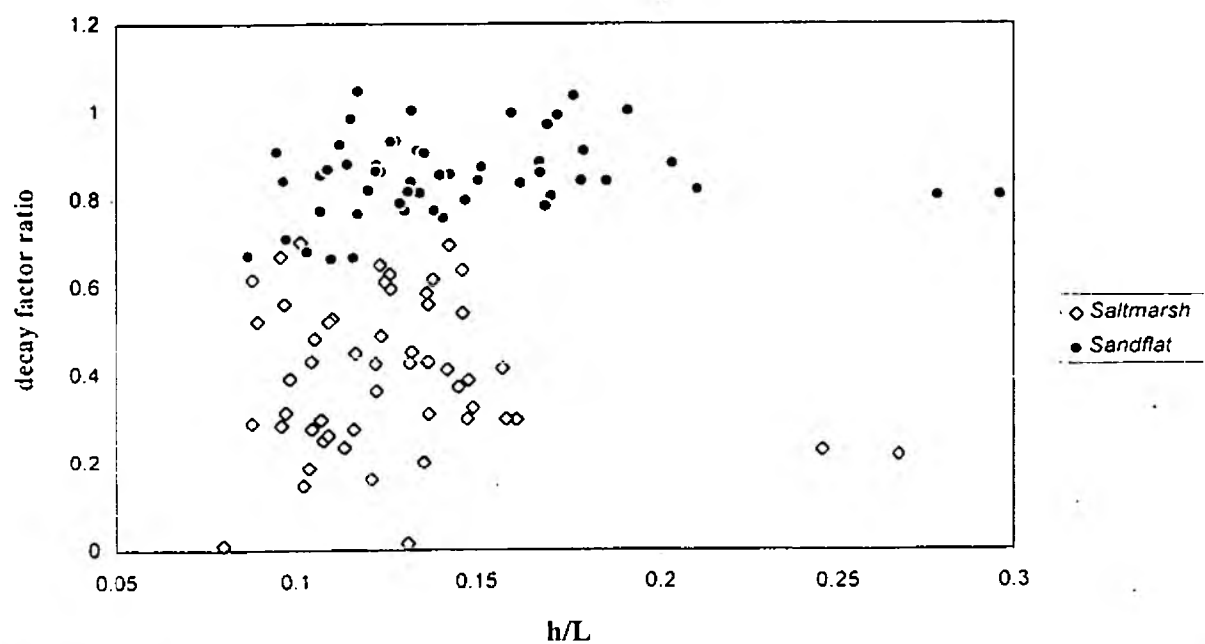


Fig. 5.14: Variation of  $K_{obs}/K_{mod}$  for sandflat and salt marsh



than observed attenuation over the sandflat. Over the salt marsh, the model predicts and average increase in wave height, whereas observed wave heights decrease (Table 5.3).

Table 5.2: Values of  $K_{obs}/K_{mod}$  for the sandflat and salt marsh transects, Stiffkey (N = 54)

	$K_{obs}/K_{mod}$	
	Sandflat	Salt marsh
Mean	0.86	0.40
St.dev	0.09	0.17
Median	0.86	0.41
Minimum	0.67	0.01
Maximum	1.05	0.70

Table 5.3: Observed and modelled wave height attenuation (excluding effect of surface friction in model)

	% wave height attenuation			
	Sandflat		Salt marsh	
	mod	obs	mod	obs
Mean	0.28	14.64	-3.47*	58.34
St.dev	1.09	9.10	2.96	17.47
Maximum	3.85	33.09	5.29	98.75
m				
Minimum	-1.43*	-5.30*	-16.11*	27.46
Median	-0.05*	14.58	-3.09*	58.06

\* note: negative values indicate % wave height increase.

The mean percentage difference between observed wave heights ( $H_{2obs}$ ) at the end of the transect and those predicted ( $H_{2mod}$ ) on the basis of modelled  $K_s$ ,  $K_v$ ,  $K_p$ , was more than 25 times as large for the salt marsh compared to the sandflat (Table 11). The difference between  $H_{2mod}$  and  $H_{2obs}$  over the salt marsh is >42% for all 54 records. The fact that the distribution in the case of the salt marsh is not normal and extremely negatively skewed (the mean being approximately three times larger than the median), however, means that no statement can be made as to whether the mean  $H$ -difference in this case is significantly different from zero. The standard deviation of the difference between predicted and observed heights over the sandflat is relatively low (Table 5.4) the distribution appears to be normally distributed (mean = median), and the mean wave height difference is significantly different from zero at the 95% confidence level. This confirms that wave attenuation over the sandflat and the salt marsh is underestimated

by the model. In addition, it appears that wave attenuation over the salt marsh has a higher variability for a given set of water depth and wave length conditions. This again suggests that non-linear interaction of individual dissipation processes is involved or that a separate energy dissipation process operates which is in itself highly variable.

Table 5.4: Percentage difference between expected wave heights (on basis of shoaling, viscous friction, and percolation) and observed wave heights (N = 54)

	$H_{2cal}-H_{2obs}$ (%)	
	Sandflat	Salt marsh
Mean	18.18	459.02
St.dev	13.10	1471.83
Median	16.88	141.85
Minimum	-4.53	42.28
Maximum	50.29	9155.82

### 5.5.3.3 Role of surface friction - model suggestions for values of $f$

The overestimation of wave heights by the model suggests that additional processes operate which dissipate wave energy in the field and have not been accounted for in the model. As mentioned above, one such process is linked to the influence of friction caused by surface roughness. As there is no direct way of estimating surface roughness accurately *a priori* (especially in the case of vegetated surfaces), the reverse procedure is adopted here: the estimates of surface friction from the comparison of wave decay measured in the field with wave decay expected due to all other main dissipation processes. This procedure assumes that all energy dissipation *not* explained by shoaling, percolation, and viscous friction is in fact due to surface roughness. Mathematically, this means that the ratio between the wave heights expected (calculated by the above model) and those actually observed is assumed to be equal to the friction decay factor,  $K_f$ :

$$H_{2obs} = H_{2mod} K_f \quad \text{where} \quad H_{2mod} = H_{1obs} K_s K_v K_p \quad (24)$$

The ratio  $H_{2obs}/H_{2mod}$  (and therefore  $K_f$ ) was determined for each of the 54 wave records of the sandflat and the salt marsh transect stations.  $K_f$  itself is a function of  $h$ ,  $T$ ,  $L$ ,  $K_s$ ,  $Dx$ , and  $f$  (equation 10). A Matlab program was written to solve this equation for  $f$  for each of the 54 wave records of known  $h$ ,  $T$ ,  $L$ ,  $K_s$ , and  $Dx$ , so that:

$$f = \left( \frac{1}{K_f} - 1 \right) \frac{1}{b}$$

where

(25)

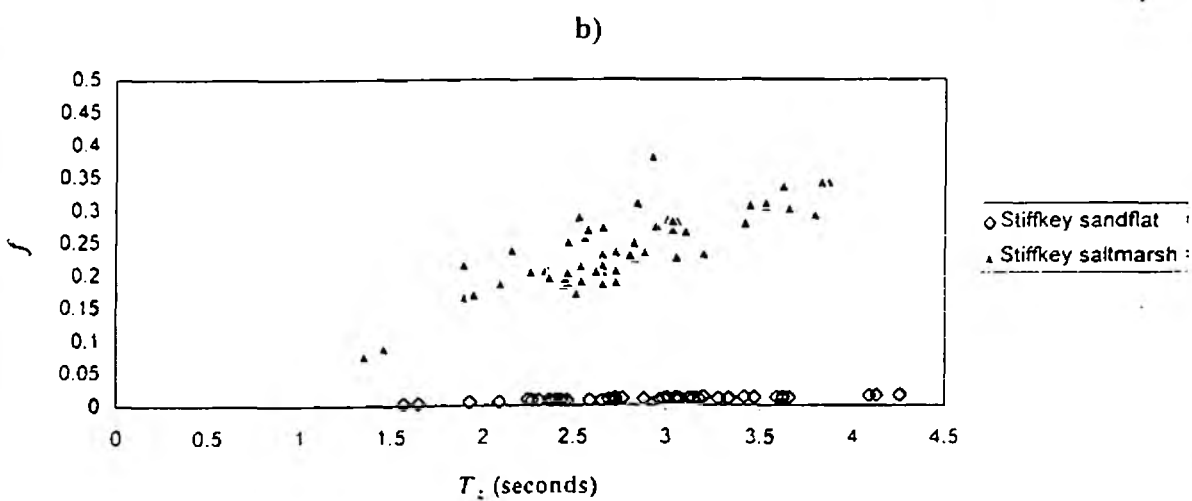
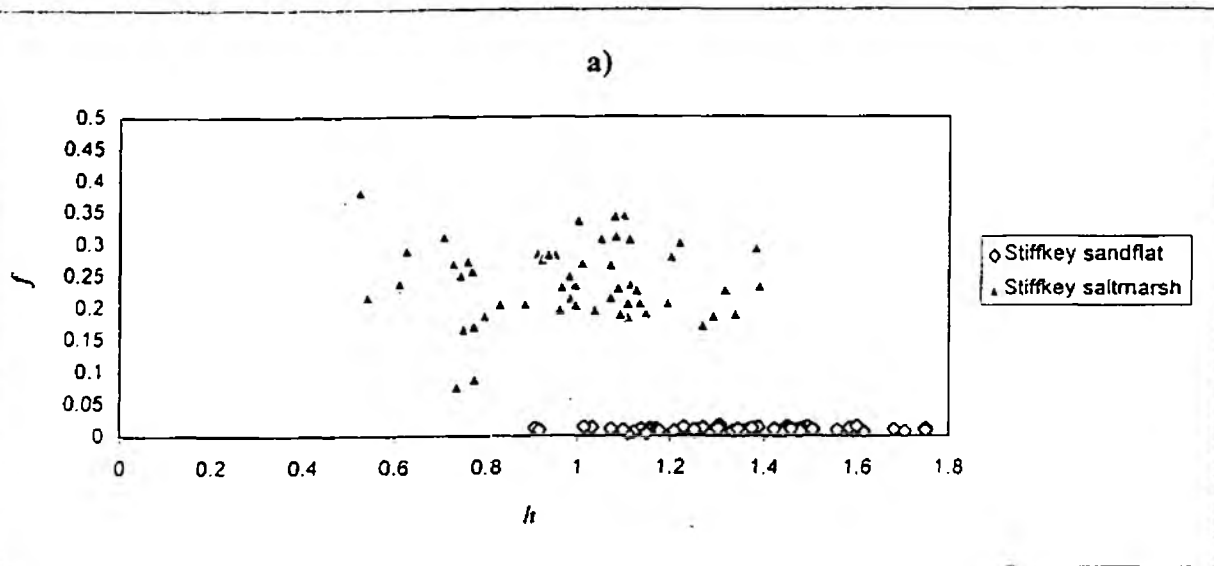
$$b = \frac{64\pi^3 H_1 \Delta x h^2 K_s^2}{3g^2 h^2 T^4 \sinh^3(2\pi h/L)}$$

The resulting values for  $f_{mod}$  appeared normally distributed. Values of  $f_{mod}$  were several orders of magnitude higher and more variable for the salt marsh transect than for the sandflat transect (Table 5.5):

Table 5.5: Values for the friction factor,  $f$ , derived from the attenuation model

	modelled friction factor, $f_{mod}$ ( $\times 10^{-2}$ )	
	Sandflat	Salt marsh
Mean	1.04	24.01
St. dev	0.30	5.95
Median	1.06	23.40
Minimum	0.32	7.71
Maximum	1.75	38.27

The modelled friction factors do not vary with water depth as suggested by Figure 5.3 (CERC, 1984) but vary with wave period (see Figure 5.15(a and b)). The increase in  $f_{mod}$  with increasing wave period is more pronounced over the salt marsh, where modelled values of  $f_{mod}$  are an order of magnitude higher than over the sandflat. The response of  $f_{mod}$  to combined changes in all three variable factors of equation 25 (i.e.  $H_1$ ,  $K_s$ , and  $h/L$ ) is illustrated in Figure 5.15(c) and shows that there is no significant tendency for  $f_{mod}$  to vary with the term in 25 that contains  $H_1$ ,  $K_s$ , and  $h/L$  (neither over the sandflat nor over the salt marsh). The relationship between wave period and modelled friction factors is reflected in Figure 5.16 where  $f_{mod}$  is plotted against relative water depth. The curve defined by the variation of modelled  $f$  with  $h/L$  corresponds very closely to the curve for 'dense marsh grass' in Figure 5.3 (CERC, 1984) if a fixed wavelength of 21.25m is assumed for Figure 5.3. This wave length value was derived from a comparison of water depth (in Figure 5.3) with the  $h/L$  value of the model corresponding to the same friction factor. It is not clear what actual wavelength or wave period the figure from CERC (1984) is based on. For longer and shorter waves ( $L = 30\text{m}$  and  $10\text{m}$  respectively), the CERC curve falls below and above the line defined by the  $f_{mod}$  values modelled for Stiffkey but retains its main characteristic shape.



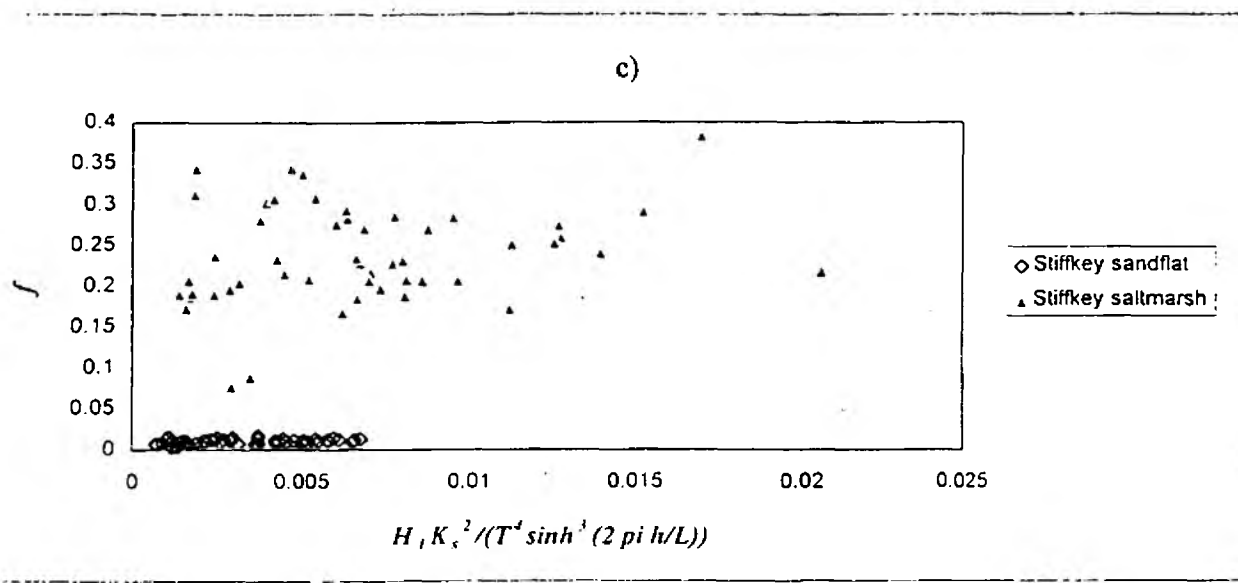


Fig. 5.15: Variation of  $f_{mod}$  with (a)  $h$ , (b)  $T$ , and (c)  $\frac{H_1 K_s^2}{T^4 \sinh^3(2 \pi h/L)}$

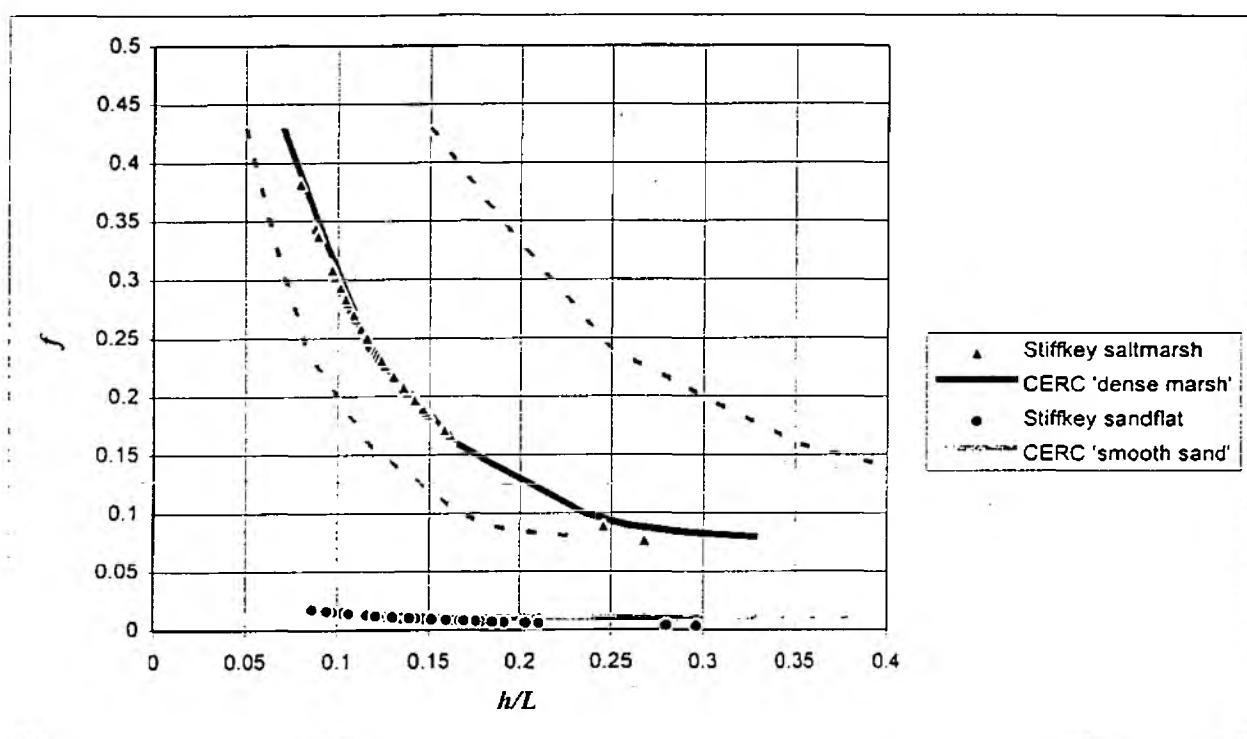


Fig. 5.16: Modelled  $f$  values for Stiffkey sandflat and saltmarsh compared to those given in Figure 5.3 (CERC 1984) (note: solid lines assume  $L = 21.25$  m in Figure 5.3, top and bottom dashed lines assume  $L = 10$  m and  $L = 30$  m respectively).

With regard to the sandflat friction factors calculated for the Stiffkey sandflat an increase with decreasing  $h/L$  and a rise to values exceeding those predicted by the CERC (1984) curve for  $h/L < 0.14$  can be observed (Figures 5.16 and 5.17). This increase in  $f_{mod}$  may be the result of an increased surface roughness due to sand ripples on the Stiffkey sandflat compared to the 'smooth sandy bottom' surface category of the CERC figure.

According to CERC (1984), the friction factor does not vary in response to water depth and/or wave length over a smooth sandy bottom. Assuming a different wave length for the computation of Figure 5.17 from Figure 5.3, therefore, has no effect on the line representing the CERC sand friction factor. In addition to the lack of information regarding the wave lengths used in Figure 5.3, however, it is unclear, whether this figure was developed for a sloping or non-sloping surface. The changes to the curve in response to changing shoaling coefficients, however, will be negligible, as the squared  $K_s$  term in equation 25 is small compared to the wave period and relative water depth terms. Figures 36 and 37 can therefore be regarded as a good approximation to the friction factors responsible for wave attenuation over the salt marsh and the sandflat in the particular  $h/L$  conditions encountered in this study.

#### 5.5.3.4 Alternative estimates of sandflat friction factors

To assess whether the friction factors determined above for the sandflat correspond to expected values derived from other sources, alternative equations may be used to derive  $f$  values applicable to the Stiffkey sandflat. An agreement between the friction values computed above and the friction factors derived from other sources would support the above claim that this modelling approach provides a good quantitative means of determining the effect of surface roughness on wave attenuation. Using equation 13 above, for example, it is possible to derive an estimate for  $f$  from the ripple dimensions or the grain size distribution of the sediment and from the amplitude of the horizontal displacement of the water just outside the boundary layer at the bed given by CERC (1984) as:

$$a = \frac{H}{2} \frac{\cosh(2\pi \frac{z+h}{L})}{\sinh(2\pi \frac{h}{L})} \quad (26)$$

For the given wave height, water depth, and wave length conditions at the outer sandflat station, values for  $a$  vary from 30 to 250mm with an average of 110mm. Values of  $k_s$  in equation 13 can be approximated by  $2D_{90}$  (Sleath, 1984) which has been determined to be approximately 0.242mm in the case of the Stiffkey sandflat substrate. As a result  $a/k_s$  varies

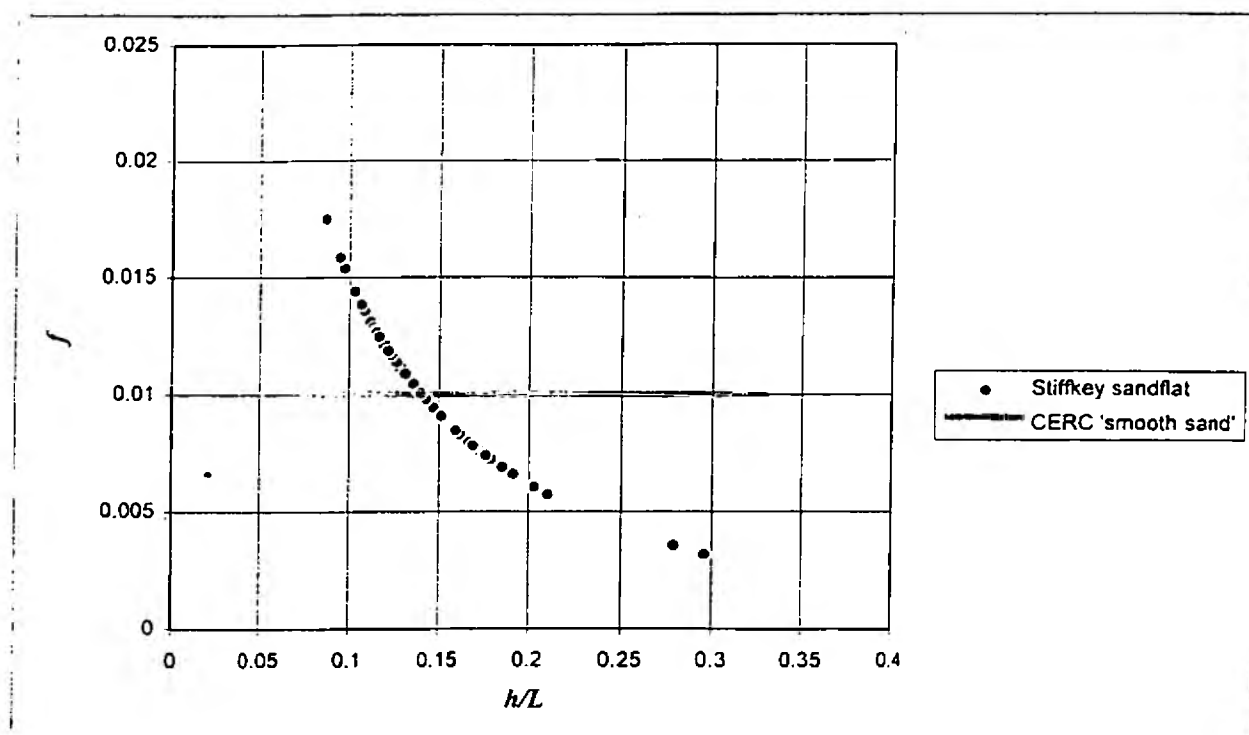


Fig. 5.17: Modelled  $f$  values for Stiffkey sandflat compared to those given in Figure 5.3 (CERC 1984) (note: solid line assumes  $L = 21.25$  m in Fig.5.3, dashed lines assume  $L = 10$ m and  $L = 30$  m.



from 123.94 to 1033.06 and according to equation 13 the respective values of  $f$  should lie between 0.0102 and 0.0203. This range is slightly higher than but includes most of the range of  $f_{mod}$  values determined by the modelling approach above (Table 5.1).

As an alternative to  $2D_{90}$ , the spacing between ripple crests (their wave length  $L_r$ ) and the height of surface ripples ( $h_r$ ) can be used to estimate  $k_r$  as  $k_r = 25h_r^2/L_r$  (Sleath (1984)). Although no regular measurements of sand surface ripples were undertaken during the field wave recording period, occasional measurements suggest that  $L_r$  and  $h_r$  at Stiffkey vary from 40 to 140mm and from 10 to 20mm respectively. According to this alternative formula,  $k_r$  would vary from 17.9 to 250mm, resulting in values of  $a/k_r$  of between 0.12 and 14. Values of  $f$  derived from these vary from 0.059 to 0.3 (equation 13), defining a range larger than that derived by using  $2D_{90}$  to estimate  $k_r$ . In this context it has to be remembered, however, that the estimates of  $L_r$  and  $h_r$  are not based on a detailed field investigation and were only used as a first and rough approximation of possible ripple dimensions in the field. The dimensions used here are likely to represent extreme conditions as the measurements were obtained after high tides with onshore winds. It is possible, that many of the 54 wave measurements were collected during times of no or little ripple formation. Using  $2D_{90}$  as an estimate of  $k_r$  may therefore provide a more realistic estimate of  $f$ .

Another way of estimating  $f$  for small amplitude waves is given by equation 11(b) in which  $U_*$ , the amplitude of the horizontal velocity just outside the boundary layer, is approximated by

$$U_* = \frac{H}{2} \frac{gT}{L} \frac{\cosh(2\pi \frac{z+h}{L})}{\cosh(2\pi \frac{h}{L})} \quad (\text{CERC, 1984}). \quad (27)$$

For the wave/water depth conditions encountered at the outer sandflat station, values of  $U_*$  vary from 0.068m to 0.0411m. Using the values of  $a$  mentioned above and a value of  $1.36 \cdot 10^{-6} \text{m}^2 \text{s}^{-1}$  for dynamic viscosity together with equation 11(b), values of  $f$  would be expected to lie between 0.007 and 0.052, a range which overlaps with the range of  $f$  derived from the attenuation model and which includes the range derived from equation 13 (using  $2D_{90}$  instead of ripple dimensions).

The ranges of  $f$  derived from the different formulae and from the attenuation model are listed for comparison in Table 5.6 below. All friction factor maxima determined from the theoretical formulae exceed the friction factor maxima derived from the attenuation model. With the exception of the range determined from equation 13 using  $L_r$  and  $h_r$ , however, the ranges overlap with those determined by the model. Lack of a disagreement between these

various estimates of  $f$  and those values of  $f$  estimated from the attenuation model suggests that the model can be used to calculate values of  $f$  which approximate actual surface friction factors.

Table 5.6: Friction factors as estimated from various equations and from the wave attenuation model

	friction factor, $f$ ( $\times 10^{-2}$ )	
	Minimum	Maximum
Attenuation model	0.32	1.75
Equation 13 (using $k_s = 2D_{90}$ )	1.0	2.03
Equation 13 (using $k_s = 25h_r^2/L_r$ )	5.91	30.00
Equation 11(b)	0.70	5.20

#### 5.5.3.5 Wave attenuation change as a result of marsh removal

It has been shown above, that wave attenuation across the sandflat can be accurately reproduced by the proposed model on the basis of known surface slope, grain size distribution of the surface sediment, incident wave and water depth conditions, and estimated friction factors. In addition, it was noted that if marsh surface friction (due to the presence of vegetation) is ignored, modelled wave attenuation over the salt marsh is much less than that actually observed, giving an indication of the possible effect of the removal of vegetation. The model can now be applied to assess the possible effect of a transformation of the salt marsh to sandflat, i.e. a complete removal of the marsh. Such a conversion may, for example, be the result of marsh edge erosion due to an increase in incident wave energy and/or a decreased sediment supply. 'Atmodel2.m' calculates expected wave heights for the innermost station on the basis of observed wave heights at the marsh edge station. These calculations are based on the observed marsh surface elevation and slope. Permeability and sediment characteristics are assumed to be similar to the respective values for the sandflat and surface friction is varied with  $f = 0.02$ , 0.052, and 0.3, three values which represent the highest estimated maxima for the sandflat (Table 5.6). By setting the friction factor equal to the highest values estimated for the sandflat, there is no danger of overestimating the reduction in attenuation resulting from the conversion from vegetated marsh to unvegetated sand. As a result, the calculated wave heights at the innermost station are conservative estimates of the wave heights one would expect if a sandflat instead of a salt marsh was fronting the wave station.

Table 5.7 summarises the results of the simulated salt marsh-to-sandflat conversion. Only in the case of very (and possibly unrealistically) high sandflat friction ( $f = 0.3$ ) does wave attenuation

over the simulated sandflat exceed that observed over the existing salt marsh (by 6.21%). The difference between the mean % wave height reduction observed and that predicted for various values of sandflat friction is significant at the 95% confidence level (the data approximates the normal distribution).

It is worth noting that, even in the case of  $f = 0.3$ , for the conditions given here, the maximum wave height attenuation observed over the existing salt marsh still exceeds the maximum attenuation to be expected over the simulated sandflat by more than 10%. Would the existing salt marsh be replaced by sandflat of the same elevation and surface slope and with a friction factor  $f = 0.052$ , wave heights landward of the transect would therefore on average be at least 78% higher.

Table 5.7: Observed values of wave height decrease over the salt marsh compared to computed values for salt marsh-to-sandflat conversion assuming three different values of  $f$ .

	% wave height decrease between middle and inner station			
	observed	$f = 0.02$	$f = 0.052$	$f = 0.3$
Mean	58.34	10.72	25.58	64.55
St. dev	17.47	6.42	11.79	14.85
Maximum	98.75	28.39	53.47	87.47
Minimum	27.46	-0.36*	6.18	32.56
Median	58.06	11.69	26.38	69.10

\* note: negative value indicates % wave height increase.

#### 5.5.4 Summary and discussion

The application of 'attmodel' to the Stiffkey sandflat/salt marsh transect showed that percolation into the surface substrate, shoaling, and viscous friction, account on average for less than 2% of observed attenuation over the sandflat. For the salt marsh, the model predicts an average increase in wave height, whereas average observed attenuation is as high as 58%. It has been suggested that an additional energy sink exists in the field which has not been considered in the initial model. Assuming that this energy sink is related to surface friction due to roughness, friction factors were calculated and correspond closely to friction factors quoted in the literature for similar surfaces. The close correspondence between friction factors for 'dense marsh' and 'smooth sand' predicted by CERC (1984) with those computed from the model presented here

supports the theory that surface friction is responsible for the previously unexplained additional energy dissipation. On the basis of the values given in Table 5.3, this would mean that surface friction accounts for at least 90% of the attenuation over the salt marsh and for at least 70% of the attenuation over the sandflat, with percolation, water viscosity, and wave breaking accounting for the remainder of wave attenuation. The model results suggest that the presence of vegetation on the salt marsh raises friction factors by at least a factor of 3 compared to friction of the sandflat. This means that even if the friction of the sandflat is assumed to be raised by the presence of surface ripples, salt marsh friction is larger than or at least comparable to sandflat friction. Only when sandflat friction is raised to the maximum value predicted from sediment properties and/or ripple dimensions does it exceed the friction computed for the Stiffkey salt marsh. Even in these extreme conditions, sandflat friction factors are at most 25% larger than salt marsh friction factors and wave attenuation over the salt marsh would still be comparable to attenuation over the sandflat (the average difference being approximately 6%). As such high values of sandflat friction are extremely unlikely (Sleath, 1984), one can conclude, that the replacement of the salt marsh by a sandflat has considerable consequences for the wave climate in the surf zone and for the wave energies reaching the shore. The model developed here shows that as a result of converting the Stiffkey salt marsh to a sandflat wave heights at the shore would on average (without taking into account the critical breaker height) be approximately 50% higher. Although actual wave heights would be smaller due to the limiting wave steepness of shoaling waves, the increase in breaking waves would have an important influence on sediment suspension, movement, and deposition, and on the ability of salt marsh plants to colonise the area.

One of the major draw-backs of the model developed and used above is the lack of consideration given to marsh surface topography. The nature of the marsh surface itself is extremely complex. It is likely that the mud-mound topography characterising the marsh edge and the creek network dissecting the marsh are of primary importance in determining wave transformation. Wave diffraction, reflection, and refraction around and over mud-mounds and creeks may be responsible for a substantial proportion of the wave attenuation which has above been attributed to surface friction. It is unclear from the results of the model, how far the increased surface friction can be attributed to the marsh vegetation or to the marsh surface topography. Further detailed field experiments investigating wave attenuation over smooth marsh surfaces and/or creek channels are needed to extend the model and determine the relative importance of these processes. In addition, it is unclear as to how the increased surface roughness interacts with the processes of percolation, shoaling, and viscous friction. These processes are treated as separate and independent energy dissipating mechanisms in the attenuation model, but may well interact considerable in the field so that the equations describing the behaviour of the individual coefficients become inaccurate. In addition, the equations on which the model is based assume a steady wave-propagation along the direction of

the transect. Meteorological and tidal conditions, however, may influence wave decay or growth, undermine this model assumption, and lead to an unexplained variability in wave attenuation in the field.

In spite of the model shortfalls discussed above, the model was able to predict surface friction factors for the sandflat and the salt marsh consistently (Table 5.5). Although it is not clear what causes the increased surface friction of the salt marsh, there can be little doubt that the surface friction over the salt marsh is significantly higher (by at least an order of magnitude) than the friction over the sandflat. As a result of the dominant influence of surface friction on wave energy dissipation (overruling the effect of shoaling, percolation, and viscous friction), this results in a pronounced difference in wave attenuation over the two different surfaces. The value of the mathematical model lies in its use as a tool for the visualisation, understanding, and simulation of the complex relationships between a large number of individual variables. The complete model (including the friction factors for marsh surfaces determined above) can now be used to provide first estimates of wave attenuation over salt marshes in any location comparable to the Stiffkey open coast marsh provided information on incident wave, water depth, and sediment characteristics is available. The comparison of such estimates with field measurements of wave attenuation provides a useful means of further improving our understanding of the processes involved in wave transformation over salt marsh surfaces.

## 6. CONCLUSIONS

The mathematical model based on hydrodynamic theory proved to be a useful tool for determining the relative importance of shoaling, viscous boundary friction, percolation, and bottom friction in the water depth/wave conditions encountered in shallow coastal environments. With respect to the field conditions encountered at the Stiffkey sandflat/salt marsh transect, the model was found to predict wave attenuation accurately with friction factors that were in close agreement with those quoted in the literature for similar surfaces. These friction factors vary with relative water depth and are several orders of magnitude higher for the salt marsh compared to the sandflat surface. This difference is significant in spite of the possible model inaccuracies due to the assumptions about the direction of wave travel and the nature of the marsh surface. The main conclusions are summarised below:

- i) Percolation has negligible effects on the height transformation of waves occurring in the relative water depth conditions encountered in shallow coastal environments. Viscous boundary layer friction has a maximum effect on waves of small period (ca 1.5s) in very shallow water (< 0.5m), reducing wave heights by just over 10%. According to the attenuation model, the effect of wave height increase due to shoaling is small compared to the effect of viscous boundary friction, percolation, and bottom friction in the water depth/wave conditions encountered in shallow coastal environments (slopes  $\approx 1.25 \cdot 10^{-5}$ ).
- ii) The difference between wave attenuation over the Stiffkey sandflat and salt marsh is due to a difference in surface roughness. It can not be explained purely by a difference in surface slope and/or water depth/incident wave conditions. It is not clear, however, what the relative importance of the marsh vegetation and the marsh (creek and mound) topography is in determining the increased surface roughness.
- iii) This difference in surface roughness amounts to several orders of magnitude. Values for surface friction factors,  $f$ , can be estimated using the attenuation model and field data on surface slope, sediment characteristics, and wave/water depth conditions at either end of the wave transect.
- iv) The presence of an open coast salt marsh such as the Stiffkey 'low' marsh is an important wave energy buffer. The removal of this area of increased wave attenuation would significantly alter local sediment dynamics and is likely to increase local coastal erosion as waves would retain their height (and therefore their energy) longer and dispense the energy closer to shore through viscous friction and/or breaking, resulting in higher current velocities at the bed and therefore a greater potential for the suspension and movement of sediments.

There is a certain inherent variability in the model accuracy due to the difficulty in providing accurate input variables, many of which (such as incident wave heights derived from pressure spectra and the permeability of submerged sediments) can only be determined indirectly in the field. The value of the model, therefore, lies not in the accurate calculation of individual wave heights or friction factors, but in its use as a tool for the prediction of average wave attenuation and average friction factors in shallow coastal environments for which wave, water depth, sedimentological, and topographical data is available. To improve and extend the use of the model such data is needed for a variety of open coast marshes, so that the model predictions can be compared with actual data and, most importantly, modelled friction factors can be compared for a variety of marsh surfaces. It may then be possible to relate these friction factors to measures of marsh vegetation characteristics and to marsh topography both of which are likely to play a role in determining marsh surface roughness.

## 7. RECOMMENDATIONS

This project reports a methodology for the reliable collection of water level records and their processing to extract wave summary statistics. The tower array used in this study was, however, visually intrusive and might not be acceptable in all locations. Further development of alternative data gathering systems should be investigated, including the remote accessing of stored datasets. Improved data storage systems, allowing greater flexibility of data collection and fewer site visits during monitoring periods, should also be investigated.

Mathematical modelling has confirmed that surface friction due to roughness is the major control on wave attenuation across salt marsh surfaces. What is less clear, however, is the relative importance of the frictional role of marsh vegetation on the one hand and the more neglected control of marsh surface topography on the other. Wave diffraction, reflection, and refraction around and over mud-mounds and creeks may be responsible for a substantial proportion of the wave attenuation which has been attributed to surface friction. Further detailed field experiments investigating wave attenuation over marsh surfaces of varying topography, with and without creek channels, are needed to extend the model and determine the relative importance of these processes. Such studies would have implications for the design and construction of artificial marshes in front of coastal defence structures.

This project was concerned with wave attenuation at one site only. Such studies might usefully be extended to make research applicable to all locations nationally. Future investigations might cover a range of marsh widths / marsh heights; look further at marsh responses to changing seasonal energy inputs; and investigate a much wider range of UK marsh types, with extension to both South coast and West coast systems. Such studies ought to form part of a National Saltmarsh Research Strategy.

The ultimate aim of a wave attenuation research programme should be to provide a series of field guidelines for Environment Agency field managers to rapidly assess salt marsh characteristics in relation to wave attenuation potential at individual sites and to evaluate the likely flood defence impacts of natural and anthropogenic modification to the salt marsh environment.



## 8. REFERENCES

- Brampton A H (1992) Engineering significance of British saltmarshes. in: Allen, J.R.L., and Pye, K. (eds.), *'Saltmarshes: Morphodynamics, conservation and engineering significance.'* Cambridge: Cambridge University Press, 115-122.
- Bretschneider C L and Reid R O (1954) 'Modification of wave height due to bottom friction, percolation, and refraction' *Beach Erosion Board, Corps of Engineers, Technical Memorandum* No. 45, 21pp.
- Burd F (1995) *'Managed retreat: A practical guide'* English Nature, Peterborough, 28pp.
- Camfield F E (1983) 'Wind-wave growth with high friction' *Journal of Waterway, Port, Coastal and Ocean Engineering*, Vol. 109 (1), 115-116.
- CERC (Coastal Engineering Research Council) (1984) *'Shore protection manual'*, Vol.1&2, US Corps of Engineers, Washington D.C.
- Dalrymple R A and Liu P L-F (1978) 'Waves over soft muds: A two-layer fluid model' *Journal of Physical Oceanography*, Vol. 8, 1121-1131.
- Dalrymple R A, Kirby J T and Hwang P A (1984) 'Wave diffraction due to areas of energy dissipation' *Journal of Waterway, Port, Coastal and Ocean Engineering*, Vol. 110 (1), 67-79.
- Dean R G (1970) 'Relative validities of water wave theories' *Journal of the Waterways and Harbours Division, ASCE*, Vol. 96 (WW1), Proceedings Paper 7092, 105-119.
- Dean R G and Dalrymple R A (1984) *'Water wave mechanics for engineers and scientists'*, Prentice-Hall New Jersey.
- Denny M W (1988) *'Biology and the mechanics of the wave-swept environments'* Princeton University Press, Princeton, New Jersey, 329pp.
- Fonseca M S and Cahalan J A (1992) 'A preliminary evaluation of wave attenuation by four species of seagrass' *Estuarine, Coastal and Shelf Science*, 35, 565-576.

Fonseca M S, Fisher J S, Zieman J C, Thayer G W (1982) 'Influence of the seagrass, *Zostera maina* L., on current flow' *Estuarine, Coastal and Shelf Science*, 15, 351-364.

Fox W T (1985) 'Modelling coastal environments' in: Davis Jr R A (ed.) '*Coastal Sedimentary Environments*', Springer Verlag, New York, 665-705.

Gardiner V and Dackombe R (1983) '*Geomorphological Field Manual*', Allen and Unwin, London, 254pp.

Horikawa K (1978) '*Coastal engineering. An introduction to ocean engineering*', University of Tokyo Press, Japan.

Hydrographer of the Navy (1996) '*Admiralty Tide Tables Vol. I European Waters 1996*', The Hydrographer of the Navy, Taunton.

Knutson P L (1988) 'Role of coastal marshes in energy dissipation and shore protection' in: Hook D D (ed.) '*The ecology and management of wetlands. Vol. I Ecology of Wetlands*' Timber Press, Portland, Oregon.

Knutson P L, Brochu R A, Seelig W N, and Inskeep M (1982) 'Wave damping in *Spartina alterniflora* marshes. *Wetlands*, 2, 87-104.

Kobayashi N, Raichle A W and Asano T (1993) 'Wave attenuation by vegetation' *Journal of Waterway, Port, Coastal and Ocean Engineering*, Vol. 119 (1), 30-48.

Leggett D J and Dixon M (1994) 'Management of the Essex saltmarshes for flood defence' in: Falconr R and Goodwin P (eds.) *Wetland Management*, I C E, London, 232-245.

Macpherson H (1980) 'The attenuation of water waves over a non-rigid bed' *Journal of Fluid Mechanics*, Vol. 97 (4), 721-742.

Martinez P A and Harbaugh J W (1993) '*Simulating nearshore environments*' Pergamon Press, Oxford, 265pp.

Meerschaert M M (1993) '*Mathematical modelling*' Academic Press, London, 287pp.

Milbradt P and Holz K P (1992) 'Modelling wave propagation in large areas' in: Partridge P W (ed.) '*Computer modelling of seas and coastal regions*' Elsevier Applied Science Publishers, London, 524pp.

Pethick J, Leggett D, Husain L (1990) 'Boundary layers under salt marsh vegetation developed in tidal currents', in: Thorne J B (ed) '*Vegetation and erosion*', John Wiley & Sons.

Price W A, Tomlinson K W and Hunt J N (1968) 'The effect of artificial seaweed in promoting the build-up of beaches' *Proceedings of the 11th Coastal Engineering Conference, ASCE*, 1, 570-578.

Putman J A (1949) 'Loss of wave energy due to percolation in a permeable sea bottom' *Transactions, American Geophysical Union*, Vol. 30 (3), 349-356.

Putman J A and Johnson J W (1949) 'The dissipation of wave energy by bottom friction' *Transactions, American Geophysical Union*, Vol. 30 (1), 67-74.

Reid R O and Kajiura K (1957) 'On the damping of gravity waves over a permeable sea bed' *Transaction, American Geophysical Union*, Vol. 38 (5), 662-666.

Seath J F A (1984) '*Sea bed mechanics*' John Wiley & Sons, New York, 335pp.

Silvester R (1974) '*Coastal engineering. I. Generation, propagation and influence of waves*'. Developments in Geotechnical Engineering 4A, Elsevier Scientific Publishing Company, London, 456pp.

Sleath J F A (1982) 'Friction coefficients of rippled beds in oscillatory flow' *Continental Shelf Research*, Vol.1 (1), 33-47.

Vogel S (1994) '*Life in moving fluids. The physical biology of flow*' Princeton University Press, Princeton, New Jersey, 467pp.

## 9. APPENDICES

**Appendix 1: Time periods for which water level and wave records were available from the NRA at individual locations along the north Norfolk coast:**

Location	Dates of water level record	Missing data within record
Thornham	19 Nov 94 - 4 Mar 95	1.1.95(pm)-4.1.95(pm)
Brancaster	2 Nov 94 - 3 Mar 95	4.12.95(pm)-9.12.95(am) 2.1.95(pm)-4.1.95(pm) 3.2.95(pm)-4.2.95(pm)
Wells-next-the-sea	1 Jan 95 - 31 Jan 95	none
Blakeney	19 Nov 94 - 4 Mar 95	none

**Appendix 2: The calculation of directional means according to Davis (1986).**

Directional means were computed by calculating the 'vector resultant' of the set of  $N$  vectors. The  $x$  and  $y$  coordinates of the vector resultant ( $X_r$  and  $Y_r$ ) are obtained by taking the sum of the sines and cosines of the vector angles ( $\theta$ ) respectively:

$$X_r = \sum_i^N \sin \theta_i$$

$$Y_r = \sum_i^N \cos \theta_i$$

The direction of the vector resultant (i.e. the 'mean direction') is obtained by taking the inverse tangens from the ratio of the sum of the sines of all angles and the sum of the cosines of all angles:

$$\text{mean direction} = \theta = \tan^{-1} \left( \frac{\sum_i^N \sin \theta_i}{\sum_i^N \cos \theta_i} \right)$$

**Appendix 3: Regression analysis ( $r$  values) of offshore wave heights versus wave heights ( $H_s$ ) at coastal stations**

$H_s$ at	offshore total H	offshore swell H	offshore wind wave H
Thornham	0.02	0.00	0.03
Brancaster	0.20	0.12	0.15
Blakeney	0.14	0.04	0.11

# APPENDIX 4: Wave parameters and summary statistics for the S4 wave record time-series

A)	$E_{sw}$ (J/m <sup>2</sup> )				$T_s$ (seconds)				$T_s$ change (secs)			
	Time	Outer	Middle	Inner	Total	Marsh	Sand	Inner	Total	Marsh	Sand	Inner
21-Sep-94 am(a)	7:50	78.73	53.49	3.30	-32.06	-93.83	-95.81	3.01	2.56	-0.45	0.85	0.85
21-Sep-94 am(b)	8:00	83.70	49.76	3.52	-40.55	-92.92	-95.79	3.06	2.66	-0.40	0.80	0.80
21-Sep-94 am(c)	8:10	74.80	44.84	3.83	-40.06	-91.47	-94.88	2.77	2.47	-0.30	0.74	0.74
22-Sep-94 am(a)	8:30	63.29	28.31	0.73	-55.27	-97.43	-98.85	3.06	2.53	-0.53	0.97	0.97
22-Sep-94 am(b)	8:45	46.52	21.85	0.66	-52.81	-96.99	-98.58	3.20	2.16	-1.04	1.51	1.51
5-Oct-94 am	6:59	137.56	95.28	10.43	-30.74	-89.05	-92.42	2.43	2.45	0.01	1.82	1.82
6-Oct-94 am(a)	7:40	57.46	42.70	1.65	-25.69	-96.13	-97.13	3.41	3.01	-0.40	4.27	4.27
6-Oct-94 am(b)	7:20	45.12	34.54	2.92	-23.45	-91.54	-93.52	3.41	3.06	-0.36	7.88	7.88
7-Oct-94 am(a)	8:15	10.99	10.76	1.67	-2.07	-84.51	-84.83	2.47	2.66	0.19	2.64	2.64
7-Oct-94 am(b)	8:30	10.98	10.29	1.80	-6.30	-82.50	-83.60	2.66	2.51	-0.15	3.53	3.53
8-Oct-94 am(a)	9:00	8.68	7.22	1.03	-16.76	-85.68	-88.08	3.08	2.54	-0.54	2.48	2.48
8-Oct-94 am(b)	9:15	8.43	5.61	1.08	-33.38	-80.73	-87.16	3.06	2.66	-0.40	2.93	2.93
4-Nov-94 pm	18:50	57.65	26.90	2.62	-53.35	-90.25	-95.45	4.27	2.95	-1.32	2.33	2.33
5-Nov-94 am(a)	6:30	44.95	38.98	3.64	-13.28	-90.65	-91.89	3.59	3.86	0.27	2.23	2.23
5-Nov-94 am(b)	6:50	42.69	33.52	8.36	-21.49	-75.07	-80.43	3.66	3.41	-0.24	3.30	3.30
5-Nov-94 am(c)	7:10	55.07	39.92	6.60	-27.51	-83.46	-88.01	4.27	3.66	-0.61	3.53	3.53
5-Nov-94 am(d)	7:30	58.59	30.26	3.27	-48.35	-89.21	-94.42	4.10	3.53	-0.57	3.59	3.59
4-Dec-94 am	6:55	8.70	8.43	3.54	-3.15	-58.01	-59.33	2.73	2.73	0.00	2.86	2.86
4-Dec-94 pm(a)	19:20	18.30	10.52	1.48	-42.55	-85.96	-91.93	2.97	2.88	-0.08	3.66	3.66
4-Dec-94 pm(b)	19:40	10.42	6.25	1.21	-40.00	-80.81	-88.37	2.88	2.73	-0.15	4.76	4.76
5-Dec-94 am	7:45	25.22	18.84	0.80	-25.31	-95.73	-96.81	2.09	2.35	0.26	1.81	1.81
6-Jan-95 pm(a)	21:45	61.45	39.02	4.02	-36.50	-89.71	-93.47	2.31	2.26	-0.05	1.69	1.69
6-Jan-95 pm(b)	22:00	47.69	32.63	3.10	-31.57	-90.51	-93.51	2.37	2.09	-0.28	1.57	1.57
3-Feb-95 pm	20:50	13.73	11.12	3.36	-19.01	-69.81	-75.55	2.47	2.47	0.00	3.72	3.72
17-Feb-95 pm(a)	19:40	20.94	21.95	4.74	4.82	-78.41	-77.36	2.39	2.54	0.15	2.90	2.90
17-Feb-95 pm(b)	19:50	22.32	17.15	4.39	-23.14	-74.43	-80.35	2.47	2.66	0.19	2.81	2.81
18-Feb-95 am	8:20	27.91	17.85	1.64	-36.02	-90.82	-94.13	1.93	1.90	-0.04	2.07	2.07
19-Feb-95 pm(a)	20:50	6.65	5.61	2.36	-15.60	-64.48	-64.48	4.14	3.83	-0.31	4.31	4.31
19-Feb-95 pm(b)	21:00	5.16	5.07	2.49	-1.87	-50.83	-51.75	3.47	3.53	0.06	4.27	4.27
20-Feb-95 am	9:30	7.59	6.60	0.63	-13.01	-90.48	-91.72	2.73	2.84	0.11	4.76	4.76
2-Mar-95 pm(a)	19:00	12.18	12.28	6.19	0.80	-49.62	-49.21	3.06	2.45	-0.60	2.14	2.14

A) (continued)		$E_{tot}$ (J/m <sup>2</sup> )		$E_{tot}$ change (%)			$T_t$ (seconds)			$T_t$ change (secs)			
Recording date	Time	Outer	Middle	Inner	Sand	Marsh	Total	Outer	Middle	Inner	Sand	Marsh	Total
2-Mar-95 pm(b)	19:20	12.23	12.00	4.80	-1.92	-59.99	-60.76	2.59	2.47	1.91	-0.12	-0.56	-0.69
3-Mar-95 am	7:50	106.60	63.86	5.94	-40.09	-90.69	-94.42	2.28	1.95	1.51	-0.33	-0.44	-0.77
3-Mar-95 pm(a)	19:40	179.69	113.11	33.89	-37.05	-70.03	-81.14	3.15	3.10	2.84	-0.05	-0.26	-0.31
3-Mar-95 pm(b)	20:00	140.10	85.27	25.03	-39.14	-70.65	-82.14	3.62	3.03	2.79	-0.59	-0.25	-0.84
4-Mar-95 am	8:20	34.82	15.59	0.00	-55.23	-99.98	-99.99	2.73	2.93	3.66	0.20	0.73	0.93
17-Mar-95 pm(a)	18:50	64.20	38.93	1.87	-39.36	-95.20	-97.09	1.65	1.46	2.66	-0.19	1.20	1.01
17-Mar-95 pm(b)	19:05	62.88	38.05	1.62	-39.49	-95.75	-97.43	1.57	1.35	2.42	-0.22	1.07	0.85
18-Mar-95 am	7:20	113.76	78.36	15.01	-31.12	-80.84	-86.81	2.38	2.66	3.01	0.28	0.35	0.63
18-Mar-95 pm(a)	19:25	45.60	39.83	13.74	-12.66	-65.50	-69.87	3.18	3.44	3.69	0.27	0.25	0.51
18-Mar-95 pm(b)	19:40	26.42	29.30	8.83	10.86	-69.86	-66.59	3.33	3.62	4.10	0.29	0.47	0.77
19-Mar-95 am	7:55	127.45	92.96	30.52	-27.06	-67.17	-76.05	2.59	2.63	2.38	0.03	-0.24	-0.21
19-Mar-95 pm(a)	20:10	222.14	173.28	91.21	-21.99	-47.36	-58.94	3.62	3.79	3.59	0.17	-0.20	-0.03
19-Mar-95 pm(b)	20:25	230.96	163.89	68.25	-29.04	-58.36	-70.45	3.33	3.06	3.13	-0.27	0.07	-0.20
20-Mar-95 am	8:30	277.09	196.41	87.40	-29.12	-55.50	-68.46	3.06	3.20	3.20	0.14	0.00	0.14
20-Mar-95 pm(a)	20:45	136.03	111.82	42.03	-17.80	-62.41	-69.10	3.08	2.82	2.95	-0.25	0.12	-0.13
20-Mar-95 pm(b)	21:00	136.24	102.45	40.77	-24.80	-60.20	-70.07	3.28	2.81	2.86	-0.47	0.06	-0.41
21-Mar-95 am	9:10	44.41	27.62	0.01	-37.80	-99.97	-99.98	2.25	1.90	1.08	-0.35	-0.81	-1.17
15-Apr-95 pm	18:03	90.59	66.08	12.91	-27.05	-80.46	-85.75	2.69	2.34	1.85	-0.35	-0.49	-0.84
16-Apr-95 pm	18:47	95.39	71.92	14.68	-24.60	-79.58	-84.61	3.13	3.03	2.79	-0.09	-0.25	-0.34
15-May-95 am	6:30	15.75	11.83	0.92	-24.91	-92.19	-94.14	2.41	2.58	3.08	0.17	0.50	0.67
16-May-95 am	7:00	62.83	57.91	10.26	-7.83	-82.29	-83.68	2.44	2.37	1.67	-0.07	-0.70	-0.77
16-May-95 pm	19:30	187.65	125.66	27.33	-33.03	-78.25	-85.44	2.99	2.82	1.98	-0.17	-0.85	-1.01
17-May-95 am	7:40	232.85	170.48	61.16	-26.79	-64.13	-73.73	3.06	2.73	2.68	-0.33	-0.05	-0.38

	$E_{tot}$ (J/m <sup>2</sup> )		$E_{tot}$ change (%)			$T_t$ (seconds)			$T_t$ change (secs)			
	Outer	Middle	Inner	Sand	Marsh	Total	Outer	Middle	Inner	Sand	Marsh	Total
mean	70.72	49.52	12.87	-26.34	-79.64	-83.80	2.92	2.74	2.79	-0.18	0.05	-0.14
st.dev.	66.82	47.77	21.19	15.59	14.57	13.22	0.60	0.55	1.23	0.33	1.07	1.17
max	277.09	196.41	91.21	10.86	-47.36	-49.21	4.27	3.86	7.88	0.29	4.82	4.46
min	5.16	5.07	0.00	-55.27	-99.98	-99.99	1.57	1.35	0.74	-1.32	-1.86	-2.25
median	51.38	34.03	3.59	-27.06	-82.39	-86.98	3.00	2.66	2.80	-0.16	-0.04	-0.24

B) Recording date	Time	$T_p$ (seconds)			$T_p$ change (secs)	
		Outer	Middle	Inner	Sand	Marsh
21-Sep-94 am(a)	7:50	4.45	6.83	102.40	2.37	95.57
21-Sep-94 am(b)	8:00	4.45	5.39	0.64	0.94	-4.75
21-Sep-94 am(c)	8:10	5.39	1.86	0.64	-3.53	-1.22
22-Sep-94 am(a)	8:30	6.02	3.10	102.40	-2.92	99.30
22-Sep-94 am(b)	8:45	6.02	6.83	102.40	0.80	95.57
5-Oct-94 am	6:59	1.52	4.31	81.92	2.79	77.61
6-Oct-94 am(a)	7:40	9.31	3.79	34.13	-5.52	30.34
6-Oct-94 am(b)	7:20	6.83	4.45	102.40	-2.37	97.95
7-Oct-94 am(a)	8:15	2.97	3.72	204.80	0.76	201.08
7-Oct-94 am(b)	8:30	6.21	3.36	204.80	-2.85	201.44
8-Oct-94 am(a)	9:00	13.65	2.25	15.75	-11.40	13.50
8-Oct-94 am(b)	9:15	13.65	13.65	15.75	0.00	2.10
4-Nov-94 pm	18:50	6.21	7.06	40.96	0.86	33.90
5-Nov-94 am(a)	6:30	6.83	6.02	9.31	-0.80	3.29
5-Nov-94 am(b)	6:50	6.83	6.83	6.83	0.00	0.00
5-Nov-94 am(c)	7:10	5.39	5.39	6.02	0.00	0.63
5-Nov-94 am(d)	7:30	5.39	5.39	102.40	0.00	97.01
4-Dec-94 am	6:55	3.86	3.72	5.85	-0.14	2.13
4-Dec-94 pm(a)	19:20	3.10	3.30	6.83	0.20	3.52
4-Dec-94 pm(b)	19:40	3.53	3.79	9.31	0.26	5.52
5-Dec-94 am	7:45	3.53	3.53	102.40	0.00	98.87
6-Jan-95 pm(a)	21:45	1.39	3.86	204.80	2.47	200.94
6-Jan-95 pm(b)	22:00	3.25	2.41	68.27	-0.84	65.86
3-Feb-95 pm	20:50	7.59	5.85	6.61	-1.73	0.76
17-Feb-95 pm(a)	19:40	4.02	4.02	18.62	0.00	14.60
17-Feb-95 pm(b)	19:50	3.53	6.83	4.45	3.30	-2.37
18-Feb-95 am	8:20	1.58	4.88	102.40	3.30	97.52
19-Feb-95 pm(a)	20:50	6.21	6.61	5.85	0.40	-0.76
19-Feb-95 pm(b)	21:00	6.02	5.39	5.39	-0.63	0.00
20-Feb-95 am	9:30	3.79	3.79	20.48	0.00	16.69
2-Mar-95 pm(a)	19:00	4.76	5.00	204.80	0.23	199.80

$T_1$ (seconds)			$T_2$ change (secs)			
Total	Outer	Middle	Inner	Sand	Marsh	Total
97.95	6.83	2.93	0.61	-3.90	-2.31	-6.21
-3.82	6.83	3.53	102.40	-3.30	98.87	95.57
-4.75	6.83	3.79	0.58	-3.03	-3.21	-6.25
96.38	5.39	4.45	34.13	-0.94	29.68	28.74
96.38	4.88	4.10	34.13	-0.78	30.04	29.26
80.40	8.03	5.06	136.53	-2.97	131.48	128.50
24.82	6.02	6.83	20.48	0.60	13.65	14.46
95.57	4.88	3.10	34.13	-1.77	31.03	29.26
201.83	3.06	3.86	3.36	0.81	-0.51	0.30
198.59	3.36	3.15	4.02	-0.21	0.86	0.66
2.10	15.75	15.75	13.65	0.00	-2.10	-2.10
2.10	15.75	10.78	13.65	-4.97	2.87	-2.10
34.75	7.06	3.47	68.27	-3.59	64.80	61.20
2.48	6.02	5.39	4.88	-0.63	-0.51	-1.15
0.00	4.45	4.10	6.02	-0.36	1.93	1.57
0.63	4.88	7.88	4.45	3.00	-3.42	-0.42
97.01	6.02	6.83	7.88	0.80	1.05	1.85
1.99	5.85	5.54	6.61	-0.32	1.07	0.76
3.72	4.45	3.53	4.10	-0.92	0.57	-0.36
5.78	7.88	3.53	4.10	-4.35	0.57	-3.78
98.87	1.44	3.79	11.38	2.35	7.59	9.94
203.41	3.47	4.55	40.96	1.08	36.41	37.49
65.02	5.25	4.36	204.80	-0.89	200.44	199.55
-0.98	12.05	3.25	8.19	-8.80	4.94	-3.86
14.60	1.45	3.86	68.27	2.41	64.40	66.81
0.92	6.02	5.39	3.79	-0.63	-1.60	-2.23
100.82	1.48	6.02	34.13	4.54	28.11	32.65
-0.35	7.06	2.88	5.54	-4.18	2.65	-1.53
-0.63	5.39	3.10	4.88	-2.29	1.77	-0.51
16.69	3.30	3.53	34.13	0.23	30.60	30.83
200.04	5.25	3.86	8.19	-1.39	4.33	2.94



B) (contidued)		$T_p$ (seconds)						$T_p$ change (secs)					
ecording date	Time	Outer	Middle	Inner	Sand	Marsh	Total	Outer	Middle	Inner	Sand	Marsh	Total
2-Mar-95 pm(b)	19:20	4.18	4.36	68.27	0.18	63.91	64.09	5.54	5.00	8.90	-0.54	3.91	3.37
3-Mar-95 am	7:50	4.45	3.53	102.40	-0.92	98.87	97.95	1.86	1.74	34.13	-0.13	32.40	32.27
3-Mar-95 pm(a)	19:40	6.61	2.66	68.27	-3.95	65.61	61.66	3.47	3.15	4.02	-0.32	0.86	0.54
3-Mar-95 pm(b)	20:00	12.05	3.36	68.27	-8.69	64.91	56.22	5.25	5.85	204.80	0.60	198.95	199.55
4-Mar-95 am	8:20	7.88	3.10	102.40	-4.77	99.30	94.52	3.79	6.83	34.13	3.03	27.31	30.34
17-Mar-95 pm(a)	18:50	1.45	1.30	68.27	-0.15	66.96	66.81	1.61	1.13	22.76	-0.48	21.62	21.14
17-Mar-95 pm(b)	19:05	1.34	1.13	68.27	-0.21	67.14	66.93	1.47	1.11	204.80	-0.37	203.69	203.33
18-Mar-95 am	7:20	6.02	4.10	5.39	-1.93	1.29	-0.63	5.39	4.45	4.45	-0.94	0.00	-0.94
18-Mar-95 pm(a)	19:25	3.47	4.02	204.80	0.54	200.78	201.33	5.00	5.85	4.76	0.86	-1.09	-0.23
18-Mar-95 pm(b)	19:40	6.61	6.61	18.62	0.00	12.01	12.01	5.85	4.36	204.80	-1.49	200.44	198.95
19-Mar-95 am	7:55	9.31	6.02	11.38	-3.29	5.35	2.07	4.45	5.39	14.63	0.94	9.24	10.18
19-Mar-95 pm(a)	20:10	7.06	4.36	68.27	-2.70	63.91	61.20	4.36	4.76	3.47	0.41	-1.29	-0.89
19-Mar-95 pm(b)	20:25	5.54	3.59	68.27	-1.94	64.67	62.73	8.90	3.86	204.80	-5.04	200.94	195.90
20-Mar-95 am	8:30	7.88	4.88	14.63	-3.00	9.75	6.75	5.39	4.10	0.43	-1.29	-3.67	-4.96
20-Mar-95 pm(a)	20:45	6.61	8.19	6.61	1.59	-1.59	0.00	18.62	4.18	204.80	-14.44	200.62	186.18
20-Mar-95 pm(b)	21:00	8.19	2.73	204.80	-5.46	202.07	196.61	5.00	5.85	15.75	0.86	9.90	10.76
21-Mar-95 am	9:10	9.31	3.79	102.40	-5.52	98.61	93.09	5.39	4.10	0.43	-1.29	-3.67	-4.96
15-Apr-95 pm	18:03	6.21	3.06	68.27	-3.15	65.21	62.06	6.61	2.88	204.80	-3.72	201.92	198.19
16-Apr-95 pm	18:47	4.36	4.02	6.61	-0.34	2.59	2.25	7.06	3.47	68.27	-3.59	64.80	61.20
15-May-95 am	6:30	4.76	3.72	204.80	-1.04	201.08	200.04	5.54	7.06	68.27	1.53	61.20	62.73
16-May-95 am	7:00	5.54	2.73	68.27	-2.80	65.54	62.73	5.85	6.61	204.80	0.76	198.19	198.95
16-May-95 pm	19:30	5.85	2.73	3.25	-3.12	0.52	-2.60	4.76	5.85	7.59	1.09	1.73	2.82
17-May-95 am	7:40	4.02	4.18	4.76	0.16	0.58	0.75	5.85	2.66	3.36	-3.19	0.70	-2.49

	$T_p$ (seconds)						$T_p$ change (secs)					
	Outer	Middle	Inner	Sand	Marsh	Total	Outer	Middle	Inner	Sand	Marsh	Total
mean	5.67	4.47	64.94	-1.20	60.47	59.28	5.80	4.67	49.21	-1.13	44.53	43.40
st.dev.	2.70	2.01	65.80	2.78	66.32	66.40	3.33	2.29	70.71	3.01	70.98	70.23
max	13.65	13.65	204.80	3.30	202.07	203.41	18.62	15.75	204.80	4.54	203.69	203.33
min	1.34	1.13	0.64	-11.40	-4.75	-4.75	1.44	1.11	0.43	-14.44	-3.67	-6.25
median	5.54	4.02	68.27	-0.18	63.91	58.71	5.39	4.10	13.65	-0.59	6.26	6.65

C)		$H_r$ (m)			$H_r$ change (%)	
Recording date	Time	Outer	Middle	Inner	Sand	Marsh
21-Sep-94 am(a)	7:50	0.35	0.29	0.07	-17.59	-75.17
21-Sep-94 am(b)	8:00	0.37	0.28	0.08	-22.88	-73.38
21-Sep-94 am(c)	8:10	0.35	0.27	0.08	-22.56	-70.80
22-Sep-94 am(a)	8:30	0.32	0.21	0.03	-33.10	-83.98
22-Sep-94 am(b)	8:45	0.27	0.19	0.03	-31.28	-82.66
5-Oct-94 am	6:59	0.47	0.39	0.13	-16.78	-66.90
6-Oct-94 am(a)	7:40	0.30	0.26	0.05	-13.79	-80.33
6-Oct-94 am(b)	7:20	0.27	0.24	0.07	-12.51	-70.94
7-Oct-94 am(a)	8:15	0.13	0.13	0.05	-1.06	-60.67
7-Oct-94 am(b)	8:30	0.13	0.13	0.05	-3.17	-58.14
8-Oct-94 am(a)	9:00	0.12	0.11	0.04	-8.74	-62.14
8-Oct-94 am(b)	9:15	0.12	0.09	0.04	-18.43	-56.07
4-Nov-94 pm	18:50	0.30	0.21	0.06	-31.69	-68.80
5-Nov-94 am(a)	6:30	0.27	0.25	0.08	-6.86	-69.44
5-Nov-94 am(b)	6:50	0.26	0.23	0.12	-11.40	-50.06
5-Nov-94 am(c)	7:10	0.30	0.25	0.10	-14.86	-59.32
5-Nov-94 am(d)	7:30	0.31	0.22	0.07	-28.13	-67.14
4-Dec-94 am	6:55	0.12	0.12	0.08	-1.61	-35.23
4-Dec-94 pm(a)	19:20	0.17	0.13	0.05	-24.20	-62.53
4-Dec-94 pm(b)	19:40	0.13	0.10	0.04	-22.54	-56.00
5-Dec-94 am	7:45	0.20	0.17	0.04	-13.55	-79.32
6-Jan-95 pm(a)	21:45	0.31	0.25	0.08	-20.32	-67.93
6-Jan-95 pm(b)	22:00	0.28	0.23	0.07	-17.28	-69.18
3-Feb-95 pm	20:50	0.15	0.13	0.07	-9.99	-45.05
17-Feb-95 pm(a)	19:40	0.18	0.19	0.09	2.35	-53.50
17-Feb-95 pm(b)	19:50	0.19	0.17	0.08	-12.33	-49.46
18-Feb-95 am	8:20	0.21	0.17	0.05	-19.98	-69.70
19-Feb-95 pm(a)	20:50	0.10	0.09	0.06	-8.15	-35.06
19-Feb-95 pm(b)	21:00	0.09	0.09	0.06	-0.99	-29.89
20-Feb-95 am	9:30	0.11	0.10	0.03	-6.72	-69.16
2-Mar-95 pm(a)	19:00	0.14	0.14	0.10	0.36	-28.98

<i>H<sub>rms</sub></i> (m)			<i>H<sub>rms</sub></i> change (%)			
Total	Outer	Middle	Inner	Sand	Marsh	Total
-79.54	0.25	0.21	0.05	-17.58	-75.19	-79.55
-79.47	0.26	0.20	0.05	-22.88	-73.38	-79.47
-77.39	0.24	0.19	0.06	-22.58	-70.79	-77.38
-89.28	0.22	0.15	0.02	-33.08	-83.99	-89.28
-88.08	0.19	0.13	0.02	-31.31	-82.64	-88.08
-72.45	0.33	0.28	0.09	-16.77	-66.92	-72.47
-83.04	0.21	0.18	0.04	-13.77	-80.36	-83.06
-74.57	0.19	0.17	0.05	-12.48	-70.94	-74.57
-61.09	0.09	0.09	0.04	-0.96	-60.67	-61.05
-59.47	0.09	0.09	0.04	-3.20	-58.21	-59.55
-65.45	0.08	0.08	0.03	-8.76	-62.11	-65.43
-64.17	0.08	0.07	0.03	-18.39	-56.12	-64.19
-78.69	0.21	0.15	0.05	-31.72	-68.76	-78.67
-71.54	0.19	0.18	0.05	-6.91	-69.41	-71.52
-55.76	0.18	0.16	0.08	-11.37	-50.09	-55.77
-65.36	0.21	0.18	0.07	-14.82	-59.32	-65.35
-76.38	0.22	0.16	0.05	-28.14	-67.14	-76.39
-36.27	0.08	0.08	0.05	-1.56	-35.20	-36.21
-71.60	0.12	0.09	0.03	-24.21	-62.49	-71.57
-65.92	0.09	0.07	0.03	-22.56	-56.01	-65.94
-82.12	0.14	0.12	0.03	-13.59	-79.30	-82.11
-74.45	0.22	0.18	0.06	-20.34	-67.89	-74.42
-74.50	0.20	0.16	0.05	-17.31	-69.23	-74.55
-50.54	0.10	0.09	0.05	-10.02	-45.07	-50.57
-52.40	0.13	0.13	0.06	2.40	-53.51	-52.40
-55.69	0.13	0.12	0.06	-12.35	-49.44	-55.69
-75.76	0.15	0.12	0.04	-20.01	-69.71	-75.77
-40.35	0.07	0.07	0.04	-8.09	-35.07	-40.33
-30.58	0.06	0.06	0.04	-0.93	-29.98	-30.64
-71.23	0.08	0.07	0.02	-6.68	-69.19	-71.25
-28.72	0.10	0.10	0.07	0.41	-29.06	-28.77

C) (continued)		$H_s$ (m)		$H_s$ change (%)			$H_{rms}$ (m)			$H_{rms}$ change (%)			
Recording date	Time	Outer	Middle	Inner	Sand	Marsh	Total	Outer	Middle	Inner	Sand	Marsh	Total
2-Mar-95 pm(b)	19:20	0.14	0.14	0.09	-0.93	-36.75	-37.34	0.10	0.10	0.06	-1.01	-36.77	-37.41
3-Mar-95 am	7:50	0.41	0.32	0.10	-22.60	-69.49	-76.39	0.29	0.23	0.07	-22.58	-69.51	-76.40
3-Mar-95 pm(a)	19:40	0.54	0.43	0.23	-20.65	-45.26	-56.57	0.38	0.30	0.16	-20.66	-45.26	-56.57
3-Mar-95 pm(b)	20:00	0.47	0.37	0.20	-21.97	-45.84	-57.74	0.33	0.26	0.14	-21.99	-45.81	-57.72
4-Mar-95 am	8:20	0.24	0.16	0.00	-33.06	-98.73	-99.15	0.17	0.11	0.00	-33.09	-98.75	-99.16
17-Mar-95 pm(a)	18:50	0.32	0.25	0.05	-22.13	-78.08	-82.93	0.23	0.18	0.04	-22.15	-78.06	-82.92
17-Mar-95 pm(b)	19:05	0.32	0.25	0.05	-22.20	-79.37	-83.95	0.22	0.17	0.04	-22.21	-79.36	-83.94
18-Mar-95 am	7:20	0.43	0.35	0.15	-17.00	-56.24	-63.68	0.30	0.25	0.11	-17.01	-56.25	-63.69
18-Mar-95 pm(a)	19:25	0.27	0.25	0.15	-6.52	-41.28	-45.11	0.19	0.18	0.10	-6.55	-41.26	-45.10
18-Mar-95 pm(b)	19:40	0.21	0.22	0.12	5.25	-45.10	-42.22	0.15	0.15	0.08	5.30	-45.10	-42.19
19-Mar-95 am	7:55	0.45	0.39	0.22	-14.60	-42.70	-51.06	0.32	0.27	0.16	-14.60	-42.70	-51.07
19-Mar-95 pm(a)	20:10	0.60	0.53	0.38	-11.68	-27.45	-35.92	0.42	0.37	0.27	-11.68	-27.46	-35.93
19-Mar-95 pm(b)	20:25	0.61	0.51	0.33	-15.76	-35.48	-45.65	0.43	0.36	0.23	-15.76	-35.47	-45.64
20-Mar-95 am	8:30	0.67	0.56	0.37	-15.81	-33.30	-43.84	0.47	0.40	0.26	-15.81	-33.31	-43.85
20-Mar-95 pm(a)	20:45	0.47	0.42	0.26	-9.35	-38.69	-44.43	0.33	0.30	0.18	-9.34	-38.70	-44.42
20-Mar-95 pm(b)	21:00	0.47	0.40	0.26	-13.28	-36.92	-45.30	0.33	0.29	0.18	-13.27	-36.93	-45.30
21-Mar-95 am	9:10	0.27	0.21	0.00	-21.13	-98.33	-98.69	0.19	0.15	0.00	-21.13	-98.32	-98.67
15-Apr-95 pm	18:03	0.38	0.33	0.14	-14.58	-55.80	-62.24	0.27	0.23	0.10	-14.57	-55.81	-62.24
16-Apr-95 pm	18:47	0.39	0.34	0.15	-13.16	-54.82	-60.77	0.28	0.24	0.11	-13.18	-54.80	-60.75
15-May-95 am	6:30	0.16	0.14	0.04	-13.36	-72.07	-75.80	0.11	0.10	0.03	-13.37	-72.02	-75.76
16-May-95 am	7:00	0.32	0.30	0.13	-4.01	-57.90	-59.59	0.22	0.22	0.09	-3.97	-57.90	-59.57
16-May-95 pm	19:30	0.55	0.45	0.21	-18.16	-53.38	-61.85	0.39	0.32	0.15	-18.15	-53.38	-61.84
17-May-95 am	7:40	0.61	0.52	0.31	-14.44	-40.11	-48.75	0.43	0.37	0.22	-14.44	-40.11	-48.76

	$H_s$ (m)		$H_s$ change (%)			$H_{rms}$ (m)			$H_{rms}$ change (%)			
	Outer	Middle	Inner	Sand	Marsh	Total	Outer	Middle	Inner	Sand	Marsh	Total
mean	0.30	0.25	0.11	-14.65	-58.33	-63.53	0.21	0.18	0.08	-14.64	-58.34	-63.54
st.dev.	0.15	0.12	0.09	9.08	17.48	17.18	0.11	0.09	0.06	9.10	17.47	17.17
max	0.67	0.56	0.38	5.25	-27.45	-28.72	0.47	0.40	0.27	5.30	-27.46	-28.77
min	0.09	0.09	0.00	-33.10	-98.73	-99.15	0.06	0.08	0.00	-33.09	-98.75	-99.16
median	0.29	0.23	0.08	-14.59	-58.02	-63.92	0.20	0.16	0.05	-14.58	-58.06	-63.94

D) recording date	Time	$E_p$ (J/m <sup>3</sup> )			$E_p$ change (%)	
		Outer	Middle	Inner	Sand	Marsh
21-Sep-94 am(a)	7:50	10.06	3.52	0.38	-65.03	-89.11
21-Sep-94 am(b)	8:00	9.37	4.23	0.29	-54.79	-93.12
21-Sep-94 am(c)	8:10	4.84	3.15	0.32	-34.89	-89.92
22-Sep-94 am(a)	8:30	10.08	2.44	0.14	-75.79	-94.10
22-Sep-94 am(b)	8:45	6.21	1.85	0.27	-70.25	-85.18
5-Oct-94 am	6:59	3.21	2.98	1.57	-7.19	-47.33
6-Oct-94 am(a)	7:40	5.96	4.08	0.79	-31.55	-80.58
6-Oct-94 am(b)	7:20	4.74	2.66	1.23	-43.99	-53.81
7-Oct-94 am(a)	8:15	0.52	0.72	0.30	38.04	-58.36
7-Oct-94 am(b)	8:30	0.50	0.66	0.60	31.58	-8.03
8-Oct-94 am(a)	9:00	0.93	0.38	0.13	-59.06	-67.01
8-Oct-94 am(b)	9:15	0.80	0.28	0.19	-65.47	-30.14
4-Nov-94 pm	18:50	11.84	2.31	0.34	-80.48	-85.34
5-Nov-94 am(a)	6:30	6.32	5.73	0.36	-9.38	-93.71
5-Nov-94 am(b)	6:50	5.28	4.19	0.92	-20.55	-78.01
5-Nov-94 am(c)	7:10	10.36	5.31	1.09	-48.72	-79.46
5-Nov-94 am(d)	7:30	9.23	3.78	0.53	-59.04	-86.07
4-Dec-94 am	6:55	0.51	0.47	0.41	-6.34	-14.36
4-Dec-94 pm(a)	19:20	1.20	1.05	0.19	-12.33	-81.55
4-Dec-94 pm(b)	19:40	0.98	0.57	0.13	-42.05	-77.58
5-Dec-94 am	7:45	2.24	4.24	0.06	89.31	-98.65
6-Jan-95 pm(a)	21:45	2.27	2.16	0.53	-5.03	-75.62
6-Jan-95 pm(b)	22:00	1.79	1.34	0.38	-25.07	-71.90
3-Feb-95 pm	20:50	1.36	0.54	0.31	-60.54	-41.62
17-Feb-95 pm(a)	19:40	0.99	1.02	0.26	3.06	-74.12
17-Feb-95 pm(b)	19:50	2.40	1.24	0.42	-48.31	-66.17
18-Feb-95 am	8:20	2.62	1.14	0.22	-56.58	-80.68
19-Feb-95 pm(a)	20:50	0.92	0.61	0.18	-33.69	-69.83
19-Feb-95 pm(b)	21:00	0.72	0.56	0.36	-22.91	-35.13
20-Feb-95 am	9:30	1.04	0.81	0.08	-22.77	-89.60
2-Mar-95 pm(a)	19:00	0.84	0.74	0.52	-11.77	-29.56

$E_z$ (J/m <sup>3</sup> )			$E_z$ change (%)			Total
Total	Outer	Middle	Inner	Sand	Marsh	
-96.19	7.74	3.26	0.32	-57.87	-90.13	-95.84
-96.89	6.51	3.01	0.26	-53.70	-91.24	-95.94
-93.44	4.41	2.97	0.28	-32.64	-90.57	-93.65
-98.57	5.45	2.01	0.10	-63.07	-95.04	-98.17
-95.59	4.51	1.60	0.14	-64.61	-91.31	-96.92
-51.12	2.54	2.13	0.87	-16.11	-59.24	-65.81
-86.71	4.67	3.56	0.18	-23.85	-94.97	-96.17
-74.13	3.17	2.53	0.61	-19.95	-75.80	-80.63
-42.53	0.52	0.58	0.08	11.41	-85.43	-83.77
21.01	0.50	0.55	0.09	10.64	-83.28	-81.50
-86.49	0.63	0.38	0.12	-40.21	-67.83	-80.77
-75.87	0.57	0.24	0.10	-58.32	-57.01	-82.08
-97.14	6.56	1.63	0.18	-75.18	-88.76	-97.21
-94.30	5.57	4.40	0.31	-20.99	-93.07	-94.52
-82.53	3.77	2.73	0.90	-27.44	-67.09	-76.12
-89.47	7.53	3.74	0.68	-50.34	-81.84	-90.98
-94.29	8.68	3.69	0.35	-57.46	-90.55	-95.98
-19.79	0.39	0.45	0.32	14.02	-29.97	-20.15
-83.83	1.18	0.99	0.14	-16.21	-85.80	-88.11
-87.01	0.80	0.55	0.13	-31.52	-76.91	-84.19
-97.44	1.29	1.98	0.06	53.17	-97.20	-95.72
-76.85	2.13	1.65	0.29	-22.78	-82.51	-86.50
-78.94	1.44	1.27	0.35	-11.55	-72.58	-75.75
-76.96	0.83	0.52	0.27	-37.10	-48.55	-67.64
-73.33	0.76	0.99	0.21	30.46	-78.80	-72.34
-82.51	1.21	1.22	0.34	0.75	-71.69	-71.48
-91.61	2.31	1.04	0.14	-54.98	-86.76	-94.04
-80.00	0.87	0.35	0.17	-59.13	-51.58	-80.21
-49.99	0.59	0.55	0.30	-7.53	-44.44	-48.63
-91.97	0.90	0.68	0.08	-24.94	-88.51	-91.38
-37.85	0.74	0.63	0.24	-13.84	-61.57	-66.88

01/569/3/A

D) (continued) Recording date	Time	$E_p$ (J/m <sup>2</sup> )			$E_p$ change (%)			$E_s$ (J/m <sup>2</sup> )			$E_s$ change (%)		
		Outer	Middle	Inner	Sand	Marsh	Total	Outer	Middle	Inner	Sand	Marsh	Total
2-Mar-95 pm(b)	19:20	0.61	0.55	0.17	-8.60	-69.43	-72.06	0.57	0.38	0.15	-33.35	-59.80	-73.20
3-Mar-95 am	7:50	7.44	4.73	1.18	-36.44	-75.01	-84.12	6.17	3.36	0.55	-45.51	-83.56	-91.04
3-Mar-95 pm(a)	19:40	10.24	4.58	2.95	-55.23	-35.66	-71.19	7.97	4.17	1.25	-47.73	-69.91	-84.27
3-Mar-95 pm(b)	20:00	6.68	3.58	1.93	-46.42	-46.00	-71.06	6.40	3.01	1.08	-53.01	-64.14	-83.15
4-Mar-95 am	8:20	2.31	1.40	0.00	-39.68	-99.94	-99.97	2.27	1.30	0.00	-42.64	-99.98	-99.99
17-Mar-95 pm(a)	18:50	4.02	1.66	0.22	-58.80	-86.53	-94.45	3.28	1.50	0.12	-54.35	-91.81	-96.26
17-Mar-95 pm(b)	19:05	3.17	2.82	0.23	-11.02	-91.92	-92.81	3.16	2.48	0.16	-21.64	-93.68	-95.05
18-Mar-95 am	7:20	9.98	9.18	1.40	-7.94	-84.77	-85.98	9.96	6.29	1.08	-36.86	-82.84	-89.16
18-Mar-95 pm(a)	19:25	2.15	2.78	1.82	29.40	-34.52	-15.27	2.09	2.29	0.63	9.56	-72.53	-69.90
18-Mar-95 pm(b)	19:40	1.81	1.82	0.50	0.89	-72.72	-72.47	1.49	1.77	0.47	18.89	-73.33	-68.29
19-Mar-95 am	7:55	9.48	5.17	2.52	-45.46	-51.34	-73.46	8.31	4.27	2.37	-48.70	-44.52	-71.54
19-Mar-95 pm(a)	20:10	14.60	8.18	7.02	-43.96	-14.13	-51.88	10.34	7.55	3.35	-26.98	-55.60	-67.58
19-Mar-95 pm(b)	20:25	10.59	6.55	7.61	-38.14	16.26	-28.09	10.54	5.40	5.02	-48.77	-6.91	-52.31
20-Mar-95 am	8:30	23.60	24.16	5.81	2.39	-75.98	-75.39	14.66	11.52	5.72	-21.40	-50.34	-60.97
20-Mar-95 pm(a)	20:45	5.35	3.98	1.82	-25.62	-54.42	-66.09	5.13	3.90	1.65	-23.94	-57.70	-67.83
20-Mar-95 pm(b)	21:00	5.68	4.58	3.42	-19.40	-25.25	-39.74	5.64	3.73	1.76	-33.80	-52.79	-68.75
21-Mar-95 am	9:10	3.70	1.80	0.00	-51.49	-99.96	-99.98	3.36	1.68	0.00	-50.14	-99.98	-99.99
15-Apr-95 pm	18:03	5.86	3.19	0.88	-45.52	-72.31	-84.92	4.06	2.81	0.87	-30.91	-68.88	-78.50
16-Apr-95 pm	18:47	4.05	3.66	0.59	-9.71	-83.96	-85.52	3.97	2.50	-0.57	-36.94	-77.36	-85.72
15-May-95 am	6:30	0.78	0.61	0.12	-21.92	-80.81	-85.01	0.61	0.43	0.10	-30.23	-77.26	-84.13
16-May-95 am	7:00	2.96	2.15	0.48	-27.46	-77.75	-83.86	2.41	2.11	0.41	-12.65	-80.37	-82.86
16-May-95 pm	19:30	12.33	5.06	1.38	-58.96	-72.80	-88.84	10.18	4.86	0.91	-52.22	-81.39	-91.11
17-May-95 am	7:40	16.92	9.90	2.66	-41.49	-73.17	-84.30	14.30	8.49	2.24	-40.65	-73.64	-84.36

	$E_p$ (J/m <sup>2</sup> )			$E_p$ change (%)			$E_s$ (J/m <sup>2</sup> )			$E_s$ change (%)		
	Outer	Middle	Inner	Sand	Marsh	Total	Outer	Middle	Inner	Sand	Marsh	Total
mean	5.27	3.27	1.08	-29.11	-66.44	-75.35	4.18	2.55	0.72	-29.35	-74.04	-81.39
st.dev.	4.85	3.66	1.62	31.31	26.36	24.49	3.64	2.21	1.13	26.06	18.78	15.03
max	23.60	24.16	7.61	89.31	16.26	21.01	14.66	11.52	5.72	53.17	-6.91	-20.15
min	0.50	0.28	0.00	-80.48	-99.96	-99.98	0.39	0.24	0.00	-75.18	-99.98	-99.99
median	3.86	2.55	0.41	-34.29	-74.57	-83.85	3.22	2.06	0.30	-32.08	-77.31	-83.95

E) Recording date	Time	$E_j$ (J/m <sup>2</sup> )
		Outer
21-Sep-94 am(a)	7:50	5.14
21-Sep-94 am(b)	8:00	6.26
21-Sep-94 am(c)	8:10	4.37
22-Sep-94 am(a)	8:30	3.41
22-Sep-94 am(b)	8:45	3.66
5-Oct-94 am	6:59	2.25
6-Oct-94 am(a)	7:40	3.94
6-Oct-94 am(b)	7:20	2.83
7-Oct-94 am(a)	8:15	0.44
7-Oct-94 am(b)	8:30	0.43
8-Oct-94 am(a)	9:00	0.38
8-Oct-94 am(b)	9:15	0.54
4-Nov-94 pm	18:50	2.85
5-Nov-94 am(a)	6:30	3.64
5-Nov-94 am(b)	6:50	3.76
5-Nov-94 am(c)	7:10	4.95
5-Nov-94 am(d)	7:30	7.86
4-Dec-94 am	6:55	0.39
4-Dec-94 pm(a)	19:20	1.10
4-Dec-94 pm(b)	19:40	0.79
5-Dec-94 am	7:45	1.25
6-Jan-95 pm(a)	21:45	1.89
6-Jan-95 pm(b)	22:00	1.20
3-Feb-95 pm	20:50	0.67
17-Feb-95 pm(a)	19:40	0.75
17-Feb-95 pm(b)	19:50	1.19
18-Feb-95 am	8:20	1.52
19-Feb-95 pm(a)	20:50	0.44
19-Feb-95 pm(b)	21:00	0.58
20-Feb-95 am	9:30	0.67
2-Mar-95 pm(a)	19:00	0.70



*E<sub>j</sub>* change (%)

Middle	Inner	Sand	Marsh	Total
3.25	0.18	-36.87	-94.38	-96.45
2.95	0.22	-52.81	-92.66	-96.54
2.90	0.27	-33.63	-90.77	-93.88
1.90	0.07	-44.24	-96.53	-98.06
1.19	0.02	-67.62	-98.21	-99.42
2.06	0.38	-8.55	-81.77	-83.33
2.49	0.15	-36.83	-94.12	-96.28
2.26	0.28	-19.99	-87.60	-90.08
0.54	0.07	22.94	-86.28	-83.14
0.48	0.07	10.91	-84.88	-83.23
0.32	0.06	-13.69	-82.16	-84.60
0.22	0.06	-58.50	-73.62	-89.05
1.60	0.15	-43.91	-90.88	-94.89
2.49	0.23	-31.51	-90.62	-93.58
2.70	0.66	-28.13	-75.57	-82.44
3.67	0.65	-25.80	-82.42	-86.96
3.54	0.28	-54.91	-91.98	-96.38
0.39	0.25	-0.90	-35.47	-36.05
0.72	0.14	-34.21	-80.78	-87.35
0.55	0.11	-31.09	-79.23	-85.69
1.38	0.05	10.50	-96.27	-95.88
1.17	0.21	-38.43	-82.31	-89.11
0.93	0.31	-22.76	-66.22	-73.91
0.49	0.18	-26.84	-63.63	-73.39
0.84	0.18	12.28	-78.41	-75.76
1.08	0.31	-9.78	-71.36	-74.16
0.82	0.12	-45.74	-86.04	-92.43
0.29	0.16	-33.63	-44.41	-63.11
0.46	0.29	-20.89	-35.71	-49.14
0.47	0.06	-29.35	-86.47	-90.44
0.57	0.23	-18.10	-60.66	-67.78

E) (continued) recording date	Time	$E_j$ (J/m <sup>2</sup> )		$E_j$ change (%)			
		Outer	Middle	Inner	Sand	Marsh	Total
2-Mar-95 pm(b)	19:20	0.49	0.37	0.14	-24.26	-60.88	-70.45
3-Mar-95 am	7:50	5.92	2.79	0.39	-52.95	-85.95	-93.39
3-Mar-95 pm(a)	19:40	6.90	4.09	1.13	-40.72	-72.32	-83.59
3-Mar-95 pm(b)	20:00	5.84	2.68	0.91	-53.99	-68.10	-84.40
4-Mar-95 am	8:20	1.83	0.80	0.00	-56.35	-99.99	-99.99
17-Mar-95 pm(a)	18:50	3.09	1.40	0.11	-54.54	-92.47	-96.58
17-Mar-95 pm(b)	19:05	2.84	1.73	0.11	-38.99	-83.55	-96.07
18-Mar-95 am	7:20	8.75	5.36	1.02	-38.72	-80.90	-88.29
18-Mar-95 pm(a)	19:25	2.07	2.25	0.50	8.44	-77.98	-78.12
18-Mar-95 pm(b)	19:40	1.00	1.51	0.39	50.28	-74.00	-60.93
19-Mar-95 am	7:55	7.43	4.10	1.79	-44.78	-56.31	-75.87
19-Mar-95 pm(a)	20:10	7.45	6.62	2.90	-11.19	-56.16	-61.06
19-Mar-95 pm(b)	20:25	8.15	4.91	2.87	-39.75	-41.61	-64.82
20-Mar-95 am	8:30	13.40	10.90	4.91	-18.63	-54.98	-63.35
20-Mar-95 pm(a)	20:45	4.50	3.39	1.48	-24.85	-56.42	-67.17
20-Mar-95 pm(b)	21:00	5.28	3.29	1.58	-37.76	-52.40	-70.37
21-Mar-95 am	9:10	2.42	1.23	0.00	-49.01	-99.88	-99.99
15-Apr-95 pm	18:03	3.19	1.89	0.36	-40.87	-80.72	-88.60
16-Apr-95 pm	18:47	3.31	2.20	0.50	-33.34	-77.48	-84.99
15-May-95 am	6:30	0.57	0.43	0.06	-25.47	-84.89	-88.74
16-May-95 am	7:00	2.34	1.72	0.28	-26.52	-83.41	-87.81
16-May-95 pm	19:30	9.04	4.82	0.74	-46.66	-84.61	-91.79
17-May-95 am	7:40	10.15	8.31	2.11	-18.18	-74.63	-79.24

	$E_j$ (J/m <sup>2</sup> )	$E_j$ change (%)			
		Outer	Middle	Inner	Total
mean		3.44	2.25	0.57	-82.89
st.dev.		3.00	2.09	0.89	13.70
max		13.40	10.90	4.91	-35.05
min		0.38	0.22	0.00	-99.99
median		2.83	1.73	0.24	-81.33